EUROPEAN MECHANICS SOCIETY

EUROMECH COLLOQUIUM 591

Three dimensional instability mechanisms in transitional and turbulent flows

Bari, Italy / 18-20 September 2017

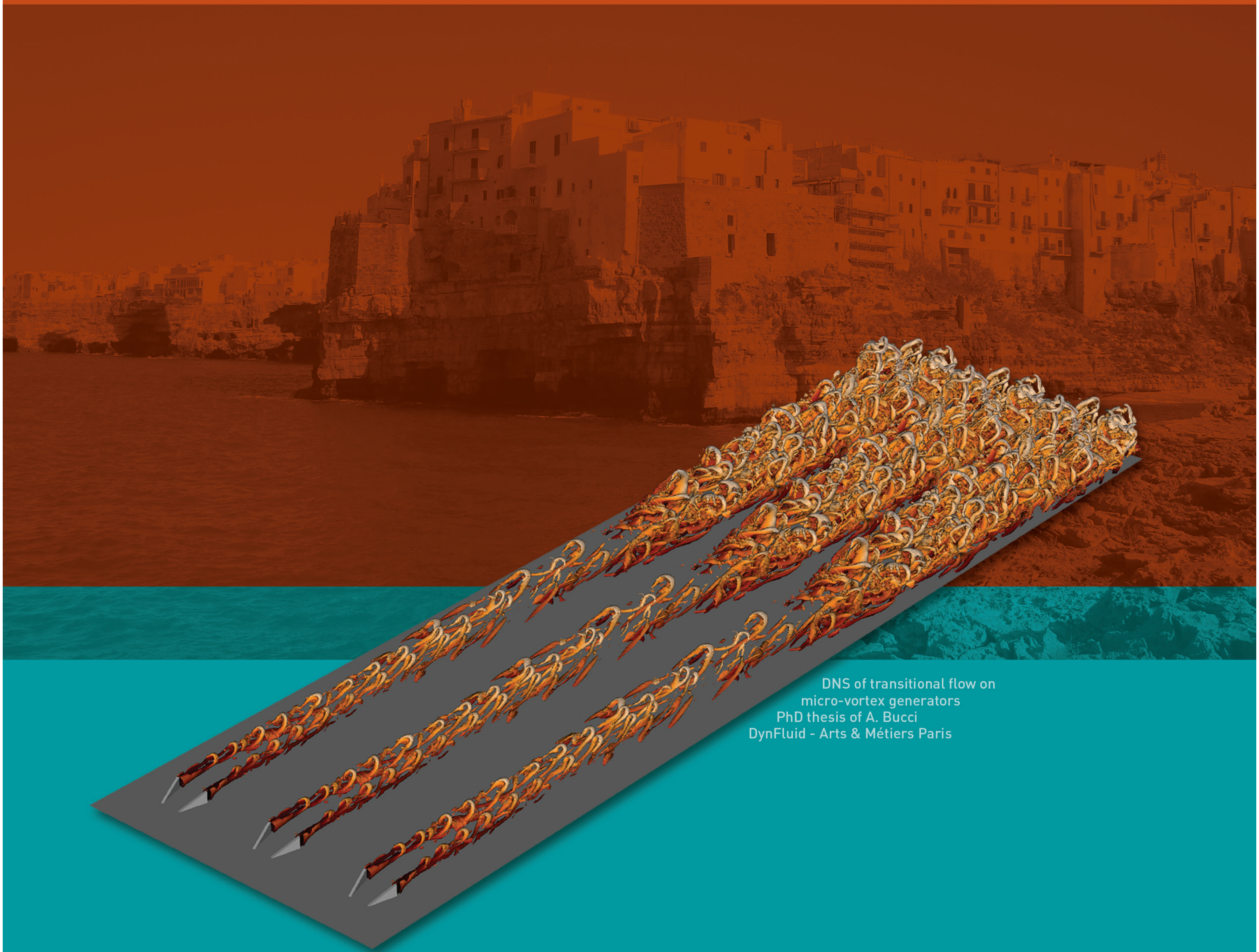

DNS of transitional flow on
micro-vortex generators
PhD thesis of A. Bucci
DynFluid - Arts & Métiers Paris

SCHEDULE
& BOOK OF ABSTRACT

ARTS ET MÉTIERS ParisTech Paris

POLITECNICO DI BARI

We gratefully acknowledge the Sponsors of the EUROMECH Colloquium 591:

- Politecnico Di Bari,
- EUROMECH (the European Mechanics Society),

Practical Information

Room location & Registration The EUROMECH-Colloquium 591 will be held at the Polytechnical University of Bari (Via Amendola 126/B, Bari, you'll find a map in figure 1), about 20 minutes walking distance from the Railway Station.

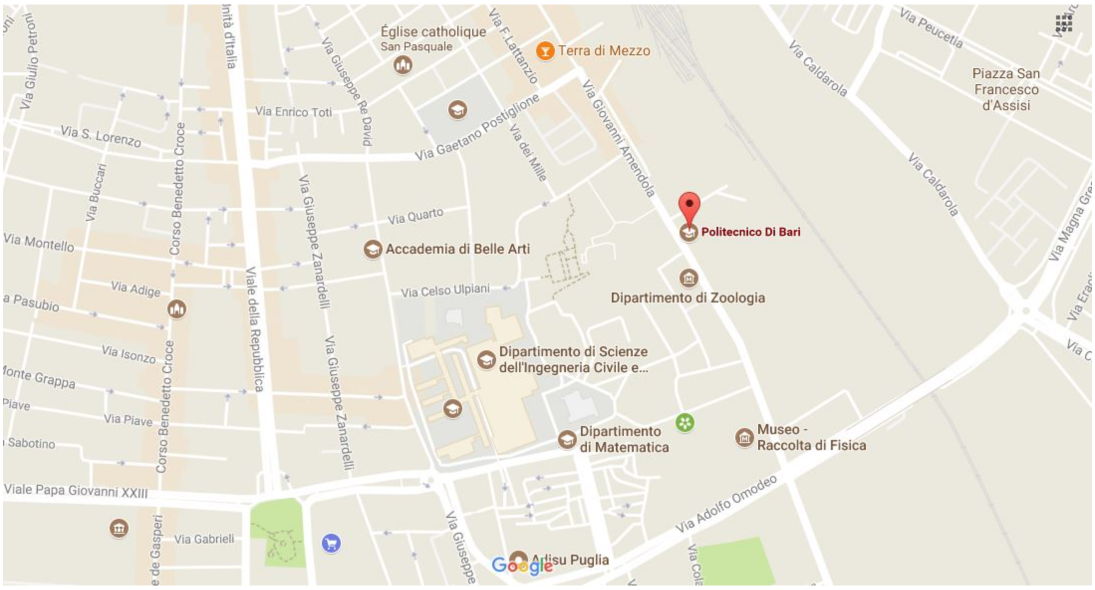

Figure 1: Map of the neighbourhood of the Politecnico di Bari, where the Euromech 591 will be held.

Following the signs at the entrance of the building (Via Amendola 126/B) you'll find the registration desk that will be open on 18th and 19th September from 8 to 8:45 am for registration.

Social Events Lunches and coffee breaks are planned during the conference according to the time plan and will be served right in front of the conference room. Furthermore, two social events are planned:

- Monday, the 18th of September (from 7 pm): The Conference participants are invited to a welcoming cocktail at the 'Circolo della Vela', located in Bari's marina, where drinks and snacks will be offered. For reaching the marina, a bus will be available right out of the conference room at 6 pm.
- Thuesday, the 19th of September (from 8 pm): Conference Dinner at Polignano a Mare, see map (2) and pictures (3). Polignano, a small city in province of Bari, is famous for its stunning old town placed on a rocky promontory. The high terraces on the see are the main attraction of this ancient town which was part of the Ancient Greece with the name of "Neapolis". Strolling in Polignano's alleys one can still feel a Greek flavour in the design and layout of the town. A short boat trip will allow to visit some of the vast sea caves that penetrate right under and into the old town. A bus will drive the conference participants in Polignano at 5pm leaving plenty of time for visiting the town. Then, at 8pm, Social Dinner will be served in a famous restaurant on the rocky promontory overlooking the sea.

Figure 2: Puglia map.

Figure 3: View of Polignano a Mare.

How to get to the conference?
By plane: via the Bari-Palese Airport

Be aware that there are direct flights to Bari from many European cities (from Paris Beauvais, London Stansted and so on). Don't forget to check the available flights on low-cost airlines which provide many of those direct (and very cheap) flights.

From the Airport take the train to Bari Centrale Station, whose timetable and price can be found at the following link: www.ferrovienordbarese.it/times

By train

Get off at Bari Centrale Station and enjoy a 20 minutes walk towards the Politecnico of Bari following the map in figure 4 or take bus 22 in Via Melo 230 (right in front of the railway station) to Mungivacca, and get off at the stop Amendola, ang. c. ulpiani (you'll find further information at the following link: www.amtab.it).

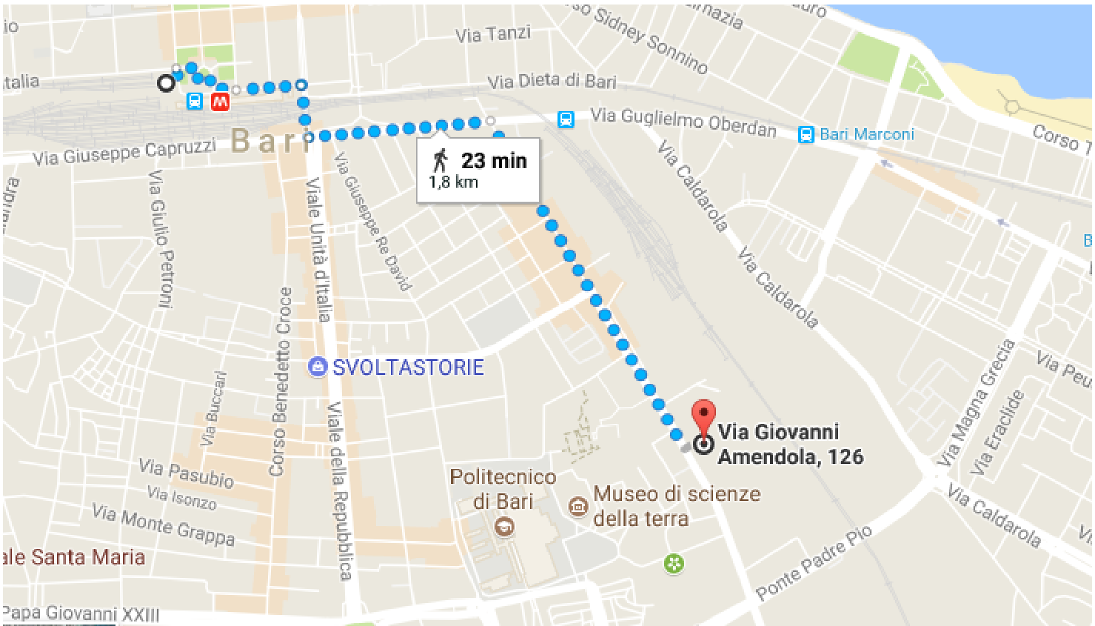

Figure 4: Walking itinerary from the Railway Station to the conference room

Wi-Fi All the campus is covered by the Wi-Fi network Eduroam. In the conference room and close to it you'll have access to a dedicated Wi-Fi network, whose access details will be provided during the registration.

Public transport For your convenience, you'll find below a map of the metro connecting the airport with the Railway Station (fig. 5) as well as a map of the city with the bus lines (fig. 6).

Figure 5: Subway map.

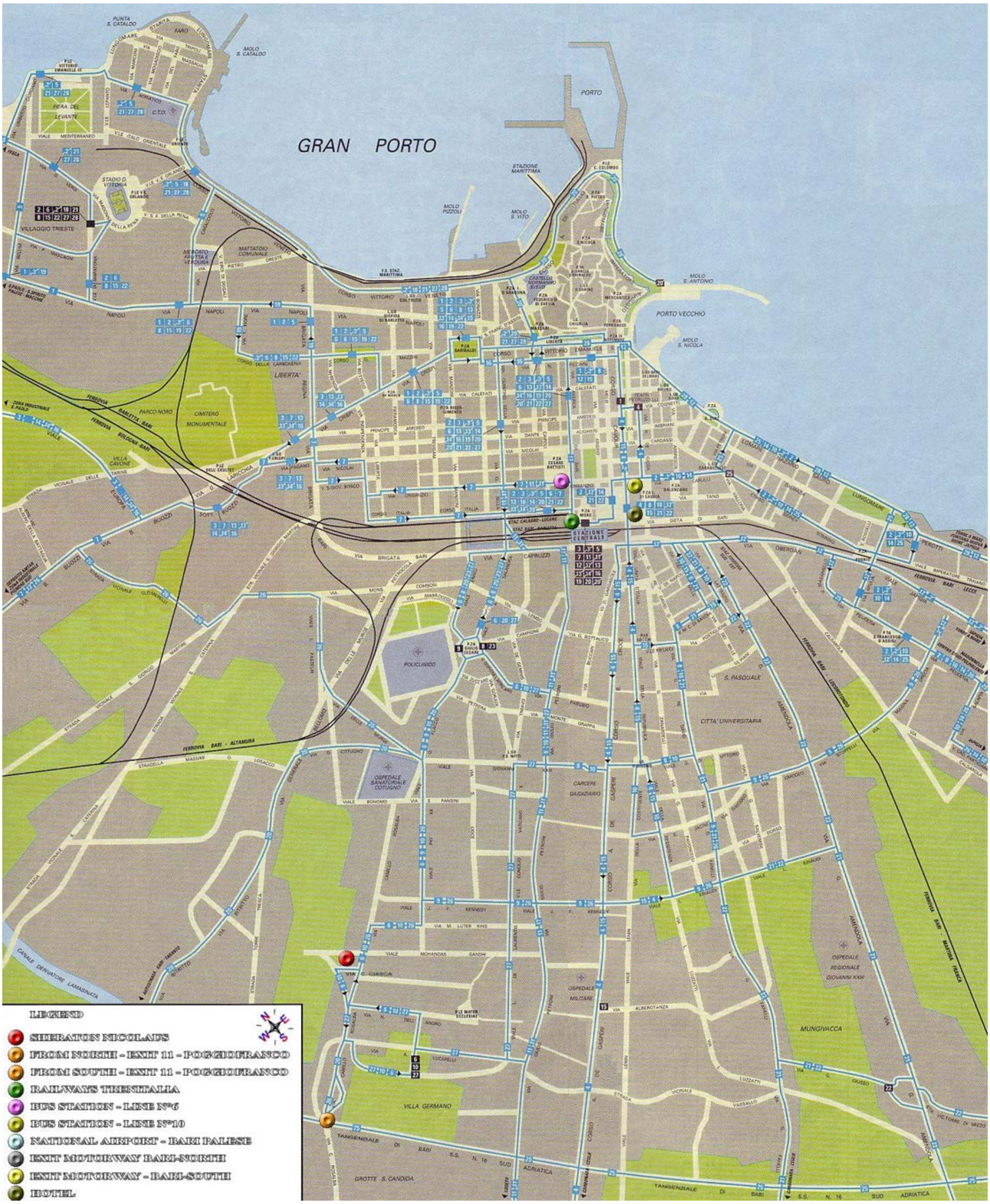

Figure 6: City map of Bari with bus connections.

Schedule

September 18, 08:00 - 18:00			
08:00 - 08:45	**Registration**		
08:45 - 09:00	**Welcome and opening remarks. S. Cherubini**		
Keynote lecture - Chair: F. Gallaire			
09:00 - 09:45	D. Sipp	DAAA ONERA-Meudon France	Mean-flow linear stability: theory and application to the identification of coherent structures, data-assimilation and flow control in turbulent flows
Session: Mean Flows and Resolvent - Chair: F. Gallaire			
09:45 - 10:00	L. Siconolfi	LFMI/EPFL Switzerland	Mode selection criteria in globally stable jet: linear and nonlinear analysis
10:00 - 10:15	L. Tuckerman	PMMH/ESPCI France	Computing optimal forcing using Laplace preconditioning
10:15 - 10:30	F. Gallaire	LFMI/EPFL Switzerland	Predicting the helical vortex breakdown precessing frequency by global stability analysis
10:30 - 10:45	Y. Bengana	PMMH/ESPCI France	Linear stability of mean flows and frequency prediction
10:45 - 11:15: **Coffee break**			
Session: Subcritical transition - Chair: L. Tuckerman			
11:15 - 11:30	Y. Duguet	LIMSI-CNRS Paris-Saclay Univ.	Solitary turbulent stripes in channel flow
11:30 - 11:45	F. Reetz	ECPS/EPFL Switzerland	Invariant solutions of turbulent-laminar stripes in plane Couette flow
11:45 - 12:00	S. Azimi	ECPS/EPFL Switzerland	Modified snaking in plan Couette flow with wall-normal suction
12:00 - 12:15	O. Semeraro	DMMM Pol. di Bari	Exploring the lower branch in Couette flows: a sensitivity analysis
12:15 - 12:30	M. Farano	DMMM Pol. di Bari	Connecting exact coherent states in plane Couette flow
12:30 - 12:45	S. Cherubini	DMMM Pol. di Bari	Optimal oblique transition
12:45 - 13:00	J.E. Wesfreid	PMMH/ESPCI France	Dynamics and large scale flows around turbulent spots
13:00 - 14:30: **Lunch**			
Session: Modal instabilities (1) - Chair: J. E. Wesfreid			
14:30 - 14:45	A. M. Bucci	DynFluid-ENSAM France	Roughness-induced transition by quasi-resonance of a varicose global mode
14:45 - 15:00	D. Puckert	IAG Stuttgart Univ.	Experimental investigation on global instability of a roughness-disturbed laminar boundary-layer
15:00 - 15:15	Y. Wu	IAG Stuttgart Univ.	Linear stability analysis of rotating-cylindrical roughness flow
15:15 - 15:30	A. Randriamampianina	Aix-Marseille Univ. France	Transition to Geostrophic turbulence within a baroclinic cavity
15:30 - 15:45	L. Pastur	LIMSI/CNRS Paris Saclay Univ.	3-D pattern organization in an open cavity flow at the onset of centrifugal instability
15:45 - 16:00	J.-C. Loiseau	DynFluid/ENSAM France	Experimental and numerical investigation of the transition scenario in a 3-D shear-driven cavity flow
16:00 - 16:30: **Coffee break**			

Session Wake instabilities - Chair: T. Colonius			
16:30 - 16:45	J. Leontini	Swinburne Univ. of Tech. Australia	3-D transition in the the wake of an elliptic cylinder
16:45 - 17:00	F. Giannetti	DIIN Università di Salerno	Effects of base-flow variations on the secondary instability in the wake of the circular cylinder
17:00 - 17:15	D. Jallas	DAAA-ONERA France	linear and non-linear perturbation analysis of the symmetry-breaking in time-periodic propulsive wake
17:15 - 17:30	O. Cadot	IMSIA-ENSTA France	Disturbed feedback flow of the static turbulent symmetry breaking mode of the Ahmed body
17:30 - 17:45	M. Lorite-Díez	Univ. de Jaén Spain	wake control of D-shaped bodies through optimized rear cavity
17:45 - 18:00	L. Magri	Univ. of Cambridge	Symmetry breaking in 3-D bluff-body wakes
19:00 - 20:00: **Welcoming cocktail**			

September 19, 08:45 - 16:30			
Keynote lecture - Chair: P. de Palma			
08:45 - 09:30	B. Barkley	Mathematics Institute University of Warwick UK	Something old, something new in transition and instability
Session: Transitional and turbulent flows - Chair: P. de Palma			
09:30 - 09:45	Y. Hwang	Dep. of Aeronautics Imperial College	Energy production and self-sustained turbulence at the Kolmogorov microscale
09:45 - 10:00	M. Chantry	PMMH/ESPCI France	Universal continuous transition to turbulence in a planar channel flow
10:00 - 10:15	T. Schneider	ECPS-EPFL Switzerland	From Turbulence transition to shell buckling - what load can a cylinder shell carry?
10:15 - 10:30	G. Chini	Univ. of New Hampshire Durham USA	A self-sustaining process theory for coupled uniform momentum zones and vortical fissures in the inertial region of turbulent wall flows
10:30 - 10:45	G. Gallino	LFMI-EPFL Switzerland	Edge states control droplet break-up in uniaxial extensional flows
10:45 - 11:15: **Coffee break**			
Session: Modal and non-modal Instabilities - Chair: S. Cherubini			
11:15 - 11:30	A. Cadiou	LMFA Univ. de Lyon France	Linear and nonlinear space-time dynamics of optimal wavepackets for streaks in a channel entrance flow
11:30 - 11:45	E. Heifetz	Dep. of Geosciences Tel-Aviv Univ. Israel	On the role of vortex stretching in energy optimal growth of 3-D perturbations on plane parallel shear flows
11:45 - 12:00	N. Navrose	DAAA-ONERA Meudon, France	Non-linear optimal perturbation in single and double vortex systems
12:00 - 12:15	G. Rigas	Caltech Pasadena, USA	one-way Navier-Stokes equations: optimal disturbances
12:15 - 12:30	B. Lebon	LOMC Univ. du Havre	Experiments with disturbances on the flow through a sudden-expansion in a circular pipe
12:30 - 12:45	F. Picella	DynFluid-ENSAM France	Passive transition control in superhydrophobic channel flow
12:45 - 13:00	M. Safdari-Shadloo	CORIA-CNRS France	Transition to turbulence in sudden-expansion pipe flow
13:00 - 14:30: **Lunch**			
Session: Rotating Flows and Centrifugal instabilities - Chair: L. Pastur			
14:30 - 14:45	H. Herrero	Dep. Matemáticas Univ. de Castilla-La Mancha	Route to chaos from axisymmetric thermal vertical vortices in a rotating cylinder
14:45 - 15:00	J. O. Rodríguez	Universidad de Navarra Spain	Experimental study of a rotating split-cylinder flow. First results
15:00 - 15:15	S. Viaro	Univ. of Sheffield Sheffield UK	Linear evolution of compressible Görtler instability triggered by free-stream vortical disturbances
15:15 - 15:30	M. Mendez-González	CORIA-CNRS France	Boundary-layer transition over concave surfaces caused by centrifugal forces
15:30 - 16:00: **Coffee break**			
17:30: **Departure for dinner**			
20:00 - 24:00: **Conference Dinner at Polignano a Mare**			

September 20, 08:45 - 14:45			
Keynote lecture - Chair: D. Sipp			
08:45 - 09:30	M. Juniper	Engineering Department University of Cambridge UK	Nonlinear thermoacoustics: flames on the edge of chaos
Session: Control and Reduced Models - Chair: D. Sipp			
09:30 - 09:45	C. Leclercq	DAAA-ONERA Meudon-France	Closed-loop flow control using a linearized approach around the mean flow
09:45 - 10:00	C. Mimeau	M2N-CNAM Paris, France	Effect of porous coatings on flows around 3-D hemisphere: application to flow control
10:00 - 10:15	S. Le Clainche	Univ. Politécnica de Madrid Madrid, Spain	A method to study flow structures
10:15 - 10:30	A. Towne	CTR Stanford Univ. CA, USA	Spectral POD and its connection with DMD and resolvent analysis
10:30 - 10:45	O. Schmidt	Caltech Pasadena, USA	Low-rank behavior of turbulent jets
10:45 - 11:00	K. Y. Volokh	Technion, I.I.T. Israel	Delay of the pipe flow instability via polymer solute
11:00 - 11:30: **Coffee break**			
Session: Modal instabilities (2) - Chair: J.-C. Loiseau			
11:30 - 11:45	Y. Guevel	Univ. Bretagne Sud Lorient, France	Numerical bifurcation analysis of 3-D steady flows in a sudden-expansion
11:45 - 12:00	A. Sansica	DynFluid-ENSAM Paris, France	3-D instability of flow around the sphere
12:00 - 12:15	J. Canton	Linné Flow Center KTH, Stockholm, Sweden	Subcritical and supercritical transition in curved pipes
12:15 - 12:30	T. Colonius	Caltech Pasadena USA	One-way Navier-Stokes equations: Global stability analysis via efficient spatial marching
12:30 - 12:45	R. Longobardi	IMFT Toulouse, France	Instability of the flow across a circular aperture in a thick plate
12:45 - 13:00	C. G. Hernandez	Dep. of Mathematics Imperial College, UK	Receptivity of a compressible boundary-layer to interactions between impinging acoustic waves
13:00 - 13:15	**Closing remarks. J.-C. Robinet**		
13:15 - 14:45: **Lunch**			

Book of Abstract

Mean-flow linear stability: theory and applications to the identification of coherent structures, data-assimilation and flow control in turbulent flows

Denis Sipp[1], Samir Beneddine[1], Robin Yegavian[1], Colin Leclerq[1], Benjamin Leclaire[1]
[1]ONERA/DAAA, Meudon, France

In this talk, we will present the basics of mean-flow linear stability analysis in turbulent flows. We will highlight in particular the importance of the resolvent operator and of its optimal singular modes and stress their relationship with the two-point correlation function $R(x, x', \tau)$ which is classically introduced in turbulence. We will then illustrate applications of these concepts for:

- the identification of coherent structures in a turbulent backward facing step flow [2];
- the reconstruction of unsteady data in a transitional jet flow from the sole knowledge of the mean-flow and unsteady data at one point [1]
- open-loop flow control of the vortex-shedding frequency in a D-shaped bluff-body [3]
- closed-loop control in an open-cavity flow at Re=7500.

Finally, we will hightlight current limitations of this approach.

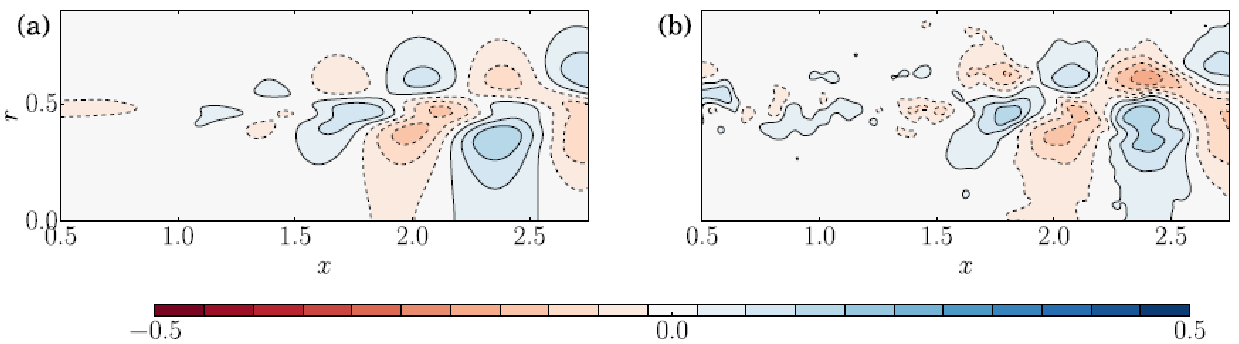

Figure 1. Comparison of the jet axial velocity fluctuation between (a): the reconstructed field and (b): the PIV field at some specific time. [1]

References

[1] S. Beneddine, R. Yegavian, D. Sipp and B. Leclaire. Unsteady flow dynamics reconstruction from mean-fow and point sensors: an experimental study. *Journal of Fluid Mechanics*, in press, 2017.

[2] *S. Beneddine, D. Sipp, A. Arnault, J. Dandois and L. Lesshafft. Conditions for validity of mean flow stability analysis. J. Fluid Mech.,* ***798****: 485-504, 2016.*

[3] *C. Mettot, D. Sipp and H. Bézard. Quasi-laminar stability and sensitivity analyses for turbulent flows: Prediction of low-frequency unsteadiness and passive control. Phys. Fluids,* **26**: 045112, 2014.

MODE SELECTION CRITERIA IN A GLOBALLY STABLE JET: LINEAR AND NONLINEAR ANALYSIS

Lorenzo Siconolfi, Francesco Viola & François Gallaire
Laboratory of Fluid Mechanics and Instabilities, École Polytechnique Fédérale de Lausanne, Lausanne, CH-1015, Switzerland

When jet flows are considered, large-scale orderly perturbations occur both in laminar and turbulent regimes. In the case of an isothermal jet, these perturbations have been experimentally studied in the seminal work documented in [1]. In particular, it was shown that increasing the Reynolds number from 10^2 to 10^3 (based on the diameter of the jet D and the centreline velocity at the exit jet plane U_0) led to the sequential observation of sinusoidal, helical and axisymmetric periodic structures, with a dominant Strouhal number of about 0.3. Moreover, when a controlled harmonic forcing is applied, the maximum disturbance amplification was obtained for a larger Strouhal number, typically in between 0.3 and 0.45, depending on the intensity of the external forcing.

In a locally parallel assumption, the results of a linear stability analysis [2, 3] show that the axisymmetric ($m = 0$) and helical ($m = 1$) modes are the most spatially unstable. In particular, axisymmetric perturbations are more amplified in the potential core region close to the exit jet plane. Further downstream, where the shear layers thicken, helical modes are promoted [4]. In a fully non-parallel framework, modal and non-modal analyses show that the flow is globally stable and thus the periodic structures are the result of a strong amplification experienced by external disturbances [5]. Moreover, considering mainly axisymmetric forcing and perturbations, the largest amplification of external forcing has been found for a Strouhal number around 0.45.

In this perspective, we study here the amplification of spiralling modes developing on a submerged incompressible jet. The mode competition between axisymmetric and single helical structures is investigated numerically by means of linear and nonlinear approaches. In the framework of global resolvent analysis, the linear optimal perturbations to a harmonic inlet forcing at different frequencies and azimuthal modes are computed (figure 1a). Consequently, the nonlinear responses to the same inlet forcing are calculated through three-dimensional Direct Numerical Simulations using the open-source spectral code Nek5000 [6] (figure 1b). The energy gain of the global response and the structure of the corresponding dominant mode are studied by varying the amplitude of the forcing, thus spanning from a linear to a fully nonlinear flow response. Hence, the effect of nonlinearity on the mode selection mechanism is finally discussed.

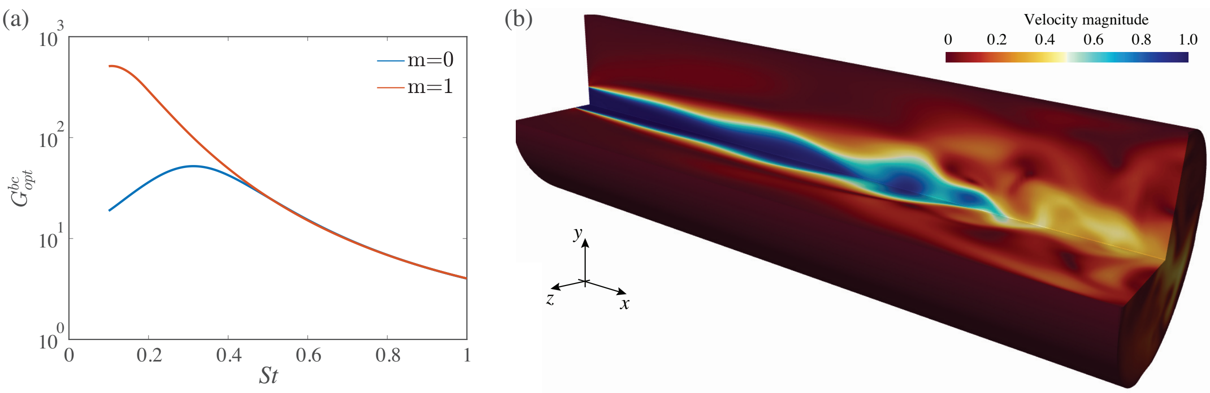

Figure 1. (a) Linear optimal amplification of harmonic forcing at the inlet for azimuthal numbers m=0,1; (b) Example of the nonlinear velocity response for an incompressible round jet at $Re = 400$ and Strouhal number $St = \omega D/2\pi U_0 = 0.4$.

References

[1] S. C. Crow and F. H. Champagne. Orderly structure in jet turbulence. *Journal of Fluid Mechanics*, 48(3):547–591, 1971.
[2] G. K. Batchelor and A. E. Gill. Analysis of the stability of axisymmetric jets. *Journal of Fluid Mechanics*, 14(4):529âĂŞ551, 1962.
[3] A. Michalke. Survey on jet instability theory. *Progress in Aerospace Sciences*, 21:159–199, 1984.
[4] J. I Jimenez-Gonzalez, P. Brancher, and C. Martinez-Bazan. Modal and non-modal evolution of perturbations for parallel round jets. *Physics of Fluids*, 27(4):044105, 2015.
[5] X. Garnaud, L. Lesshafft, P. J. Schmid, and P. Huerre. The preferred mode of incompressible jets: linear frequency response analysis. *Journal of Fluid Mechanics*, 716:189–202, 2013.
[6] P. Fischer, J. W. Lottes, and S. G. Kerkemeier. nek5000 Web page, 2008. http://nek5000.mcs.anl.gov.

COMPUTING OPTIMAL FORCING USING LAPLACE PRECONDITIONING

M. Brynjell-Rahkola[1], L.S. Tuckerman[2], P. Schlatter[1] and D. S. Henningson[1]
[1] *Linné FLOW Centre, SeRC, KTH Mechanics, Royal Institute of Technology, SE-100 44 Stockholm, Sweden*
[2] *PMMH (UMR 7636 CNRS - ESPCI - UPMC Paris 6 - UPD Paris 7), 10 rue Vauquelin, 75005 Paris, France*

Along with time integration, steady-state solving and linear stability analysis, the calculation of transient growth and of optimal forcing have become part of the toolbox of hydrodynamic stability theory. When a system is linearly stable, it may nevertheless undergo amplification due to a harmonic driving force, a situation described by

$$\frac{\partial q}{\partial t} = \mathcal{A}q + fe^{i\omega t}. \tag{1}$$

If all of the eigenvalues of $\mathcal{A}$ have negative real part, then asymptotically as $t \to \infty$, the solution q tends to

$$q(x,t) = e^{\mathcal{A}t}c(x) - (\mathcal{A} - i\omega\mathcal{I})^{-1}f(x)e^{i\omega t} \to -(\mathcal{A} - i\omega\mathcal{I})^{-1}f(x)e^{i\omega t}. \tag{2}$$

We seek the optimal forcing of the system, i.e. the frequency ω and forcing profile f that maximize the amplification

$$G(\omega) \equiv \max_{\|f\|\neq 0} \frac{\|(\mathcal{A} - i\omega\mathcal{I})^{-1}f\|}{\|f\|} = \text{ maximum eigenvalue of } \left[(\mathcal{A} - i\omega\mathcal{I})(\mathcal{A}^\dagger + i\omega\mathcal{I})\right]^{-1}. \tag{3}$$

The usual method [1] for calculating optimal forcing for large problems in two or three spatial dimensions is by repeated time integration of (1) and its adjoint. This is necessarily very time consuming because time-integration algorithms require a small timestep in order to be valid. We instead use (3) directly by calculating the largest eigenvalue of the operator $\left[(\mathcal{A} - i\omega\mathcal{I})(\mathcal{A}^\dagger + i\omega\mathcal{I})\right]^{-1}$. Because the operator is assumed to be too large to diagonalize directly, we use the power method. To perform inversions, we carry out conjugate gradient iteration, using preconditioned versions of $(\mathcal{A} - i\omega\mathcal{I})$ and its adjoint that arise naturally from their time-stepping codes when Δt is taken to be large [2, 3]. We validate the new method on the 2D lid-driven cavity. For $Re = 100$ the new method is faster than the time-integration algorithm by factors of 3 and 10, respectively, for the frequencies $\omega = 3$ and $\omega = 0$. The optimal gain, forcing and response for $Re = 8015$ are shown in figure 1. Details are given in [4].

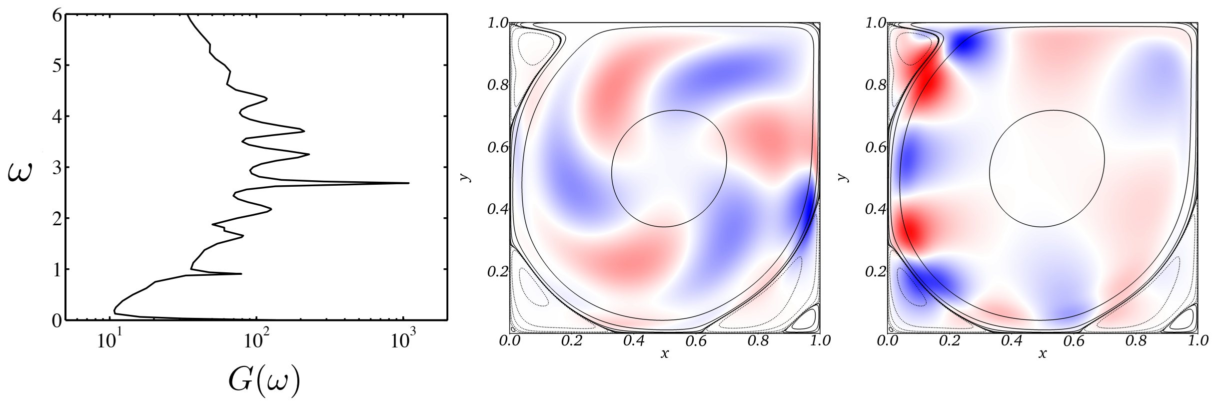

Figure 1. Optimal forcing for the 2D lid-driven cavity at $Re = 8015$. Left: amplification $G(\omega)$ has a maximum at $\omega = 2.6875$. Middle and right: real part of the optimal forcing profile $f(x)$ and response $(\mathcal{A} - i\omega\mathcal{I})^{-1}f(x)$ for these parameters. The imaginary parts of both profiles resemble rotated versions of the real parts.

References

[1] A. Monokrousos, E. Åkervik, L. Brandt, D.S. Henningson, Global three-dimensional optimal disturbances in the Blasius boundary-layer flow using time-steppers. *J. Fluid Mech.* **650**: 181-214, 2010.

[2] H.A. Dijkstra, F.W. Wubs, A.K. Cliffe, E. Doedel, I.F. Dragomirescu, B. Eckhardt, A.Y. Gelfgat, A.L. Hazel, V. Lucarini, A.G. Salinger, E.T. Phipps, J. Sanchez-Umbria, H. Schuttelaars, L.S. Tuckerman, U. Thiele, Numerical Bifurcation Methods and their Application to Fluid Dynamics: Analysis beyond Simulation. *Commun. Comput. Phys.* **15**: 1-45, 2014.

[3] L.S. Tuckerman, Laplacian Preconditioning for the Inverse Arnoldi Method. *Commun. Comput. Phys.* **18**: 1336-1351, 2015.

[4] M. Brynjell-Rahkola, L.S. Tuckerman, P. Schlatter, D.S. Henningson, A method for computing optimal forcing of globally stable flows using Laplace preconditioning. *Commun. Comput. Phys.*, in press.

PREDICTING THE HELICAL VORTEX BREAKDOWN PRECESSING FREQUENCY BY GLOBAL STABILITY ANALYSIS

François Gallaire, Simon Pasche & François Avellan
Laboratory of Fluid Mechanics and Instabilities, EPFL, Lausanne, Switzerland

Vortex breakdown is a characteristic phenomenon affecting swirling jet and wake flows. It is associated to a sudden change of the flow topology when the swirl number S, defined as the ratio between the characteristic tangential velocity and the centerline axial velocity, reaches a critical value. While the flow remains columnar below this treshold, it suddenly changes topology into several possible vortex breakdown states, like the bubble vortex breakdown characterized by an axisymmetric recirculation region or the helical vortex breakdown, which sheds a single or double spiral, which coils in space and rotates in time.

The observation that helical instabilities could become absolutely unstable in swirling wakes has led to the interpretation of spiral vortex breakdown as a secondary instability of axisymmetric vortex breakdown [1], using the flow geometry of [2]. This was confirmed by [3] and [4], who both performed a global linear stability analysis about the axisymmetric base flow, and successfully described the Hopf bifurcation and the development of the spiral vortex breakdown coiling around the axisymmetric breakdown for Reynolds number and swirl number close to $Re = 200$ and $S = 1$. Such global stability analysis about the axisymmetric base flow is relevant at the onset of the instability but one may question its validity further away from threshold. This fundamental issue for the application of global stability analysis to real flows was revived by [5], who showed that the frequency of the Bénard-von-Karman vortex street in the cylinder wake was correctly captured by a global linear stability analysis around the mean flow while the prediction from the linearization around the base flow quickly failed when the Reynolds number was increased.

In this study, we first discus the validity of the base flow and mean flow stability analysis in predicting the frequency of the self-sustained single spiral vortex breakdown mode appearing for sufficient swirl and Reynolds numbers in the flow geometry of [2]. Fixing the swirl number to $S = 1.095$, we observe that both coincide away from the critical Reynolds number at the bifurcation threshold $Re = 143$ until $Re \sim 200$. For larger Reynolds number, the mean flow eigenvalue analysis provides an excellent prediction of the dominant frequency pertaining in the nonlinear simulations, in stark contrast to the base flow stability analysis, as the consequence of an important mean flow modification. We observe for instance that, while the base flow has two recirculation bubbles at $Re = 300$, the mean flow has only a single small bubble.

In a second step, we observe the onset of chaos for $Re \sim 220$ through a Ruelle-Takens route. The flow becomes first quasi-periodic with two different non commensurable frequencies, until they become sufficiently close for nonlinearities to destructure the T_2 torus. The chaotic nature of the flow is confirmed by phase-map cross-sections as well as sensitivity to initial conditions.

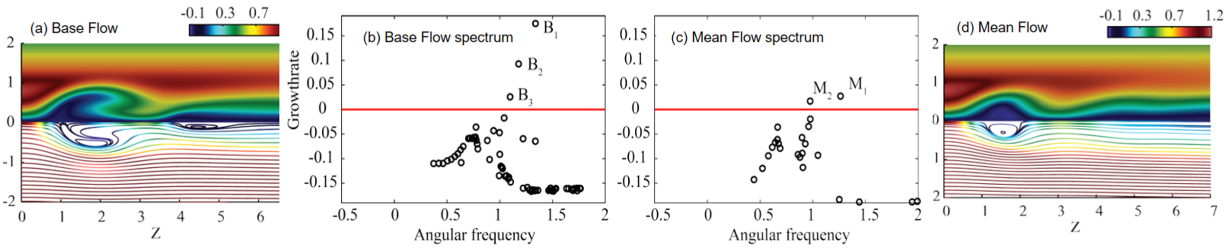

Figure 1. Base flow (a) and its spectrum (b) for the helical mode $m = 1$ at Re=300. Mean flow (d) and its spectrum (d) for the same parameters. In (a) and (d), the upper part shows the tangential velocity component and the lower part the streamsurfaces colored by the magnitude of the axial velocity component.

References

[1] F. Gallaire, M. Ruith, E. Meiburg, J.-M. Chomaz and P. Huerre. Spiral vortex breakdown as a global mode. *J. Fluid Mech.* **549**: 71–80, 2006.
[2] M. R. Ruith, P. Chen, E. Meiburg and T. Maxworthy. Three-dimensional vortex breakdown in swirling jets and wakes: direct numerical simulation. *J. Fluid Mech.* **486**: 331–378, 2003.
[3] P. Meliga, F. Gallaire and J.-M. Chomaz, A weakly nonlinear mechanism for mode selection in swirling jets. *J. Fluid Mech.* **699**: 216–262, 2012.
[4] U. A. Qadri, D. Mistry and M. P. Juniper. Structural sensitivity of spiral vortex breakdown. *J. Fluid Mech.* **720**: 558–581, 2013.
[5] D. Barkley. Linear analysis of the cylinder wake mean flow. *Europhys. Lett.* **75**: 750, 2006.

LINEAR STABILITY OF MEAN FLOWS AND FREQUENCY PREDICTION

Yacine Bengana[1] & Laurette Tuckerman[1]
[1] Laboratoire de Physique et Mécanique des Milieux Hétérogènes (PMMH), CNRS, ESPCI Paris, PSL Research University, 10 rue Vauquelin, Paris, France; Sorbonne Université, Univ. Paris Diderot.

The frequency of the von Kármán vortex street can be predicted by linear stability analysis around its mean flow. Barkley [1] has shown this to yield an eigenvalue whose real part is zero and whose imaginary part matches the nonlinear frequency This property was named RZIF by Turton et al. [2]; moreover they found that the traveling waves (TW) of thermosolutal convection have the RZIF property as shown in Figure (1). They explained this as a consequence of the fact that the temporal Fourier spectrum consists primarily of the mean flow and first harmonic. From this same idea Mantič-Lugo et al. [3] developed the Self-Consistent Model (SCM)

$$0 = \mathcal{L}\bar{U} + \mathcal{N}(\bar{U},\bar{U}) + \mathcal{N}(u_1,u_1^*) \tag{1a}$$

$$(\sigma + i\omega)u_1 = \mathcal{L}_{\bar{U}}u_1 \tag{1b}$$

$$\|u_1\| = A, \qquad \sigma = 0 \tag{1c}$$

for the base flow $\bar{U}$, the complex eigenvector u_1 and eigenvalue $\sigma + i\omega$, and its amplitude A. Mantič-Lugo et al. [3] solved these equations iteratively for the cylinder wake for each value of A by determining $\bar{U}$ via Newton's method from (1a), then determining u_1 and $\sigma + i\omega$ via diagonalization of (1b), and finally choosing the value of A such that $\sigma = 0$. We have carried out the same calculation for the traveling waves of thermosolutal convection, but we were able to obtain convergence of this procedure only up to $r = 2.25$. We then implemented a full Newton's method to solve the coupled problem (1) up to at least $r = 3$. Figure 1 shows that while the RZIF property is satisfied up to at least $r = 3$, the SCM model reproduces the exact frequency only for $r < 2.1$ and deviates entirely from it for $r > 2.5$. Thus, the nonlinear interaction of u_1 with itself yields a mean flow which is insufficiently accurate. Our next step will be to take into account higher harmonics and to apply this analysis to the standing waves, for which RZIF does not hold.

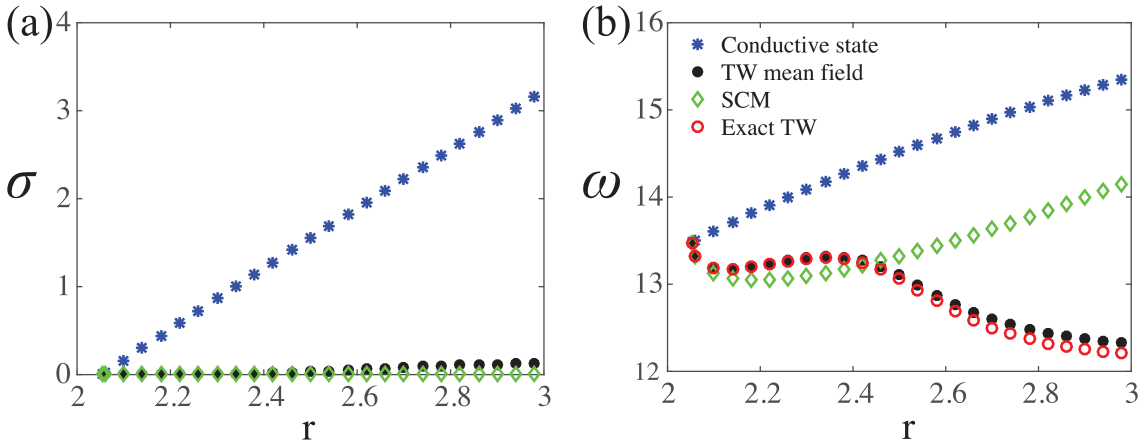

Figure 1. Growth rate (a) and frequency (b) as a function of Rayleigh number r for TW branch of thermosolutal convection. Linearization about the mean field yields eigenvalues (black filled circles) whose real part is close to zero and whose imaginary part is close to the exact nonlinear frequency (hollow red circles), i.e. the RZIF property is satisfied over the range shown. The Self-Consistent Model yields eigenvalues (green diamonds) whose real part is zero by construction, but whose imaginary part is close to the exact nonlinear frequency only for small r. The eigenvalues obtained by linearization about the conductive state are shown as blue stars.

References

[1] D. Barkley, Linear analysis of the cylinder wake mean flow. *Europhys. Lett.*, **75**: 750–756, 2006.
[2] S. E. Turton, L. S. Tuckerman, and D. Barkley, Prediction of frequencies in thermosolutal convection from mean flows. *Phys. Rev. E*, **91**: 043009, 2015.
[3] V. Mantič-Lugo, A. Cristóbal, and F. Gallaire, Self-consistent mean flow description of the nonlinear saturation of the vortex shedding in the cylinder wake. *Phys Rev Lett*, **113**: 084501, 2014.

SOLITARY TURBULENT STRIPES IN CHANNEL FLOW

Yohann Duguet[1], Chaitanya Paranjape [2] & Björn Hof [2]
[1]*LIMSI-CNRS, Université Paris-Saclay, Orsay France*
[2]*IST Austria, Klosterneuburg, Austria*

In subcritical fluid flows such as channels, pipes and boundary layers, the way turbulence manifests itself at the lowest possible flow rates has been a long-standing question. A new experimental disturbance technique applied to plane channel flow makes it possible to sustain turbulent flow at much lower values of the Reynolds number Re than previously thought. We demonstrate that these perturbations take the form of isolated stripes of turbulence oblique with respect to the flow. The angle of these stripes, however, is not determined by the Reynolds number Re only, but follows a statistical distribution [1]. In order to understand this multiplicity of angles, we use a deterministic approach in terms of unstable solutions of the Navier-Stokes equations in a slanted periodic domain, where the angle becomes one of the control parameters [2]. Edge states in the form of localised travelling waves, and their subsequent bifurcations, act as a scaffold for the turbulent dynamics down to very low values of Re consistent with the experimental thresholds. The non-uniqueness of these nonlinear waves in terms of angle provides a new theoretical framework for the rise in complexity observed experimentally as Re increases. The underlying angle selection process is fully nonlinear, and displays radical differences with the classical selection processes in linearly unstable pattern-forming systems [3].

Figure 1. Experimental realisation of growing turbulent stripes at Re=750 based on the centreline velocity, as time goes by (flow from left to right).

References

References

[1] Duguet, Y. and Schlatter, P.. Oblique laminar-turbulent interfaces in plane shear flows. *Phys. Rev. Lett.* **110**: 034502, 2013.
[2] Tuckerman, Laurette S., et al.. Turbulent-laminar patterns in plane Poiseuille flow. *Phys. Fluids* 26, **11**: 114103, 2014.
[3] Cross, M. C. and Hohenberg, P.. Pattern formation outside of equilibrium. *Rev. Mod. Physics* **65**: 851, 1993.

INVARIANT SOLUTIONS OF TURBULENT-LAMINAR STRIPES IN PLANE COUETTE FLOW

Florian Reetz[1], Tobias Kreilos [1] & Tobias M. Schneider [1]
[1]*ECPS, Ecole polytechnique fédérale de Lausanne , Lausanne, Switzerland*

A common feature of transitional turbulence in extended shear flows is the spatial coexistence of turbulent and laminar regions. For a range of transitional Reynolds numbers Re, the coexisting regions can spontaneously form a robust pattern of large scale order, known as turbulent-laminar stripes or bands [1]. The preferred orientation of these stripes is oblique, i.e. the pattern is tilted by angle θ relative to the direction of the base flow, and the selected wavelength λ is large compared to the local turbulent structures. The phenomenon of stripes is known for 50 years and has been observed in different shear flows but their emergence and dynamics remain not fully understood. Invariant solutions which represent the stripes could help to better understand the pattern.

We study turbulent-laminar stripes in plane Couette flow (PCF) numerically in a double-periodic domain. Following Barkley and Tuckerman [1], a base flow which is tilted by θ relative to the domain dimensions of suitable size allows to simulate a single period of the pattern. We look for invariant solutions in a domain with tilted base flow using the *Channelflow*-software [2] which is a pseudo-spectral code for direct numerical simulations (DNS) and for matrix-free Newton and continuation methods.

A fully nonlinear equilibrium solution is presented which closely resembles the oblique stripe pattern in PCF at Reynolds number $Re = 350$, angle $\theta = 24°$ and wavelength $\lambda = 40$ (Figure 1). The bifurcation sequence from the well studied invariant solution of wavy streaks (NBCW) [3] to the new stripe equilibrium highlights the role of the streak phase for the formation of the pattern.

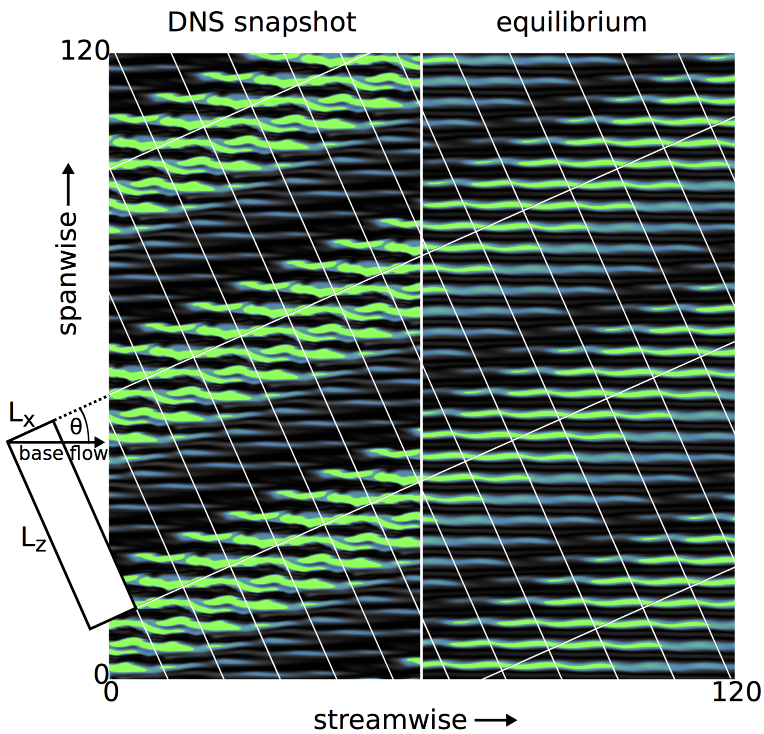

Figure 1. Turbulent-laminar stripes from DNS (left) compared to the new fully nonlinear equilibrium solution (right). Contours are kinetic energy and the total region in space is chosen to match Figure 1 of [1], as are the parameters $Re = 350$, $\theta = 24°$ and $\lambda = 40$. The tiling of replicated DNS domains (white grid) host a single stripe period with $L_z = \lambda$. The displayed cross-section is not midplane but at $y = 0.5$ to show the asymmetric fronts of the stripes.

References

[1] D Barkley and L S Tuckerman. Computational Study of Turbulent Laminar Patterns in Couette Flow. *Physical Review Letters*, **94**:14502–14505, 2005.

[2] J F Gibson, J Halcrow, and P Cvitanović. Visualizing the geometry of state space in plane Couette flow. *Journal of Fluid Mechanics*, **611**:107–130, 2008.

[3] F Waleffe. Three-dimensional coherent states in plane shear flows. *Physical Review Letters*, **81**:4140–4143, 1998.

MODIFIED SNAKING IN PLANE COUETTE FLOW WITH WALL-NORMAL SUCTION

Sajjad Azimi[1] and Tobias M. Schneider[1]
[1]*ECPS, Ecole polytechnique fèdèrale de Lausanne, Lausanne, Switzerland*

Homoclinic snaking is a process by which a localized invariant solution grows additional structures at its fronts while undergoing a sequence of saddle-node bifurcations [1]. In shear flows, the first set of snaking solutions is found in plane Couette flow. They consist of two travelling wave branches which live in a shift-reflect symmetry subspace and two equilibria which live in a central symmetry subspace [2]. These solutions are connected by multiple non-symmetric solutions, also called “rungs”, which connect the two symmetry subspaces. The travelling waves and the equlibria together with the non-symmetric solutions form a characteristic snakes-and-ladders bifurcation structure. The homoclinic snaking process is similarly observed in simpler pattern forming systems such as the 1D with 3-5 nonlinearity Swift-Honenberg equation [3]. A key feature of both systems is the symmetries of the snaking branches so that one snaking branch retains an odd symmetry and the other one retains an even symmetry and the two are connected by non-symmetric branches.

We look at the robustness of the snaking process under a smooth change of boundary conditions to a new system, which is applying suction into the bottom plate and increasing it smoothly. Finally, this leads to the asymptotic suction boundary layer flow which is an streamwise-invariant boundary layer flow. Applying suction on plane Couette flow breaks the up-down symmetry of the system and as a result the central symmetry. We show that the suction turns the snaking solutions of plane Couette flow into a modified snakes-and-ladders formed by two separate snaking branches of travelling waves which are connected by non-symmetric branches formed by what remains from the rungs and pieces of the equilibrium branches.

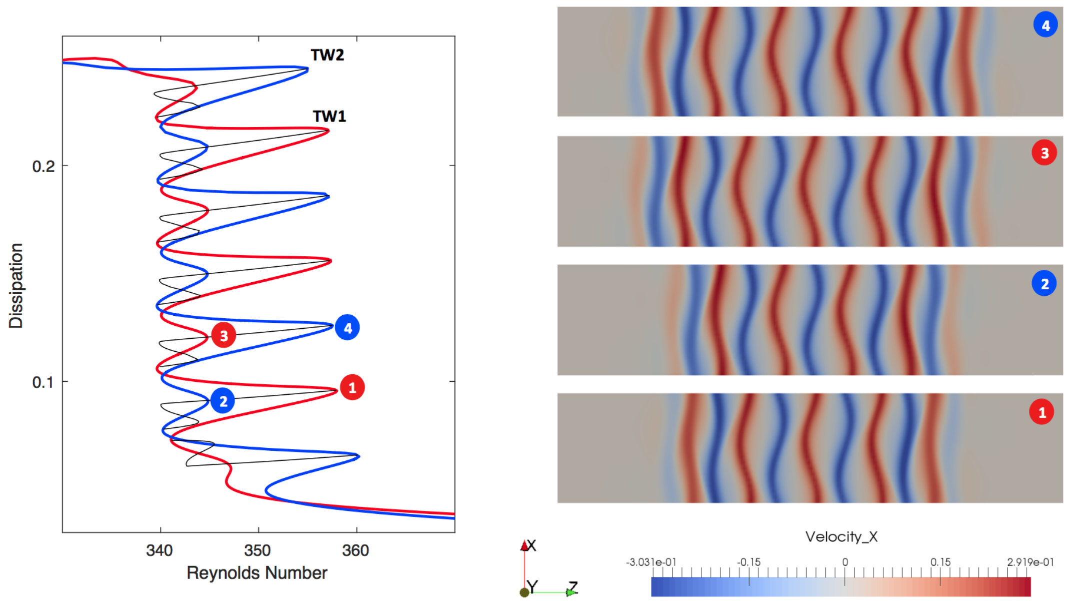

Figure 1. The traveling waves and the connecting states, in plane Couette flow with a suction of $V_s = 2e - 4$ wall speed units into the lower plate. The right panels show the velocity profiles on the midplane of the numerical cell at the points labeled in the left panel. The suction breaks the up-down symmetry and turns the snakes-and-ladders structure of the travelling waves and the equlibria into a modified snakes-and-ladders structure of travelling waves and connections between them.

References

[1] E. Knobloch. Spatial localization in dissipative systems. *conmatphys*, **6**(1): 325-359, 2015.
[2] T.M. Schneider, J.F. Gibson, and J. Burke. Snakes and ladders: localized solutions of plane Couette flow. *Physical review letters*, **104**(10): 104501, 2010.
[3] J. Burke and and E. Knobloch. Homoclinic snaking: structure and stability. *Chaos: An Interdisciplinary Journal of Nonlinear Science*, **17**(3): 037102, 2007.

EXPLORING THE LOWER BRANCH IN COUETTE FLOWS: A SENSITIVITY ANALYSIS

Onofrio Semeraro[1], Stefania Cherubini[1], Flavio Giannetti[2], Luca Brandt[3], Pietro De Palma[1]
[1]*Dipartimento di Meccanica, Matematica e Management (DMMM), Politecnico di Bari - 70126, Bari, Italy,*
[2]*Dipartimento di Ingegneria Industriale (DIIN), Universitá di Salerno - 84084, Fisciano (SA), Italy,*
[3]*Linné Flow Centre, KTH Mechanics - 10044, Stockholm, Sweden*

In recent years, canonical flows have been analysed from the dynamical system point of view to gain more insight into the transition to turbulence processes. Numerous examples can be found in literature, ranging from pipe flows to plane flows and boundary layers. Phase-space diagrams have been drawn identifying nontrivial solutions and classifying them along the bifurcation branches [3, 5].

In this contribution, we focus on Couette flows. We start from the periodic, lower-branch solution found by [4] in a minimal box with horizontal ratio $L_x/L_z = 1.458$. We explore the entire lower-branch, ranging from $Re \approx 236$, identified as the minimal Reynolds for which such a solution exists, to $Re = 400$. By applying the Floquet analysis [1], we calculate the Floquet multipliers and examine the most unstable modes and the related adjoint modes of the identified solutions. Through this analysis, the sensitivity of the unstable periodic orbits to structural perturbations is investigated, based on the framework by [2]. Finally, we consider the nonlinear sensitivity analysis with respect of limit-cycle frequency and the amplitude to feedback forcing, using the formulation introduced by [6] and further extended in [7].

The structural sensitivity analysis, based on the linear perturbations and computed over the orbit period, shows that the core of the instabilities coincides with the regions where the streaks are bent. Interestingly, preliminary results for the nonlinear sensitivity analysis reveal that the regions of the flow where the sensitivity is higher with respect of feedback forcings are localized where the velocity of the shear flow is higher. In practice, while the structural sensitivity is higher in the centre of channel at $y/H = 0$, the sensitivity to feedback forcings with respect of the limit cycle frequency and amplitude shows that the flow is more sensitive in vicinity of the walls. Based on these observations, the final goal of the investigation will be to provide indications on how to alter the self-sustaining mechanisms of the analysed flows.

References

[1] D. Barkley and R. D. Henderson *Three-dimensional Floquet stability analysis of the wake of a circular cylinder*. J. Fluid Mech. **322**, 215-241, 1996

[2] F. Giannetti et al. *Structural sensitivity of the secondary instability in the wake of a circular cylinder*. J. Fluid Mech. **651**, 319-337, 2010

[3] J. F. Gibson et al. *Visualizing the geometry of state space in place Couette flow*. J. Fluid Mech. **611**, 107-130, 2008

[4] G. Kawahara and S. Kida *Periodic motion embedded in plane Couette turbulence: regeneration cycle and burst*. J. Fluid Mech. **449**, 291-300, 2001

[5] T. Kreilos and B. Eckhardt *Periodic orbits near onset of chaos in plane Couette flow*. Chaos **22-4**, 047505, 2012

[6] P. Luchini et al. *Structural Sensitivity of Linear and Nonlinear Global Modes*. 5^{th} AIAA Theor. Fluid Conf. AIAA-2008-4227, 2008

[7] J. Pralits et al. *Sensitivity analysis of the finite-amplitude vortex shedding behind a cylinder*. In 8th ERCOFTAC SIG 33 Workshop - Global Instabilities of Open Flows, 2010.

CONNECTING EXACT COHERENT STATES IN PLANE COUETTE FLOW

M. Farano[1,2,3], P. De Palma[1] J.-C. Robinet[2], S. Cherubini[1,2] & T. M. Schneider[3]
[1]*DMMM, Politecnico di Bari, Via Re david 200, 70125 Bari, Italy*
[2]*Dynfluid Laboratory, Arts et Metiers ParisThech, 151 Boulevard de l'Hopital, 75013 Paris, France*
[3]*ECPS, École Polytechnique Fédérale de Lausanne, 1015 Lausanne, Switzerland*

The understanding of transitional and turbulent flows has been recently boosted by the discovery of exact invariant solutions of the Navier-Stokes equations, which can be equilibria, travelling waves, periodic orbits or chaotic solutions having a few unstable directions. With the improvement of the computational resources, it has been possible to compute an increasing number of these non-linear invariant solutions, which support the dynamics in the transitional and turbulent regimes [3]. Many investigations have shown how the flow spends a relevant amount of time wondering in the vicinity of one of these invariant solutions before escaping towards another [5]. The dynamics may shadow heteroclinic connections between different exact coherent states [4].

The aim of this work is to construct dynamically relevant heteroclinic connections. A new algorithm based on a non-linear adjoint optimization method [1] has been developed to detect several new heteroclinic connections between highly unstable equilibria. Our method computes trajectories which start in the neighbourhood of an initial equilibrium $\mathbf{u}_{ECS_{out}}$ ($E_0 = ||\mathbf{u}(0) - \mathbf{u}_{ECS_{out}}||_2^2 = 10^{-6}$ in this work) and end in the neighbourhood of a target equilibrium $\mathbf{u}_{ECS_{in}}$ in a finite interval of time T. Thus, the method aims at finding the time T and the initial state $\mathbf{u}(0)$ that minimize the distance $||\mathbf{u}(T) - \mathbf{u}_{ECS_{in}}||_2$. The algorithm, which has been implemented in the *channelflow* code [2], stops when this distance reaches a value lower than a chosen threshold.

In order to validate the method, we compute three of the existing heteroclinic connections in plane Couette flow at $Re = 400$ [4] and we found six previously unknown (see figure 1) using the available solutions on the database [2] (where nomenclature has been taken from).

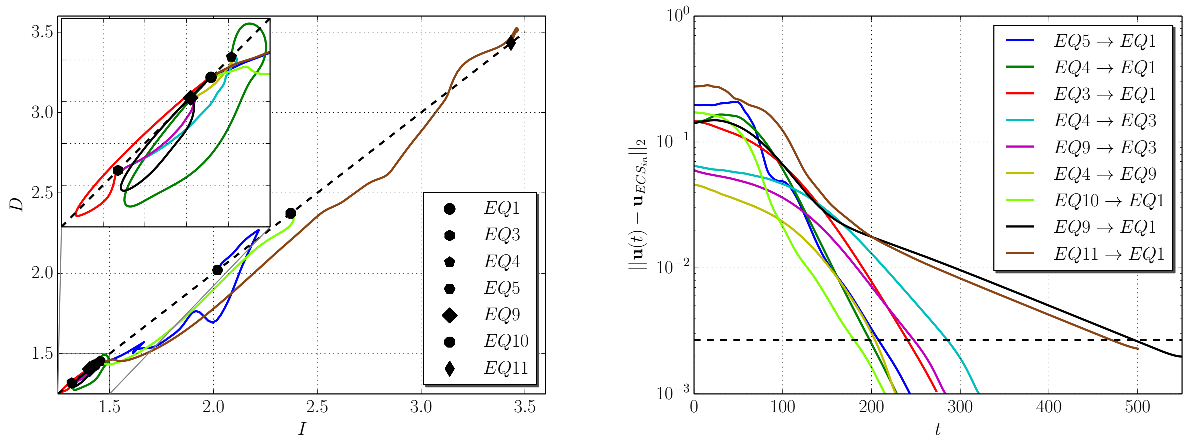

Figure 1. Left: Visualization of the nine heteroclinic connections by projecting the trajectory onto the energy input I and the dissipation rate D plane, normalized by their value in laminar flow. Right: Plots of distances of the velocity field $\mathbf{u}(t)$ to the target equilibrium $\mathbf{u}_{ECS_{in}}$ along the computed heteroclinic connections versus time. This plot represents the convergence of the computed heteroclinic connections. The dashed line indicate the highest residual value for the heteroclinic connections computed in [4].

References

[1] Stefania Cherubini, Pietro De Palma, J-Ch Robinet, and Alessandro Bottaro. Rapid path to transition via nonlinear localized optimal perturbations in a boundary-layer flow. *Physical Review E*, **82**(6):066302, 2010.

[2] J. F. Gibson. Channelflow: A spectral Navier-Stokes simulator in C++. Technical report, U. New Hampshire, 2014. `Channelflow.org`.

[3] John F Gibson, Jonathan Halcrow, and Predrag Cvitanović. Visualizing the geometry of state space in plane couette flow. *Journal of Fluid Mechanics*, **611**:107–130, 2008.

[4] Jonathan Halcrow, John F Gibson, Predrag Cvitanović, and Divakar Viswanath. Heteroclinic connections in plane couette flow. *Journal of Fluid Mechanics*, **621**:365–376, 2009.

[5] Genta Kawahara, Markus Uhlmann, and Lennaert Van Veen. The significance of simple invariant solutions in turbulent flows. *Annual Review of Fluid Mechanics*, **44**:203–225, 2012.

OPTIMAL OBLIQUE TRANSITION

Alessandro Bottaro[1], Jan Pralits [1] & Stefania Cherubini [2]
[1]*DICCA, Università di Genova, Via Montallegro 1, 16145 Genova, Italy*
[2]*DMMM, Politecnico di Bari, Bari, Italia*

Transition to turbulence in shear flows is a subcritical phenomenon, which relies on nonlinear mechanisms, possibly exploiting transient disturbance energy amplification. Recently, an approach to identify initial disturbances of finite amplitude capable to optimally initiate the transition process has been proposed, relying on nonlinear optimization algorithms (see [1, 2] for a review). However, since these methods rely on the optimisation of the full (three-dimensional) flow field, they are computationally too expensive to allow a complete exploration of the parameter space. For this reason, in this work we propose a weakly nonlinear optimisation, able to identify the couple of oblique waves capable of optimally triggering transition to turbulence in a plane shear flow. Towards this aim, we decompose the perturbation to the base flow in: i) a pair of oblique waves of wavevector $(\alpha, \pm\beta)$ and amplitude ϵ; ii) a mean flow correction $(0, 0)$ of amplitude ϵ^2; iii) a streamwise-independent streak/vortex of amplitude ϵ^2 and wavevector $(0, 2\beta)$, generated by first-generation non-linear interactions of the previous. The optimisation aims at seeking the initial optimal oblique wave pairs of given amplitude ϵ and wavenumbers $(\alpha, \pm\beta)$ inducing the maximum energy growth at a target time T, where the energy $e(t)$ takes into account the contribution of the oblique wave pairs, as well as of the mean flow correction and the streamwise streaks/vortices. The induced energy gain with respect to $(\alpha, \pm\beta)$ is provided in figure 1 for $\epsilon = 0.00450$ (left) and $\epsilon = 0.00518$ (right). An optimal oblique wave pair arises past a finite value of the amplitude, inducing energy peaks comparable to those typical of the well-known lift-up mechanism [3]. Moreover, these energy peaks are found to exist in a very narrow wavenumber range, demonstrating the strong selectivity of the identified mechanism. These oblique optimal perturbations are expected to lead to rapid breakdown past a well defined threshold value of the disturbance amplitude. Direct numerical simulations of the Navier-Stokes equations substantiate the weakly nonlinear results, providing thresholds for transition close to the predictions of the weakly non-linear model. Finally, an investigation of the transition scenario initiated by these optimal oblique perturbations is provided.

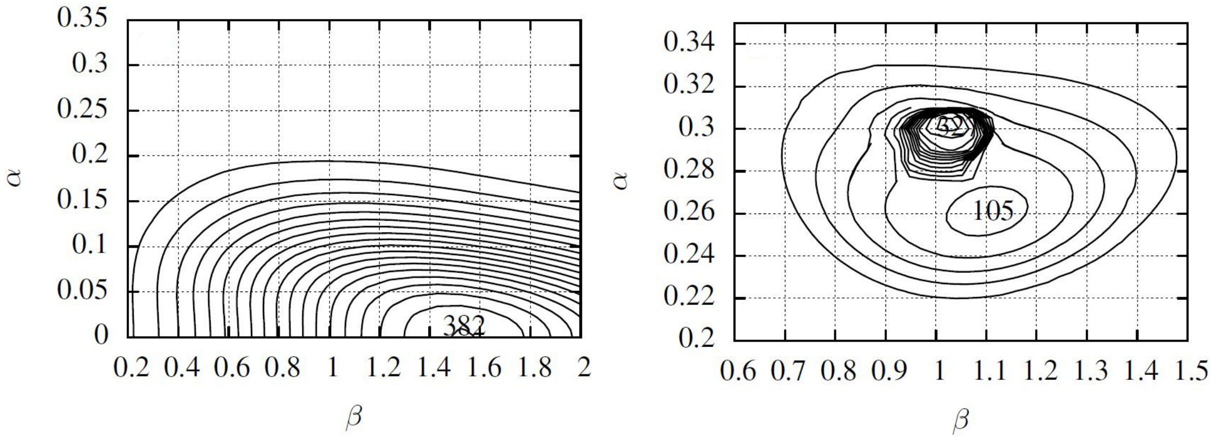

Figure 1. Iso-contours of the energy $2e_{11}(T)/e_{11}(0)$ in the $\alpha - \beta$ plane for the case of (left) $\epsilon = 0.00450$ with maximum value equal to 382 at (α, β)=(0.001,1.540) and (right) $\epsilon = 0.00518$ with maximum value equal to 327 at (α, β)=(0.303,1.020).

References

[1] P. Luchini and A. Bottaro Adjoint equations in stability analysis. *Annual Review of Fluid Mechanics*, **46**:493–517., 2014.
[2] R. R. Kerswell, C. C. T. Pringle and A. P. Willis An optimisation approach for analysing nonlinear stability with transition to turbulence in uids as an exemplar *Rep. Prog. Phys.*, **77** 085901, 2014.
[3] M. T. Landahl A note on an algebraic instability of inviscid parallel shear flows *Journal of Fluid Mechanics*, **99** 243–251, 1980.

DYNAMICS AND LARGE SCALE FLOWS AROUND TURBULENT SPOTS

Lukasz Klotz[1], Alexandr Pavlenko[2], José Eduardo Wesfreid[1]
[1] *PMMH-ESPCI (UMR CNRS 7636) 10, rue Vauquelin, 75005 Paris, France*
[2] *Institute of Theoretical and Applied Mechanics SB RAS, Institutskaya Str. 4/1, 630090 Novosibirsk, Russia*

We have recently setup an experiment to study localized turbulent spots, surrounded by laminar flow, in the subcritical transition to turbulence in confined shear flows.

It consists of a Couette-Poiseuille flow, i.e. of two parallel walls, one moving and the other fixed [1]. Since the turbulent spots move with a velocity close to the mean velocity, which is zero in this setup, they can be measured for long duration of time.

We study the evolution of spots, when a very controlled perturbation is introduced in the flow. We study dynamics of growth and decay, eventually, of these structures.of these structures.

We also study the interactions between these structures during process of sustained turbulence. In particular we measured the large-scale flow around isolated spots as well when they are organized in bands.

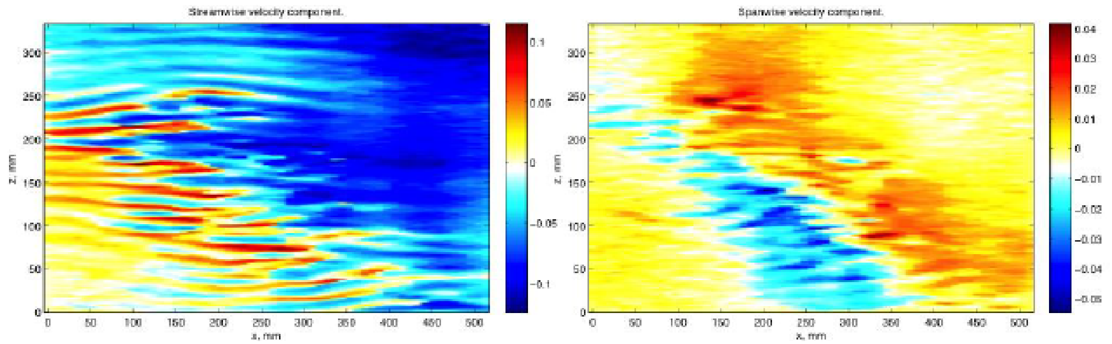

Figure 1. Left: turbulent band surrounded by laminar flow. Right: spanwise component of the large scale flow around the band

References

[1] L. Klotz, G. Lemoult, I. Frontczak, S. Tuckerman, J.E. Wesfreid, New experiment in Couette-Poiseuille flow with zero mean advection velocity: subcritical transition to turbulence. *Phys. Rev. Fluids*, 2.043904, 2017.

ROUGHNESS-INDUCED TRANSITION BY QUASI-RESONANCE OF A VARICOSE GLOBAL MODE

M. A. Bucci[1], D. K. Puckert [2], C. Andriano [1,3], J.-Ch. Loiseau [1], S. Cherubini [3], J.-Ch. Robinet [1] & U. Rist[2]
[1]*DynFluid, Arts et Métiers ParisTech, 151 Bd. de l'Hôpital, 75013, Paris, France*
[2]*Institut für Aerodynamik und Gasdynamik, Universität Stuttgart, Pfaffenwaldring 21, D-70569 Stuttgart, Germany*
[3] *DMMM, Politecnico di Bari, via Re David 200, 70100 Bari, Italy*

The effect of wall roughness elements on laminar-turbulent transition in boundary-layer flows has recently been the focus of many investigations. Despite their stabilizing effect on TS waves, in certain flow conditions they can induce bypass transition, a detrimental effect for control purposes. In an effort to provide thresholds for transition, von Doenhoff & Baslow [1] compiled a transition diagram correlating the roughness element's aspect ratio to the roughness Reynolds number, Re_h, beyond which the induced flow would transition to turbulence. With the aim of providing a more accurate estimate of the critical Reynolds number for transition, global stability analyses have been recently performed in the case of a cylindrical roughness elements [2].

In this work, the onset of unsteadiness in a boundary-layer flow past a cylindrical roughness element of unitary aspect ratio is investigated both experimentally and numerically at a subcritical Reynolds number. On the one hand, a shedding of spanwise-symmetric hairpin vortices characterized by a pulsation $\omega \simeq 1.05$ and a spatial wavelength $\lambda_x \simeq 5$ is observed experimentally. On the other hand, global stability analyses have revealed the existence of a varicose isolated mode, as well as of a sinuous one, both being linearly stable, whereas unsteadiness is observed during the experiments. Nonetheless, the isolated varicose mode, characterized by a pulsation $\omega = 1.02$ is highly sensitive, as ascertained by pseudospectrum analysis (see Fig. 1). To investigate how this mode might influence the flow dynamics, an optimal forcing analysis is performed [3]. The optimal response at $\omega = 1.02$ consists of a spanwise-symmetric perturbation with wavelength $\lambda_x = 4.7$ inducing dynamics similar to the ones observed experimentally. This indicates that the onset of unsteadiness at subcritical Reynolds number can be due to quasi-resonance of such a varicose global mode, explaining the experimental observations.

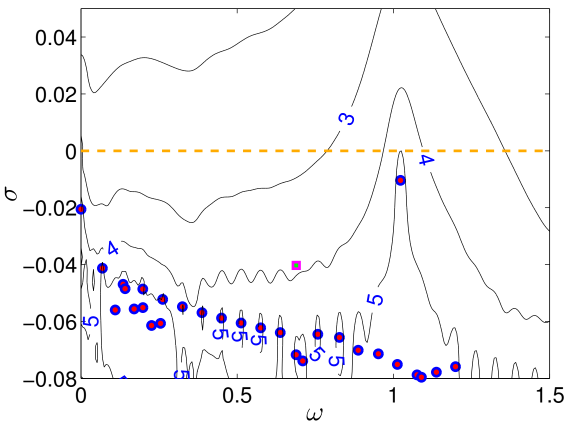

Figure 1. Eigenspectrum (colored symbols) and pseudospectrum (solid lines) of the linearised Navier-Stokes operator for $(\eta; Re)$ = (1; 700). Circles (squares) represent varicose (sinuous) modes. The iso-lines represent pseudospectrum given by $\log_{10}(\varepsilon^{-1})$ contours, with ε ranging from 10^{-6} to 10^{-3}.

References

[1] Gustav Victor Lachmann. *Boundary layer and flow control: its principles and application*. Elsevier, 2014.
[2] Jean-Christophe Loiseau, Jean-Christophe Robinet, Stefania Cherubini, and Emmanuel Leriche. Investigation of the roughness-induced transition: global stability analyses and direct numerical simulations. 2014.
[3] Antonios Monokrousos, Espen Åkervik, Luca Brandt, and Dan S Henningson. Global three-dimensional optimal disturbances in the blasius boundary-layer flow using time-steppers. *Journal of Fluid Mechanics*, **650**:181–214, 2010.

EXPERIMENTAL INVESTIGATION ON GLOBAL INSTABILITY OF A ROUGHNESS-DISTURBED LAMINAR BOUNDARY LAYER

Dominik K. Puckert, Ulrich Rist
Institut für Aerodynamik und Gasdynamik, Universität Stuttgart, Stuttgart, Germany

Roughness-induced boundary layer instabilities are investigated by means of hot-film anemometry in a water channel to provide experimental evidence of a global instability. It is shown that the roughness wake dynamics depends on extrinsic disturbances (amplifier) at subcritical Reynolds numbers whereas intrinsic, self-sustained oscillations (wavemaker) are suspected at supercritical Reynolds numbers. Further, the critical Reynolds number from recent theoretical results is successfully confirmed in this experiment, supporting the physical relevance of a global instability. The critical Reynolds number therefore separates between two fundamentally different instability mechanisms.

Figure 1 shows the distribution of root mean square (rms) of u'/U_e versus x and Re_k. The dashed line indicates the beginning of a region where the contours become more independent of Re_k and show stronger velocity fluctuations downstream of $x = 30$. The fluctuation upstream edge moves upstream with increasing Re_k until it reaches the dashed line and then remains constant at $x = 4$. These changes all occur at one distinct Reynolds number which we denote as the experimental critical Reynolds number $Re_{k,c,e}$. Most likely $Re_{k,c,e} = 556$ separates the system dynamics into convective amplification and intrinsic oscillation and is thus the value to be compared to the critical Reynolds number of 3-d global stability theory. Such computations have recently been done [1] and these authors predicted a critical Reynolds number of $Re_{k,c,t} = 564$ for exactly the same configuration. Despite the necessary but restricting assumptions of linear theory, there is very good agreement to the highly nonlinear observations in this experiment. Together with a successful frequency comparison [2] there is little doubt that the observed self-sustained oscillation originates from a linear global instability.

A similar comparison to an experiment has been done before, however, the theoretical critical Reynolds number has been compared to the transition Reynolds number, which can in the worst case be misleading. In our presentation we will discuss the problem that arises from such a comparison and provide a different experimental method.

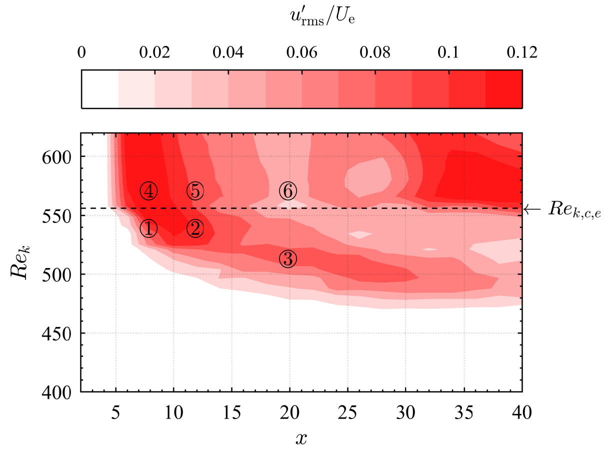

Figure 1. Dimensionless root mean square of streamwise velocity fluctuations as a function of x and Re_k.

References

[1] J. C. Loiseau, S. Cherubini, J. C. Robinet, and E. Leriche. Investigation of the roughness-induced transition: global stability analyses and direct numerical simulations. *J. Fluid Mech.*, 2014.

[2] D. K. Puckert and U. Rist. Transition downstream of an isolated cylindrical roughness element on a flat plate boundary layer. In *New results in numerical and experimental fluid mechanics XI*, **218** of *Notes on numerical fluid mechanics and multidisciplinary design*. Springer, 2017.

LINEAR STABILITY ANALYSIS OF ROTATING-CYLINDRICAL ROUGHNESS FLOW

Yongxiang Wu, Ulrich Rist
Institut für Aerodynamik und Gasdynamik, Universität Stuttgart, Stuttgart, Germany

Roughness flow is characterised by an upstream and downstream reverse flow region, and thereupon resulting vortices and shear systems. As found by recent study [1], the stability of flow with cylindrical roughness element is determined by the shear systems stemming from the roughness. In this study, the vortices and shear systems are modified by rotating the cylindrical roughness. Figure 1 shows vortices for comparison between static and rotating cylindrical roughness element. For the rotating case, the two inner vortex legs become twisted over each other at the near wake region, and further downstreams one of the inner vortices dominates. Like the modification of the base flow, the alteration of its instability property persists in the pronounced vortex as well.

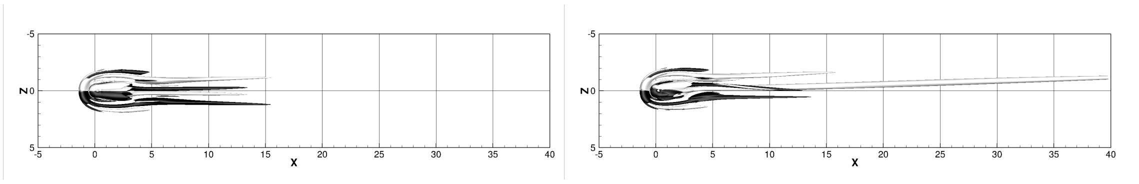

Figure 1: Vortices visualized by λ_2 criterion for $Re_h = 1000$. Left: static roughness, right: rotating cylindrical roughness element with $\omega = 38$. Shading indicates rotation sense.

Bi-global linear stability analysis is performed for a parametric study of rotating cylindrical roughness element. Figure 2 shows a comparison of leading modes between static and rotating cases for baseflow $Re_h = 1000$ with aspect ratio $\eta = 1$. For static cylindrical element, the leading mode is found to be asymmetric, while for rotating cases the mode symmetry/asymmetry sense becomes ambiguous and even lost. The amplified vortex leg futher promotes the lateral low spead streak and forms stronger vortex at higher rotation speed ($\omega = 67$). A strong inflectional velocity profile is obvious in the vortex region. As shown, the leading modes for rotating roughness are located around the promoted vortex leg. The relocation of the leading modes can be ascribed to the redistribution of the shear system caused by this promoted vortex. A pertubation kinetic energy analysis [2] reveals the physical stability mechanism. By rotating the roughness, the wall-normal production is amplified while the dissipation is inhibited. However, at a certain position (roughly $x/h = 60$) with rotation speed $\omega = 38$, the spanwise production is negative, indicating a stabilizing effect.

In this study, the influence of cylindrical roughness rotation is analyzed with a parametric study of Reynolds number Re, the aspect ratio of roughness η, and rotating speed ω. The stability mechanism is analyzed with bi-global linear stability theory. The results could provide a new flow control method.

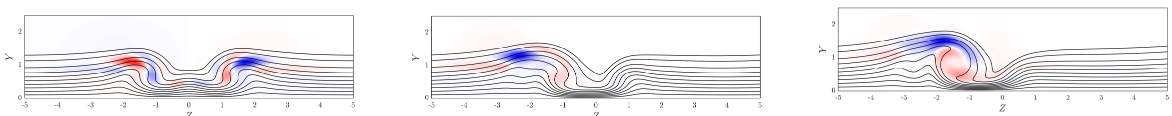

Figure 2: Leading modes of $Re_h = 1000$, $\eta = 1$ at $x/h = 40$ with wave number $\alpha = 1.5$. Left: static cylinder ($\omega = 0$), middle: rotating cylinder ($\omega = 38$), right: rotating cylinder ($\omega = 67$). Mode magnitude normalized with local maxima. Solid lines are base-flow isolines.

References

[1] Loiseau, J.-C., Robinet, J.-C., Cherubini, S., and Leriche, E. (2014). Investigation of the roughness-induced transition: global stability analyses and direct numerical simulations. *J. Fluid Mech*, **760**: 175–211, 2014.

[2] Cossu, C., and Brandt, L. On Tollmien–Schlichting-like waves in streaky boundary layers. *European Journal of Mechanics - B/Fluids* **23(6)**: 815–833, 2004.

TRANSITION TO GEOSTROPHIC TURBULENCE WITHIN A BAROCLINIC CAVITY

Anthony Randriamampianina[1], Stéphane Viazzo [1], Thomas von Larcher [2], Uwe Harlander [3] & Peter L. Read [4]
[1]*Aix Marseille Univ, CNRS, Centrale Marseille, M2P2, Marseille, France,*
[2]*Institute of Mathematics, Freie Universität Berlin, Germany,*
[3]*Department of Aerodynamics and Fluid Mechanics, Brandenburg University of Technology Cottbus-Senftenberg, Germany,*
[4]*Atmospheric, Oceanic and Planetary Physics, University of Oxford, UK*

Inside a differentially heated, rotating annulus, the so-called baroclinic cavity, it is recognized that the transition to turbulence occurs through the development of fluctuations, which are going to progressively destroy the regularity of the large-scale flow ([1]). In liquid-filled cavities, direct numerical simulations have allowed to detect, simultaneously with the baroclinic instability, the spontaneous emission of such fluctuations along the Stewartson boundary layers developing towards the inner, cold, and outer, hot, vertical cylinders. As illustrated in figure 1, these small-scale structures exhibit very different behaviours. The inner small-scale features have been identified as inertia-gravity waves from their dispersion relation, while those located towards the outer wall have been found to result from centrifugal instability ([2]).

We present results from these simulations together with available experimental measurements in the laboratory using two different liquids, and discuss the interaction between these fluctuations and the large-scale baroclinic waves during the transition.

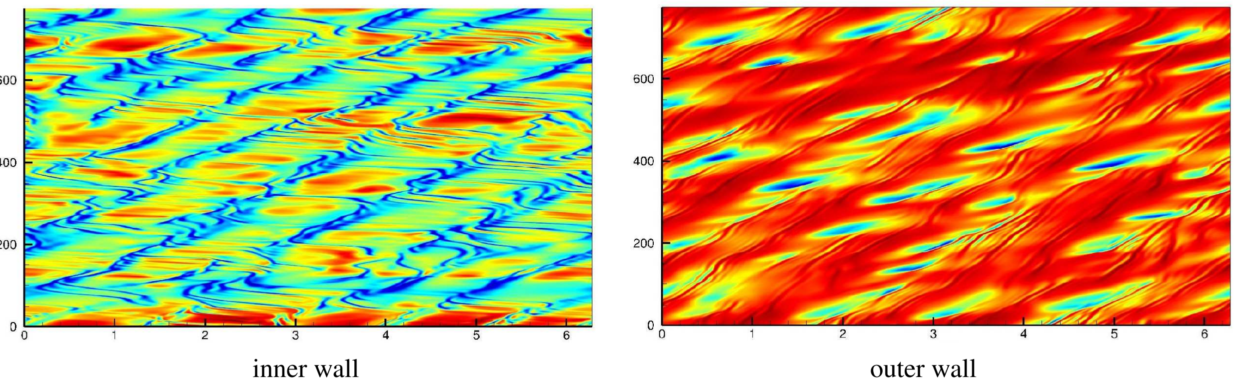

Figure 1. Hovmöller diagrams in an azimuth-time slice showing the small-scale structures developing inside the baroclinic cavity.

References

[1] READ, P. L., MAUBERT, P., RANDRIAMAMPIANINA, A. & FRÜH, W.-G. 2008 Direct numerical simulation of transitions towards Structural Vacillation in an air-filled, rotating, baroclinic annulus. *Phys. Fluids* **20**, 044107.

[2] VON LARCHER, T., VIAZZO, S., HARLANDER, U., VINCZE, M. & RANDRIAMAMPIANINA, A. 2017 Instabilities and small-scale waves within the Stewartson layers of the thermally driven rotating annulus. *J. Fluid Mech.* (submitted).

THREE-DIMENSIONAL PATTERN ORGANIZATION IN AN OPEN CAVITY FLOW AT THE ONSET OF CENTRIFUGAL INSTABILITIES

Luc Pastur[1], Christelle Douay[1,2] & François Lusseyran [1]
[1]*LIMSI-CNRS, Université Paris Sud, Université Paris Saclay, F-91400 Orsay, France*
[2] *Current address: Institut Supérieur de l'Aéronautique et de l'Espace (ISAE-SUPAERO), Université de Toulouse, F-31055 Toulouse Cedex 4, France*

We experimentally investigated the transition to pattern formation, in an open cavity flow, resulting from centrifugal instabilities. The steady inner-flow is characterized by a main recirculating flow driven by the shear layer from the cavity top-plane. Centrifugal instabilities develop on the steady inner-flow at Reynolds numbers much lower than the onset of shear-layer oscillations — the energetically dominant feature of the flow at higher Reynolds numbers. The resulting pattern is an allay of Taylor-like pairs of counter-rotating rings of vorticities, winding up around the main inner-flow recirculation. A topview visualization of the pattern, in an horizontal cut of the flow seeded with smoke, is shown in Fig. 1.

Linear stability analyses, performed on two-dimensional steady base flows with respect to spanwise Fourier modes, predict families of modes against which the base flow can destabilize [1, 2, 3]. We realized a parametric experimental study of the onset of instability in cavities of different depth D and different aspect ratio L/D, where L is the cavity length. In geometries where the span ratio S/D is large enough (S being the cavity span), theory and experiment compare well [4]. For small aspect ratios, $L/D < 1.4$, a family of (quasi)-steady modes is selected at onset, while travelling waves are observed for larger aspect ratios, as expected from the linear growth rates predicted by the linear stability analyses of [3]. When the span ratio is smaller, typically $S/D = 6$, modes at onset are (quasi)-steady for all aspect ratios between 1 and 2. In such a case, the effect of the spanwise boundaries cannot be neglected and linear stability analyses must be performed on fully three-dimensional steady base flows [5].

Preliminary comparisons between experiment and fully three-dimensional linear stability analyses show good agreement.

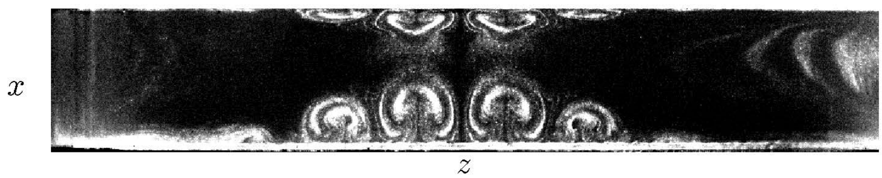

Figure 1. Smoke visualisation of the pattern at onet (topview).

References

[1] G. A. Brès, T. Colonius. Three-dimensional instabilities in compressible flow over open cavities, *Journal of Fluid Mechanics* **599**, 309–339, 2008.
[2] F. Alizard, J.C. Robinet, X. Gloerfelt. A domain decomposition matrix-free method for global linear stability, *Computers & Fluids* **66**, 63–84, 2012.
[3] F. Meseguer-Garrido, J. de Vicente, E. Valero, V. Theofilis. On linear instability mechanisms in incompressible open cavity flow, *Journal of Fluid Mechanics* **752**, 219–236, 2014.
[4] C. Douay, F. Lusseyran, L.R. Pastur. The onset of centrifugal instability in an open cavity flow, *Fluid Dynamics Research*, **48**, 061410, 2016.
[5] C. Douay, L.R. Pastur, F. Lusseyran. Centrifugal instabilities in an experimental open cavity flow, *Journal of Fluid Mechanics*, **788**, 670–694, 2016.

EXPERIMENTAL AND NUMERICAL INVESTIGATION OF THE TRANSITION SCENARIO IN A THREE-DIMENSIONAL SHEAR-DRIVEN CAVITY FLOW

J.-Ch. Loiseau[1], F. Picella[1], F. Lusseyran[2], J.-Ch. Robinet[1], S. Cherubini[3] & L. Pastur[2]
[1] *Laboratoire DynFluid, ENSAM, Paris, France.*
[2] *LIMSI, CNRS – Université Paris-Saclay, Orsay, France.*
[3] *DMMM, Politecnico di Bari, Bari, Italia.*

Centrifugal forces are ubiquitous in nature and can have a tremendous impact on a large variety of physical systems, ranging from astrophysical objects to man-made experimental devices. Typical examples are accretion disks and planetary cores where the centrifugal forces can cause an instability of the system giving rise to spatial patterns strongly affecting its dynamics. At human scale, these centrifugal forces can be found in granular or stratified flows between concentric cylinders, in separated boundary layer flows, as well as in a number of confined flows such as the flow within a lid-driven cavity [3, 1, 4].

The transition to unsteadiness of a realistic shear-driven cavity flow is investigated using the joint application of experimental observations, direct numerical simulations and fully three-dimensional linear stability analyses. Supported by experimental evidences and explained by linear stability theory, a clear understanding of the first two bifurcations occurring in the flow will be given. As for its two-dimensional counterpart, the first bifurcation is characterized by the emergence of Taylor-Görtler-like vortices resulting from a centrifugal instability of the primary vortex core. Further increasing the Reynolds number eventually triggers self-sustained periodic oscillations of the flow in the vicinity of the spanwise end-walls of the cavity. This secondary instability causes the emergence of a new set of Taylor-Görtler vortices experiencing a spanwise drift directed towards the spanwise end-walls. While a two-dimensional stability analysis would fail to capture this secondary instability due to the neglection of the lateral walls, it is the first to our knowledge that this drifting of the vortices has been fully characterized by a three-dimensional linear stability analysis of the flow. Good agreements with the experimental observations and measurements (see figure 1) strongly supports our claim that the initial stages of transition to turbulence of three-dimensional shear-driven cavity flows are solely governed by modal instabilities.

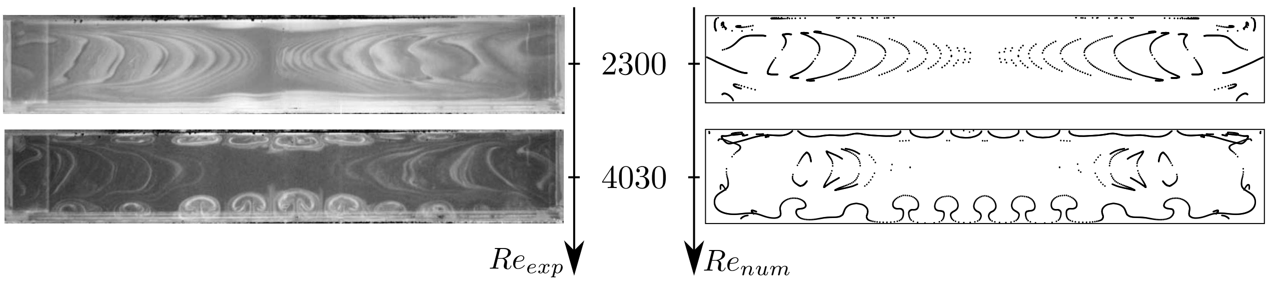

Figure 1. Experimental smoke visualization (left) [2] and numerically computed streamlines (right). The visualization tehcnique enhances the detection of mushroom-like Taylor-Görtler vortical structures. Top-views in the $y = 0.8$ plane.

References

[1] S. Albensoeder, H.C. Kuhlmann, and H.J. Rath. Three-dimensional centrifugal-flow instabilities in the lid-driven cavity problem. *Phys. Fluids*, **13**:121–135, 2001.
[2] T. Faure, P. Adrianos, F. Lusseyran, and L. Pastur. Visualizations of the flow inside an open cavity at medium range reynolds numbers. *Experiments in Fluids*, **42**:169–184, 2007.
[3] N. Ramanan and G. M. Homsy. Linear stability of lid-driven cavity flow. *Phys. Fluids*, **6**:2690–2701, 1994.
[4] V. Theofilis, P.W. Duck, and J. Owen. Viscous linear stability analysis of rectangular duct and cavity flows. *J. Fluid Mech.*, **505**:249–286, 2004.

THREE-DIMENSIONAL TRANSITION IN THE WAKE OF AN ELLIPTIC CYLINDER

Justin S. Leontini[1], David Lo Jacono [2] & Mark C. Thompson[3]
[1] *Faculty of Science, Engineering and Technology, Swinburne University of Technology, Hawthorn, Australia*
[2] *Institut de Mécanique des Fluides de Toulouse (IMFT), Université de Toulouse, CNRS, INPT, UPS, Toulouse, France*
[3] *FLAIR, Department of Mechanical and Aerospace Engineering, Monash University, Clayton, Australia*

The transition to three-dimensional flow in the wake of a circular cylinder has been extensively studied over the past 30 years [6]. It is currently understood that the flow undergoes a subcritical bifurcation to *mode A* at a Reynolds number $Re \simeq 190$. The physical mechanism of instability appears to be a cooperative elliptic instability [4]. The wake vortices that make up the Kármán vortex street are strained into an approximately elliptical shape in the near wake, triggering an elliptic instability, causing the wake vortices to become wavy along the span of the cylinder with a wavelength around four diameters. This is further amplified in the shear layers that connect these vortices.

Linear stability analysis predicts the onset Reynolds number and wavelength of mode A very accurately, via a mode that is synchronous with the base flow [1]. However in reality, the onset of three-dimensional flow also marks the end of the strict periodicity of the flow as the flow becomes chaotic (although the flow remains dominated by the vortex shedding and can appear ordered for many vortex shedding cycles) [2].

The two-dimensional wake behind an elliptic cross section, or elliptic cylinder, is very similar to that behind a circular cylinder, simply scaled down due to the more streamlined shape (when the long axis of the ellipse is aligned with the flow). It might therefore be expected that the three-dimensional transition is also similar to the circular cylinder. Here, we show that this is not the case.

We have conducted Floquet stability analysis of the elliptic cylinder wake, investigating the impact of the aspect ratio of the ellipse [3]. We have found that for aspect ratios close to unity (i.e, cross sections close to circular) the transition scenario is indeed similar to that of the circular cylinder. However, as the body becomes more streamlined, two modes that are not present in the circular cylinder wake lead the transition to three-dimensionality ("lead" in the sense that they become unstable at the lowest Reynolds number). The first of these, dubbed mode $\widehat{\mathrm{A}}$, appears to be due to similar mechanisms to mode A, but with a much longer wavelength. The second, mode $\widehat{\mathrm{B}}$, is significantly different in terms of structure, wavelength and spatio-temporal symmetry. Three-dimensional DNS shows that of these two, mode $\widehat{\mathrm{A}}$ plays the largest role in the final saturated state, regardless of which leads the transition, an example of which is shown in figure 1.

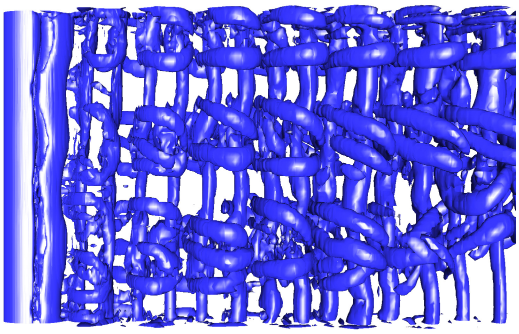

Figure 1. The final saturated state of mode $\widehat{\mathrm{A}}$. Vortices are marked in blue by isosurfaces of the λ_2 criterion. Flow is from left to right, with the cylinder running from top to bottom of the image.

References

[1] D. Barkley and R. D. Henderson. Three-dimensional Floquet stability analysis of the wake of a circular cylinder. *J. Fluid Mech.*, **322**:215–241, 1996.
[2] S. Behara and S. Mittal. Wake transition in flow past a circular cylinder. *Phys. Fluids*, **22**:114104, 2010.
[3] J.S. Leontini, D. Lo Jacono, and M.C. Thompson. Stability analysis of the elliptic cylinder wake. *J. Fluid Mech.*, **763**:302–321, 2015.
[4] M. C. Thompson, T. Leweke, and C. H. K. Williamson. The physical mechanism of transition in bluff body wakes. *J. Fluid Struct.*, **15**:607–616, 2001.
[5] P. toto, S. Titi, and J.-C. Tata. Numerical study of something. *Journal of everything*, **15**:43–62, 2017.
[6] C. H. K. Williamson. The existence of two stages in the transition to three-dimensionality of a cylinder wake. *Phys. Fluids*, **31 (11)**:3165–3168, 1988.

EFFECTS OF BASE-FLOW VARIATIONS ON THE SECONDARY INSTABILITY IN THE WAKE OF A CIRCULAR CYLINDER

Flavio Giannetti[1], Simone Camarri[2] & Vincenzo Citro[1]
[1]*DIIN, Università di Salerno, 84084 Fisciano (SA), Italy*
[2]*DICI, Università di Pisa, 56100 Pisa, Italy*

The stability properties of fluid systems can be significantly altered by small variations of the base flow. This issue has been investigated in detail in several studies: for example sensitivity analysis were carried out for parallel flows [1], boundary layers [5] and bluff body wakes [2, 4, 3]. To the authors' knowledge all sensitivity studies documented in the literature are carried out for steady base flows. However, sensitivity analysis can be relevant also for configurations characterised by a periodic base flow. For instance, the periodic wake arising behind bluff bodies due to vortex shedding may undergo a secondary bifurcation which generally leads the system towards a more complex state. As an example, this happens for the wake past a circular cylinder, which becomes unstable to 3D perturbations when the Reynolds number exceeds the threshold $Re_{2,c} \approx 189$, and this treshold can be estimated by a Floquet stability analysis. In this work we consider the sensivity analysis proposed in [4] and in [3] to study the effects of small localised structural perturbations on the stability properties of the system, and we generalize it so as to include configurations characterised by a periodic base flow. In particular, starting from a Floquet analysis of the linearised Navier Stokes equations and using a Largangian approach it is possible to estimate the variation of a particular Floquet exponent (indicating the stability of the flow) caused by a generic but localised structural perturbation of the base flow equations. This link is expressed in terms of adjoint operators and the result is used to build spatial sensitivity maps as those reported in fig. 1. These maps identify the regions of the flow where the placement of a infinitesimal small object produces the largest effect on the Floquet exponent. Such analysis may provide useful insights both for passive control strategies or for experimental investigations. In this work the proposed method is applied to the wake past a circular cylinder.

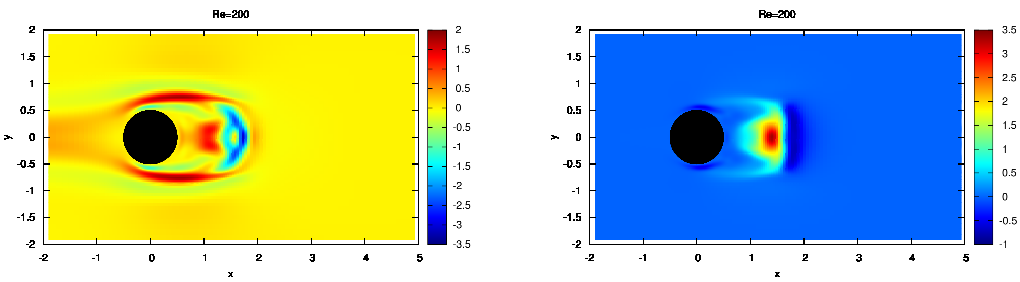

Figure 1. Sensitivity of the Floquet exponent of mode A to the application of a localized force which is proportional to the local velocity: (left figure) contribution due to the variation of the baseflow and (right figure) by the direct effect on the linearized flow equations. The global effect is the sum of the two maps.

References

[1] A. Bottaro, P. Corbett, and P. Luchini. The effect of base flow variation on flow stability. *J. Fluid Mech.*, **476**:293–302, 2003.
[2] D.C. Hill. A theoretical approach for analyzing the restabilization of wakes. In *AIAA Pap. No. 1992-0067*, 1992.
[3] P. Luchini, F. Giannetti, and J. Pralits. Structural sensitivity of linear and nonlinear global modes. In *AIAA Pap. No. 2008-4227*, 2008.
[4] O Marquet, D Sipp, and L Jacquin. Sensitivity analysis and passive control of cylinder flows. *J. Fluid Mech.*, **615**:221–252, 2008.
[5] S. Zuccher, P. Luchini, and A. Bottaro. Algebraic growth in a Blasius boundary layer: optimal and robust control by mean suction in the nonlinear regime. *J. Fluid Mech.*, **513**:135–160, 2004.

LINEAR AND NON-LINEAR PERTURBATION ANALYSIS OF THE SYMMETRY-BREAKING IN TIME-PERIODIC PROPULSIVE WAKES

Damien Jallas[1], Olivier Marquet [1] & David Fabre [2]
[1]*ONERA, The French Aerospace Lab (DAAA), 92190 Meudon, France*
[2]*Université de Toulouse, INPT, UPS (IMFT), 31400 Toulouse, France*

The deviation of the two-dimensional propulsive wake produced by a pitching foil [1] is investigated numerically by varying the flapping frequencies f at a fixed chord-based Reynolds number ($Re \sim 1000$) and flapping amplitude ($A \sim 1$). Three different regimes are observed when examining the evolution of time-averaged forces with increasing flapping frequency. In the regime I, the wake is aligned with the upstream flow velocity (Fig. 1-a) and the time-averaged lift force exerted by the flow on the foil is striclty equal to zero. In the regime II, the wake is weakly deviated (Fig. 1-b) and the mean lift is positive/negative for upward/downward deviated wakes respectively. In the regime III, the wake is strongly deviated (Fig. 1-c) and a large increase of both the mean lift and thrust is observed.

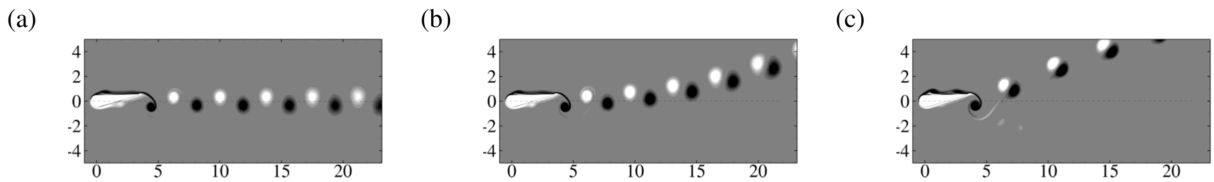

Figure 1. Vorticity snapshots of the time-periodic wake obtained for flapping frequency in (a) regime I ($f = 0.35$), (b) regime II ($f = 0.43$) and (c) regime III ($f = 0.45$).

A Floquet stability analysis of the time-periodic wake is performed to analyze the transition between the regimes I and II [2]. The base flow is the non-deviated time-periodic base flow satisfying the spatio-temporal symmetry characteristics of the foil's kinematics. For flapping frequency in regime I, it is trivially computed by marching in time the governing equations. For flapping frequency in regimes II and III, a new method is designed to compute it, based on a splitting of the flow field, as well as the governing equations, in two components that respect and break, respectively, the spatio-temporal symmetry. A damping term is introduced into the equation governing the dynamics of the symmetric-breaking component, so as to stabilize it without changing the dynamics of the symmetric component. Solving this system of coupled equations allow to obtain a spatio-temporal symmetric solution of the Navier-Stokes equations, i.e. a non-deviated time-periodic wake flow. The linear Floquet stability analysis of this time-periodic base flow show the existence of one real unstable mode, which breaks the spatio-temporal symmetry. This mode becomes unstable for the same critical frequency where the deviation occurs. It acts as an array of displacement modes [3] that provokes the deviation.

While the transition between regime I and II is explained by a linear stability analysis, the transition between the regimes II and III occurs due to non-linear effects. Anti-symmetric perturbations that result of the linear destabilisation of the wake produce and interact with perturbations that respect the spatio-temporal symmetry. These non-linear interactions between the symmetric and anti-symmetric perturbations arise closer to the foil with increasing flapping frequencies. When the non-linear effects are no longer negligeable in the vicinity of the foil, we observe the transition between the regimes II and III, associated with the large deviation of the wake flow. The increase of symmetric and anti-symmetric perturbations in the vicinity of the foil are responsible for the increase of mean thrust and lift respectively.

References

[1] R. Godoy-Diana, J.-L. Aider & J. E. Wesfreid. Transitions in the wake of a flapping foil. *Physical Review E*, v. 77(1), p. 016308. 2008.

[2] D. Jallas, O. Marquet & D. Fabre. Linear and non-linear perturbation analysis of the symmetry-breaking in time-periodic propulsive wakes. *Physical Review E*, accepted for publication. 2017.

[3] D. Fabre, D. Sipp & L. Jacquin. Kelvin waves and the singular modes of the Lamb-Oseen vortex. *Journal of Fluid Mechanics*, v. 551, p. 235-274. 2006.

DISTURBED FEEDBACK FLOW OF THE STATIC TURBULENT SYMMETRY BREAKING MODE OF THE AHMED BODY

O. Cadot[1,2], J.M. García de La Cruz[2], R.D. Brackston[2], G. Bonnavion[1] & J.F. Morrison[2]
[1] *IMSIA, ENSTA-ParisTech/CNRS/CEA/EDF, Université Paris Saclay, Palaiseau, France*
[2] *Department of Aeronautics, Imperial College London, London, UK*

A secondary small body is placed inside the recirculation bubble of the static Symmetry Breaking mode (SB mode) of a 3D squareback bluff body wake at Re=1.07×10^5. The apparatus sketched in the figures $1(a, b)$ allows angular displacements of $\pm 10°$ and radial displacements from $0.2H$ to $1.2H$ of the secondary body. This study is inspired from the stabilizing effect found in [2] using a vertical cylinder with a length l equal to the body height H. Following the same procedure as in [2], the energy of the asymmetry is estimated from the horizontal base pressure coefficient gradient:

$$A_{SB}^2 = \overline{(H\frac{\partial c_p}{\partial y})^2}$$

The velocity field of the unforced SB mode is also shown in the figures $1(a, b)$. The strong permanent horizontal asymmetry in figure $1(a)$ develops an amplitude $A_{SB} \simeq 0.15$. The preliminary result using a vertical cylinder of length $l = H$ placed at positions (x_c, y_c) recovers satisfactorily the SB mode suppression region evidenced by [2], here marked by the blue region in figure $1(c)$, but with a Reynolds number ten times larger than in [2]. A shorter cylinder with $l = 0.75H$ as set in figure $1(b)$ leads to the different sensitivity map shown in figure $1(d)$ with significantly less suppression around the symmetry axis. The purpose of the talk will be to identify these most sensitive parts inside the separated region using bodies at different vertical positions. The question of whether the SB mode is a shear layer instability, or one arising from the internal flow within the recirculation region will be addressed to shed light on the nature of the instability. In addition, the sensitivity study aims at improving the authority of actuators and their design for active flow control [1, 3].

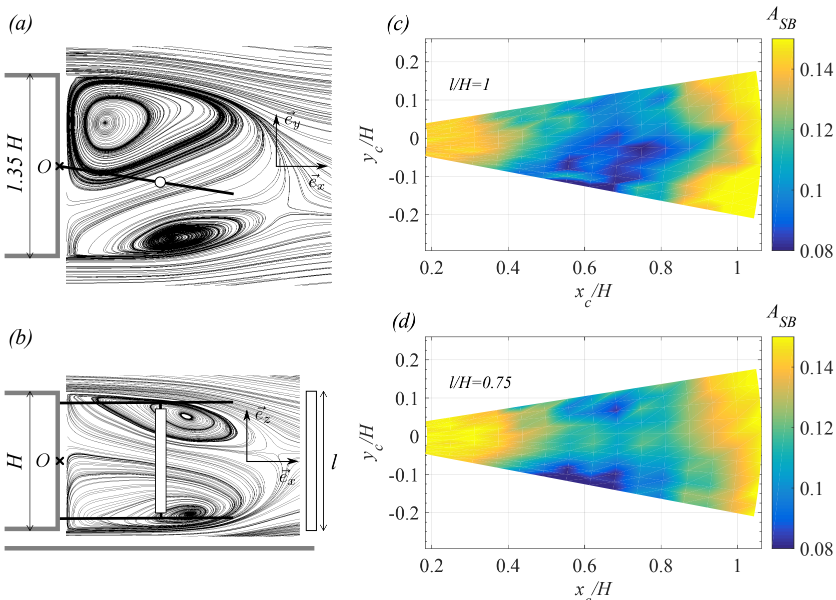

Figure 1. Top (a) and side (b) views of the squareback after body with the control cylinder placed at (x_c, y_c). Backgrounds in (a, b) display the mean streamlines of the unforced wake (i.e. the SB mode). Sensitivity maps of $A_{SB}(x_c, y_c)$ for the long, $H = l$ cylinder (c) and the short, $H = 0.75l$ cylinder (d).

References

[1] R.D. Brackston, J.M. García De La Cruz, A. Wynn, G. Rigas, and J.F. Morrison. Stochastic modelling and feedback control of bistability in a turbulent bluff body wake. *Journal of Fluid Mechanics*, **802**:726–749, 2016.

[2] M. Grandemange, M. Gohlke, and O. Cadot. Turbulent wake past a three-dimensional blunt body. Part 2. Experimental sensitivity analysis. *Journal of Fluid Mechanics*, **752**:439–461, 2014.

[3] R. Li, D. Barros, J. Borée, O. Cadot, B.R. Noack, and L. Cordier. Feedback control of bimodal wake dynamics. *Experiments in Fluids*, **57**(10), 2016.

WAKE CONTROL OF D-SHAPED BODIES THROUGH OPTIMIZED REAR CAVITIES

M. Lorite-Díez[1], J. I. Jiménez-González[1], C. Gutiérrez-Montes[1] & C. Martínez-Bazán[1]
[1]*Departamento de Ingeniería Mecánica y Minera. Universidad de Jaén. Campus de las Lagunillas, 23071, Jaén, Spain.*

We have investigated the use of the adjoint sensitivity formulation to design efficient passive control strategies aiming at reducing the drag coefficient of a slender blunt-based body with a straight rear cavity. In particular, a technique consisting in wake modifications generated by shape optimization of a cavity placed at the base of the body, has been evaluated numerically. Thus, we have computed the turbulent flow sensitivity of the drag coefficient to localized forcing for a two-dimensional body with a straight cavity at $Re = \rho U_\infty H/\mu = 2000$, where U_∞ is the free-stream velocity, ρ and μ the fluid density and viscosity respectively and H the body height, showing that the highest values of sensitivity are obtained near the rear massive separation point. The drag shape sensitivity on the body surface [1], computed using the linear adjoint formulation, has been used in combination with a free-form deformation algorithm [2], to guide the local structure deformations of the cavity, providing progressive drag reductions until the optimal, curved, shape is achieved. To deeply analyze the physical mechanisms behind the drag reduction provided by the optimal cavity, we have also performed more realistic three-dimensional numerical simulations using an IDDES model at two different Reynolds numbers, $Re = 2000$ and 20000. The results corroborate sensitivity analysis, obtaining a total drag reduction of 25.6% at $Re = 2000$ and 43.9% at $Re = 20000$, with respect to the original body without cavity, and 21.7% at $Re = 2000$ and 29.6% at $Re = 20000$ additional reduction with respect to the body with a straight cavity. These reductions are mainly achieved by the inwards deflection of the flow upon detachment and a flow deceleration at the trailing edge due to an adverse pressure gradient introduced by the curved shape of the optimal cavity walls. Both combined effects modify the near wake formed behind the body, increasing the base pressure, and consequently, decreasing the drag. Furthermore, the addition of an optimized base cavity reduces the amplitude of velocity fluctuations behind the body and stabilizes the wake, which becomes less chaotic and more two-dimensional, as observed in Fig. 1.

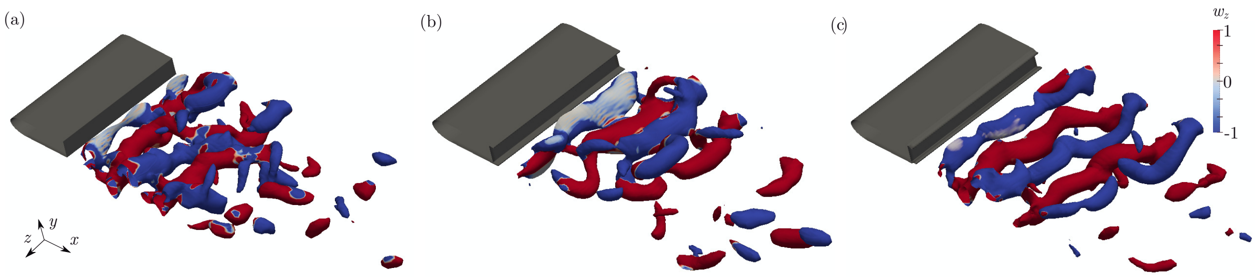

Figure 1. Contours of static pressure in the wake ($p* = -0.36$), colored by spanwise vorticity: (a) original body without cavity, (b) body with straight cavity, and (c) body with the optimized curved cavity.

References

[1] C. Othmer. Adjoint methods for car aerodynamics. *J. Math. Ind.*, **4**(1):1–23, 2014.
[2] T. Han, C. Hill, and S. Jindal. Adjoint method for aerodynamic shape improvement in comparison with surface pressure gradient method. *SAE Int. J. Passeng. Cars - Mech. Syst*, **4**(1):100 – 107, 2011.

SYMMETRY BREAKING IN 3D BLUFF-BODY WAKES

Georgios Rigas[1], Lucas Esclapez[2] & Luca Magri[3]
[1]*California Institute of Technology, Pasadena, CA, USA*
[2]*CERFACS, Toulouse, France*
[3]*University of Cambridge, Cambridge, UK*

The dynamics of a three-dimensional axisymmetric bluff-body wake are examined at low Reynolds regimes where transitions take place through spatio-temporal symmetry breaking. A linear stability analysis is employed to identify the critical Reynolds numbers associated with symmetry breaking, and the associated eigenmodes, known as global modes. The analysis shows that the axisymmetric stable base flow breaks the rotational symmetry through a pitchfork $m = 1$ bifurcation, in agreement with previously reported results for axisymmetric wakes. Above this threshold, the stable base flow is steady and three-dimensional with planar symmetry. A three-dimensional global stability analysis around the steady reflectionally symmetric base flow, assuming no homogeneous directions, predicts accurately the Hopf bifurcation threshold, which leads to asymmetric vortex shedding. DNS simulations validate the stability results and characterize the flow topology during the early chaotic regime [2, 1].

For $Re > 900$ chaotic behavior is established. The wake breaks the reflectional symmetry and random reorientations in the azimuthal direction occur. Interestingly, the laminar symmetry-breaking instabilities persist even at high Reynolds numbers [4, 3] and manifest as coherent large-scale structures. This is shown based on experimental results of the same bluff body geometry at $Re_D \approx 200,000$. A stochastic framework for the modelling of the large-scale symmetry breaking coherent structures is proposed and validated against the experimental measurements.

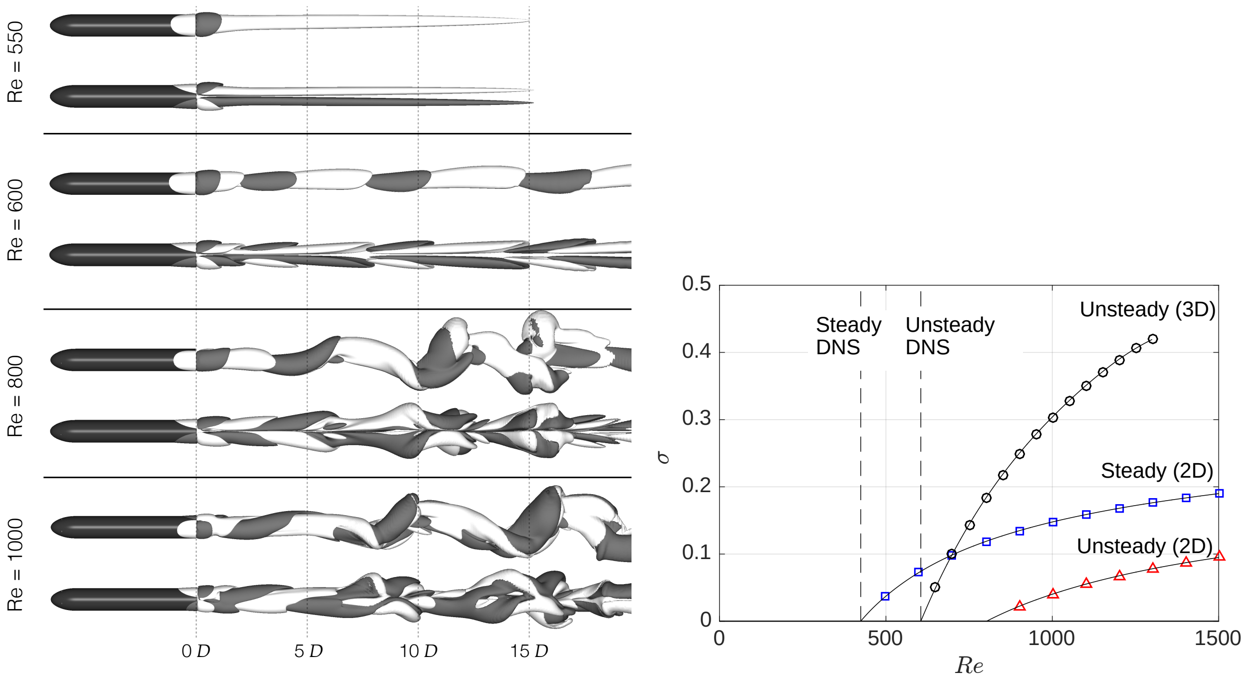

Figure 1. DNS simulations (left) and growth rates of the globally unstable modes (right). Growth rates were predicted from global stability analysis with 2 inhomogeneous directions (2D) and 3 inhomogeneous directions (3D). Streamwise vorticity contours, $\omega_z^* = \pm 0.05$, in the wake of the bluff-body; side (left-top) and plane (left-bottom) views.

References

[1] P.J. Blonigan, P. Fernandez, S.M. Murman, Q. Wang, G. Rigas, and L. Magri. Towards a chaotic adjoint for LES. In *Proceedings of the Summer Program*. Center for Turbulence Research, Stanford University, 2016.

[2] G. Rigas, L. Esclapez, and L. Magri. Symmetry breaking in 3D wakes. In *Proceedings of the Summer Program*. Center for Turbulence Research, Stanford University, 2016.

[3] G. Rigas, A. S. Morgans, R. D. Brackston, and J. F. Morrison. Diffusive dynamics and stochastic models of turbulent axisymmetric wakes. *J. Fluid Mech.*, **778**:R2, 2015.

[4] G. Rigas, A. R. Oxlade, A. S. Morgans, and J. F. Morrison. Low-dimensional dynamics of a turbulent axisymmetric wake. *J. Fluid Mech.*, **755**:R5, 2014.

SOMETHING OLD, SOMETHING NEW IN TRANSITION AND INSTABILITY

Dwight Barkley[1]
[1]*Mathematics Institute, University of Warwick, Coventry CV4 7AL, UK*

I will begin by discussing subcritical transition in the context of directed percolation. I will briefly review the basic features of spatiotemporal transition, and then focus on recent successes in obtaining critical exponents in experiments and numerical simulations. I will discuss the difficulties of such studies and the challenges for the future. I will then turn to low-viscosity flows in cylindrical geometries and discuss the interesting mathematics and physics of certain types of highly nonlinear solutions.

ENERGY PRODUCTION AND SELF-SUSTAINED TURBULENCE AT THE KOLMOGOROV MICROSCALE

Qiang Yang[1,3], Ashley P. Willis [2] & Yongyun Hwang[1]
[1] *Department of Aeronautics, Imperial College London, London, UK.*
[2] *School of Mathematics and Statistics, University of Sheffield, S3 7RH, UK*
[3] *School of Engineering and Centre for Scientific Computing, University of Warwick, Coventry CV4 7AL, UK*

Several recent studies have reported that there exists a self-similar form of invariant solutions in the form of a stationary/traveling wave down to the Kolmogorov microscale in the bulk region of Couette flow [1, 2, 3]. While their role in a fully-developed turbulent flow is yet to be identified, in this talk, we report a related mechanism of turbulence production at the Kolmogorov microscale in the bulk region of turbulent Couette flow. A set of minimal-span direct numerical simulations are performed up to friction Reynolds number $Re_\tau \simeq 800$ (see figure 1). It is found that this production mechanism essentially originates from the non-zero mean shear in the bulk region of the Couette flow and that the associated eddy turn-over dynamics in the core region of the Couette flow is remarkably similar to the so-called self-sustaining process (SSP), involving amplification of streaks, their subsequent breakdown via an instability, and regeneration of streamwise vortices. A numerical experiment that removes all the other motions except in the core region is also performed, which demonstrates that the eddies at a given wall-normal location in the bulk region are sustained in the absence of other motions at different wall-normal locations. It is proposed that the self-sustaining eddies at the Kolmogorov microscale correspond to those in uniform shear turbulence at transitional Reynolds numbers, and a quantitative comparison between the eddies in uniform shear and near-wall turbulence is subsequently made. Finally, it is shown that the turbulence production by the self-sustaining eddies at the Kolmogorov microscale is much smaller than that of full-scale simulations, and that the difference between the two increases with Reynolds number.

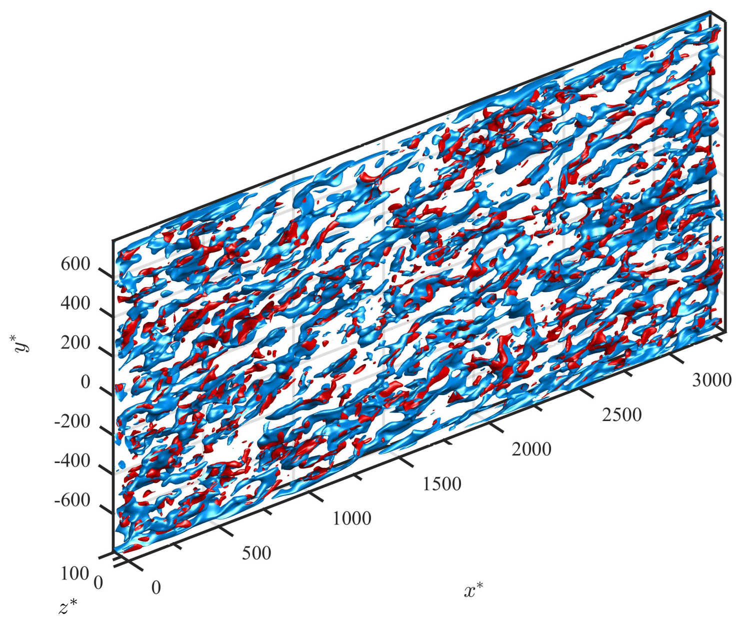

Figure 1. An instantaneous flow field of the minimal-span simulation of turbulent Couette flow at $Re_\tau \simeq 814$. Here, the blue iso-surfaces indicate $u'^* = -2$, while the red ones are $v'^* = 1.5$. Here the superscript * denotes dimensionless variables with the Kolmogorov microscale.

References

[1] H. M. Blackburn, P. Hall, and S. Sherwin. Lower branch equilibria in Couette flow: the emergence of canonical states for arbitrary shear flow. *J. Fluid Mech.*, **726**:R2, 2013.
[2] K. Deguichi. Self-sustaining states at Kolmogorov microscale. *J. Fluid Mech.*, **781**:R6, 2015.
[3] B. Eckhardt and S. Zammert. Exact coherent structures for the turbulent cascade. *Bulletin of the American Physical Society*, **61**(20):A18.008, 2016.

UNIVERSAL CONTINUOUS TRANSITION TO TURBULENCE IN A PLANAR SHEAR FLOW

Matthew Chantry[1,2,4], Laurette S. Tuckerman[2,4] and Dwight Barkley[3,4]
[1]*Atmospheric, Oceanic and Planetary Physics, University of Oxford, Clarendon Laboratory, Parks Road, Oxford OX1 3PU, UK*
[2]*Laboratoire de Physique et Mécanique des Milieux Hétérogènes (PMMH), CNRS, ESPCI Paris, PSL Research University; Sorbonne Université, Univ. Paris Diderot, France*
[3]*Mathematics Institute, University of Warwick, Coventry CV4 7AL, UK*
[4]*Kavli Institute for Theoretical Physics, University of California at Santa Barbara, Santa Barbara, CA 93106, USA*

Classifying the transition to turbulence in planar shear flows is a long-standing question without a definitive answer [1, 2, 3, 4]. More specifically, the question is one of continuous or discontinuous transition, whether an arbitrarily small turbulence fraction can be maintained in the long-time limit. To attack this problem, either in simulations or experiments, requires domains that are large relative to the building blocks of transition, turbulent spots and bands. The combination of large domains and long time integration results in a computational burden too large for 3D DNS. Instead we consider the problem in Waleffe flow – the planar shear flow between stress-free boundaries driven by a sinusoidal body force. Using a low-order truncation in the wall-normal direction we can reduced the costs and consider system sizes an order of magnitude larger than any previously simulated. Despite this truncation, the building blocks of spots and bands are still robustly created .

In this system we demonstrate a continuously increasing turbulence fraction as Reynolds number is increased beyond a critical Reynolds number. The statistics of turbulence near criticality show the hallmarks of (2+1)D directed percolation. By reconsidering the domain sizes used in previous experiments and simulations we see that their discontinuous transitions result from insufficiently large domains or insufficiently long time integrations. Our results provide a guide to the work required to confirm plane Couette flow in the universality class of directed percolation.

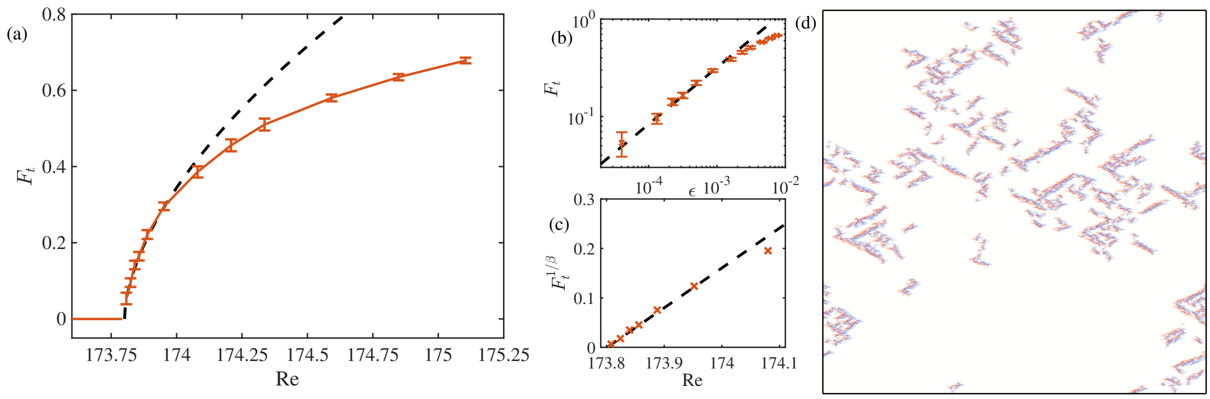

Figure 1. Bifurcation diagrams for the transition to turbulence. (a) Continuous transition in a large domain. Equilibrium turbulence fraction F_t is plotted as a function of *Re*. Points and errorbars denote mean and standard deviation of F_t. Black dashed curved shows the directed percolation power law. (b) Log-log plot of the same data in terms of $\epsilon = (Re - Re_c)/Re_c$, where $Re_c = 173.80$. Near criticality the data is consistent with $F_t \sim \epsilon^\beta$ with $\beta \simeq 0.583$. (c) $F^{1/\beta}$ against *Re* showing linear behaviour. The dashed curve is the directed-percolation power law from the large domain. (d) Streamwise velocity at the midplane for *Re* just above Re_c in our simulation domain $[2560h, 1.25h, 2560h]$.

References

[1] Sabine Bottin and Hugues Chaté. Statistical analysis of the transition to turbulence in plane Couette flow. *Eur. Phys. J. B*, **6**:143–155, 1998.
[2] Sabine Bottin, Francois Daviaud, Paul Manneville, and Olivier Dauchot. Discontinuous transition to spatiotemporal intermittency in plane Couette flow. *Europhys. Lett.*, **43**:171, 1998.
[3] Yohann Duguet, Philipp Schlatter, and D. S. Henningson. Formation of turbulent patterns near the onset of transition in plane Couette flow. *J. Fluid Mech.*, **650**:119–129, 2010.
[4] Grégoire Lemoult, Liang Shi, Kerstin Avila, Shreyas V Jalikop, Marc Avila, and Björn Hof. Directed percolation phase transition to sustained turbulence in Couette flow. *Nat. Phys.*, **12**:254–258, 2016.

FROM TURBULENCE TRANSITION TO SHELL BUCKLING - WHAT LOAD CAN A CYLINDER SHELL CARRY?

Tobias Kreilos[1], Emmanuel Virot [1,2], Shmuel M. Rubinstein[2] & Tobias M. Schneider [1]
[1]*Emergent Complexity in Physical Systems Laboratory (ECPS), École Polytechnique Fédérale de Lausanne, 1015 Lausanne, Switzerland*
[2]*Harvard John A. Paulson School of Engineering and Applied Sciences, Harvard University, Cambridge, Massachusetts 02138, USA*

Natural and engineered structures ranging from egg shells to air- and spacecrafts are built from curved thin elastic shells offering exceptional structural rigidity at minimal weight. How much load can such a shell carry before it buckles and collapses? This classical problem has not been fully resolved even for the simple geometry of an axially compressed cylinder shell. Predictions based on linear theory fail to capture experiments indicating buckling to occur well before the unbuckled state looses linear stability. We will argue that the buckling transition can be described as a finite amplitude instability similar to the transition to turbulence in linearly stable flows. Consequently the dynamical systems concepts and methods that revolutionized our understanding of transitional turbulence in recent years carry over to shell elasticity.

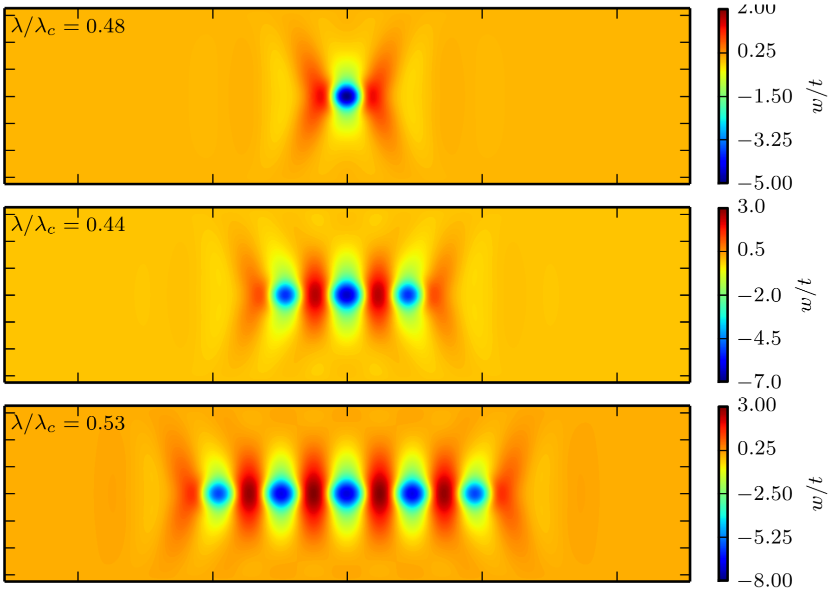

Figure 1. Unstable force equilibrium for an axially loaded cylinder of length $L = 1.6R$. The solutions represented by their normal deflection w in units of the shell thickness t are located on the stability boundary of the unbuckled base state. Under continuation in axial load λ the edge state (single dimple) undergoes homoclinic snaking, creating multi-dimple configurations.

We calculate fully nonlinear force equilibrium solutions of the loaded cylinder shell. The equilibrium solutions are dynamically unstable and located on the stability boundary of the unbuckled state. A fully localized single dimple deformation is identified as the edge state[1], the attractor for the dynamics restricted to the stability boundary. Under variation of the axial load the single dimple undergoes homoclinic snaking[2] in the azimuthal direction, creating states with multiple dimples arranged around the central circumference.[3]
Experiments suggest that the fully nonlinear solutions embedded in the stability boundary of the stable unbuckled state define critical shape deformations that trigger buckling of the shell. The solutions may thus help explain when an axially loaded cylinder shell collapses.

References

[1] T.M. Schneider, B. Eckhardt, amd J.A. Yorke. Turbulence transition and the edge of chaos in pipe flow. *Phys. Rev. Lett.* **99**:34502, 2007.
[2] E. Knobloch. Spatial Localization in Dissipative Systems. *Annu. Rev. Cond. Mat. Phys.* **6**:325–359, 2015.
[3] T. Kreilos, and T.M. Schneider. Fully localized post-buckling states of cylindrical shells under axial compression. *in review*, 2017.

A SELF-SUSTAINING PROCESS THEORY FOR COUPLED UNIFORM MOMENTUM ZONES AND VORTICAL FISSURES IN THE INERTIAL REGION OF TURBULENT WALL FLOWS

Greg Chini[1,2], Brandon Montemuro[2], Chris White[1] & Joe Klewicki[1]
[1]*Department of Mechanical Engineering, University of New Hampshire, Durham, NH 03824 USA*
[2]*Integrated Applied Mathematics Program, University of New Hampshire, Durham, NH 03824 USA*

Three-dimensional invariant solutions of the Navier–Stokes (NS) equations and the self-sustaining processes (SSPs) that support them are now widely believed to play a fundamental role in wall flows at transitional Reynolds numbers. At asymptotically large values of the friction Reynolds number Re_τ, these solutions and the associated SSPs also may be relevant to the *near-wall* dynamics of turbulent shear flows [1], where the *effective* Reynolds number is modest. Yet, there is mounting evidence that much larger-scale quasi-coherent flow structures similarly exert a controlling influence on momentum and vorticity transport away from the wall, i.e. in the inertial layer (outboard of the Reynolds stress peak), where the effective Reynolds number is asymptotically large [2]. We investigate the possibility that these outer-region 'super-structures' are directly supported by a variant of the near-wall self-sustaining process operative in the inertial layer. Specifically, we develop an asymptotic SSP theory [3] that has the potential to explain the origin and maintenance of zones of quasi-uniform streamwise momentum (UMZs) and interlaced internal shear layers (or 'vortical fissures', VFs) that comprise a characteristic structural feature of the inertial region of turbulent wall flows at sufficiently large Re_τ [4].

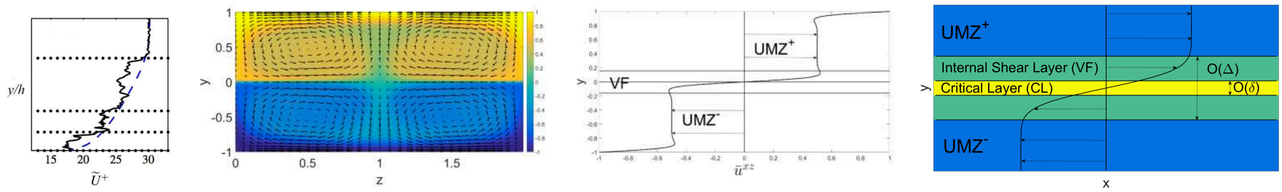

Figure 1. The proposed SSP theory aims to explain the robust staircase-like structure of the instantaneous streamwise (x) velocity (left panel, [4]) arising in the inertial layer of high-Re_τ turbulent wall flows. Middle panels: Large-scale counter-rotating roll modes, distributed in the wall-normal (y) direction, act as a homogenizing agent that creates and maintains uniform momentum zones (UMZs) while simultaneously producing concentrated regions of spanwise vorticity (VFs). Owing to this homogenization, the fluctuations (streamwise-varying fields) are largely irrotational within the UMZs, implying the roll modes are driven by nonlinear fluctuation dynamics within critical layers (CLs) embedded within the fissures, yielding a 3-region wall-normal asymptotic structure (right panel).

The proposed mechanism and the corresponding asymptotic analysis have commonalities with, respectively, the SSP theory developed by Waleffe [5] and the large Reynolds number asymptotic vortex–wave interaction (VWI) theory originally developed by Hall and Smith and subsequently applied to invariant solutions of the NS equations by Hall & Sherwin [6], but there are crucial distinctions. Firstly, we show that the streamwise-averaged roll motions, while remaining comparably weak relative to the mean streaky streamwise flow, must have a magnitude $\gg O(1/Re_\tau)$ to locally homogenize the streamwise flow. As shown in figure 1, a spanwise array of counter-rotating rolls, distributed in the wall-normal direction, then can induce – and maintain against viscous disintegration – a staircase-like profile in the instantaneous streamwise velocity, in accord with recent observations. Moreover, our asymptotic analysis highlights the active role played by the internal shear layers, where the effective Reynolds number is $O(1)$, even though viscous effects necessarily are weak over the vast majority of the inertial domain. In contrast to the near-wall SSP, here it is the strong wall-normal rather than weak spanwise inflections of the streamwise-averaged streamwise flow that are primarily responsible for the instabilities that nonlinearly interact – within even finer critical layers (i.e. embedded within the VFs) – to sustain the roll and streak flow.

References

[1] J. M. Hamilton, J. Kim & F. Waleffe. Regeneration mechanisms of near-wall turbulence structures. *J. Fluid Mech.* **287**: 317–348, 1995.
[2] N. Hutchins & I. Marusic. Evidence of very long meandering structures in the logarithmic region of turbulent boundary layers. *J. Fluid Mech.* **579**: 1–28, 2007.
[3] G. P. Chini, B. Montemuro, C. M. White & J. Klewicki. A self-sustaining process model of inertial layer dynamics in high Reynolds number turbulent wall flows. *Phil. Trans. R. Soc. A* **375**: 20160090, 2017.
[4] C. M. de Silva, N. Hutchins & I. Marusic. Uniform momentum zones in turbulent boundary layers. *J. Fluid Mech.* **786**: 309–331, 2016.
[5] F. Waleffe. On a self-sustaining process in shear flows. *Phys. Fluids* **9**:883–900, 1997.
[6] P. Hall & S. Sherwin. Streamwise vortices in shear flows: harbingers of transition and the skeleton of coherent structures. *J. Fluid Mech.* **661**:178–205, 2010.

EDGE STATES CONTROL DROPLET BREAK-UP IN UNIAXIAL EXTENSIONAL FLOWS

Giacomo Gallino[1], Tobias M. Schneider [2] & François Gallaire [1]
[1]*Laboratory of Fluid Mechanics and Instabilities, École Polytechnique Fédérale de Lausanne.*
EPFL-STI-IGM-LFMI, CH-1015 Lausanne, Switzerland
[2]*Emergent Complexity in Physical System Laboratory, École Polytechnique Fédérale de Lausanne.*
EPFL-STI-IGM-ECPS, CH-1015 Lausanne, Switzerland

When a droplet is placed in an extensional flow it elongates and can ultimately break, leading to the formation of smaller droplets. The droplet elongation is related to the strength of the applied flow, which is represented by the capillary number Ca. The seminal work from Taylor [1] shows that when the capillary number exceeds a critical value Ca_c, the droplet always breaks. This phenomenon occurs because for $Ca > Ca_c$ the steady solution disappears, as demonstrated theoretically in [2]. When $Ca < Ca_c$, the evolution of the droplet depends on its initial shape. Indeed, it has been shown experimentally [3] that an initially very elongated droplet can break up even for a subcritical capillary number. The influence of the droplet stability upon the initial deformation denotes the existence of a finite basin of attraction of the steady solution. In this work we investigate the stability of droplets for subcritical capillary number. For this purpose we characterize the boundaries of the basin of attraction, separating droplets that break from those that return to the steady state. We adapt the edge tracking technique developed to study shear flows [4] to our system. Thereby, we find the edge state, which is an unstable equilibrium configuration whose stable manifold forms the basin boundary. In figure 1a we show that starting from the edge state computed at $Ca = 0.07$, we can perform pseudo arc-length continuation in capillary number until we join the branch of the steady states observed in experiments. The two branches join in a saddle node bifurcation at $Ca = Ca_c$. The edge tracking and the continuation method are based on a spectral boundary integral method solver. In figure 1b we show the time evolution for two families of a shape A and B, projected on the second and fourth coefficient of a Legendre series. In all cases the droplet first approaches the edge state and than converges to the steady solution or breaks up through the edge pinching mechanism [5]. This shows that the edge state strongly affects the transient dynamics of the droplet shape, selecting an almost unique path towards break-up.

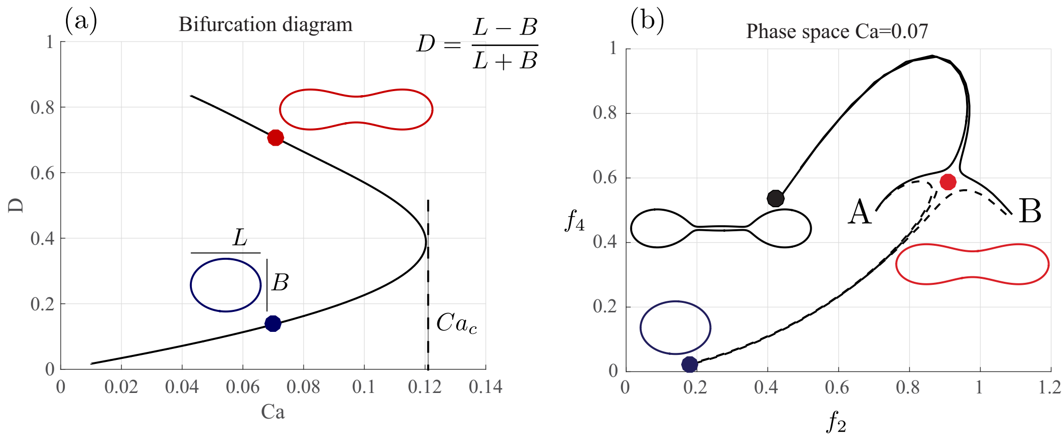

Figure 1. (a) Bifurcation diagram of the deformation parameter as a function of the capillary number. (b) Phase space for $Ca = 0.07$ of the second and fourth Legendre mode describing the droplet radius: all trajectories are first attracted to the edge state, than stable trajectories (dashed) return to the stable steady state while the others develop instabilities that leads to pinch-off.

References

[1] G. Taylor, "The formation of emulsions in definable fields of flow," *Proceedings of the Royal Society of London. Series A, Containing Papers of a Mathematical and Physical Character*, vol. 146, no. 858, pp. 501–523, 1934.
[2] D. Barthes-Biesel and A. Acrivos, "Deformation and burst of a liquid droplet freely suspended in a linear shear field," *Journal of Fluid Mechanics*, vol. 61, no. 01, pp. 1–22, 1973.
[3] H. Stone and L. Leal, "The influence of initial deformation on drop breakup in subcritical time-dependent flows at low reynolds numbers," *Journal of fluid mechanics*, vol. 206, pp. 223–263, 1989.
[4] T. M. Schneider, B. Eckhardt, and J. A. Yorke, "Turbulence transition and the edge of chaos in pipe flow," *Physical review letters*, vol. 99, no. 3, p. 034502, 2007.
[5] H. A. Stone and L. Leal, "Relaxation and breakup of an initially extended drop in an otherwise quiescent fluid," *Journal of Fluid Mechanics*, vol. 198, pp. 399–427, 1989.

Linear and nonlinear space-time dynamics of optimal wavepackets for streaks in a channel entrance flow

A. Cadiou, F. Alizard, L. Le Penven, M. Buffat, B. Di Pierro

Laboratoire de Mécanique des Fluides et d'Acoustique, Université de Lyon, Université Claude-Bernard Lyon 1/CNRS/École Centrale de Lyon/Insa de Lyon, 36, av Guy de Collongue, 69134 Écully, France

In spite of a large number of theoretical, numerical and experimental studies in bypass transition to turbulence of fully developed channel flows, less attention has been paid to the channel entrance flow [1]. This work aims at describing different paths leading to turbulence for the entrance channel flow case where the flow is uniform upstream. Due to the favorable pressure gradient, all velocity profiles are stable [3] and if transition to turbulence occurs, it excludes the path through the exponentially growing Tollmien-Schlichting mode. Scenarii are therefore based on secondary instability of streaks [4].

A linear global optimization is carried out consisting in searching for initial perturbations having the largest energy growth for given times [2], for various streaks amplitudes. For sufficiently high amplitude of the streaks, global optimal modes, both varicose and sinuous, that take the form of wavepackets, are amplified. We show that for short optimization times, varicose wavepacket grows through a combination of the Orr and lift-up effects, whereas for larger target times, both sinuous and varicose wavepackets (if exist) exhibit an instability mechanism driven by the presence of inflection points in the streaky flow.

By means of direct numerical simulations, we show that the varicose wavepacket associated with short time optimization of the streaky flow exhibits a subcritical behaviour leading to hairpin-like trains. Both varicose and sinuous wavepackets resulting for larger time optimizations yield to a supercritical behaviour that give rise to arch-like patterns and spanwise wavy motion of streaks, respectively. It is shown that for short and long time optimizations, the flow becomes turbulent futher downstream, and is very similar to a fully developed wall tubulence, with the same wall shear-stress for all cases ($Re_\tau = 166$). It is observed that in this regime, the outer part of the boundary layer is dominated by arch-like structures, independently of the symmetry of the initial wavepacket.

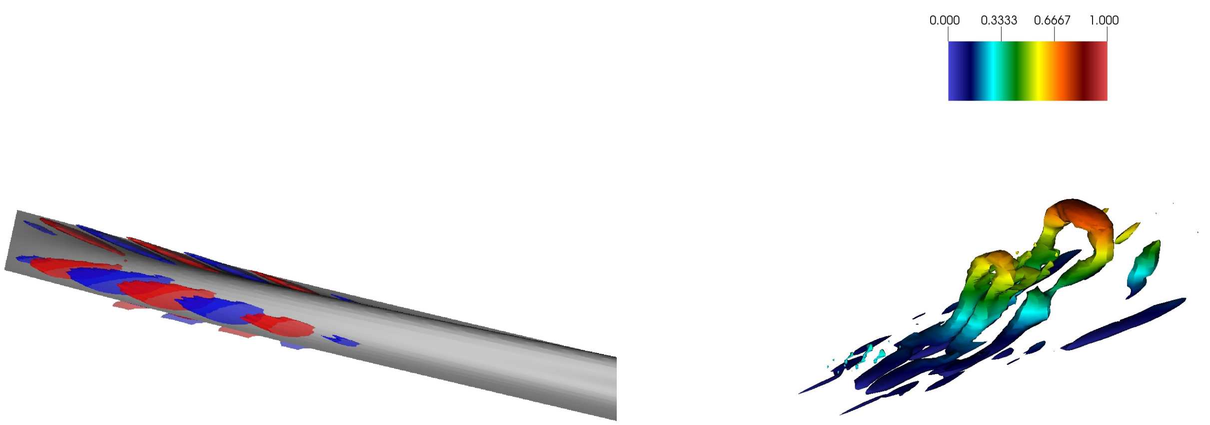

(a) Spanwise component of the vorticity of the linear optimal wavepacket at the initial time.

(b) Nonlinear evolution of the optimal wavepacket convected along low-speed streaks. Isosurface of the λ_2-criterion colored by the spanwise component of the fluctuation of the velocity.

Figure 1: Optimal varicose wavepacket for short time optimization of the secondary instability of the streaks in the channel entrance flow. The Reynolds number based on the channel half-height and the bulk velocity is $Re_h = 2500$.

[1] M. Asai and J.M. Floryan. Certain aspects of channel entrance flow. *Phys. Fluids*, 16 (4):1160–1163, 2003.

[2] D. Barkley, H.M. Blackburn, and S.J. Sherwin. Direct optimal growth analysis for timesteppers. *Int J. for Num. Methods in Fluids*, 57:1435–1458, 2008.

[3] M. Buffat, A. Cadiou, and L. Le Penven. Bypass transition at the entrance of a plane channel. In *EFMC10 Conference, 14 September - 18 September, Copenhague, Danemark*, September 2014.

[4] P. Schlatter, L. Brandt, H.C. de Lange, and D.S. Henningson. On streak breakdown in bypass transition. *PoF*, 101505(20):1–15, 2008.

On the role of vortex stretching in energy optimal growth of three-dimensional perturbations on plane parallel shear flows

Eyal Heifetz[1], Helena Vitoshkin[2], A. Yu Gelfgat[2] & N Harnik[2]
[1]*Department of Geosciences Faculty of Exact Sciences, Tel-Aviv University, Israel*
[2]*School of Mechanical Engineering, Faculty of Engineering, Tel-Aviv University, Israel*

The three-dimensional linearized optimal energy growth mechanism, in plane parallel shear flows, is re-examined in terms of the role of vortex stretching and the interplay between the spanwise vorticity and the planar divergent components. For high Reynolds numbers the structure of the optimal perturbations in Couette, Poiseuille and mixing-layer shear profiles is robust and resembles localized plane waves in regions where the background shear is large. The waves are tilted with the shear when the spanwise vorticity and the planar divergence fields are in (out of) phase when the background shear is positive (negative). A minimal model is derived to explain how this configuration enables simultaneous growth of the two fields, and how this mutual amplification affects the optimal energy growth. This perspective provides an understanding of the three-dimensional growth solely from the two-dimensional dynamics on the shear plane.

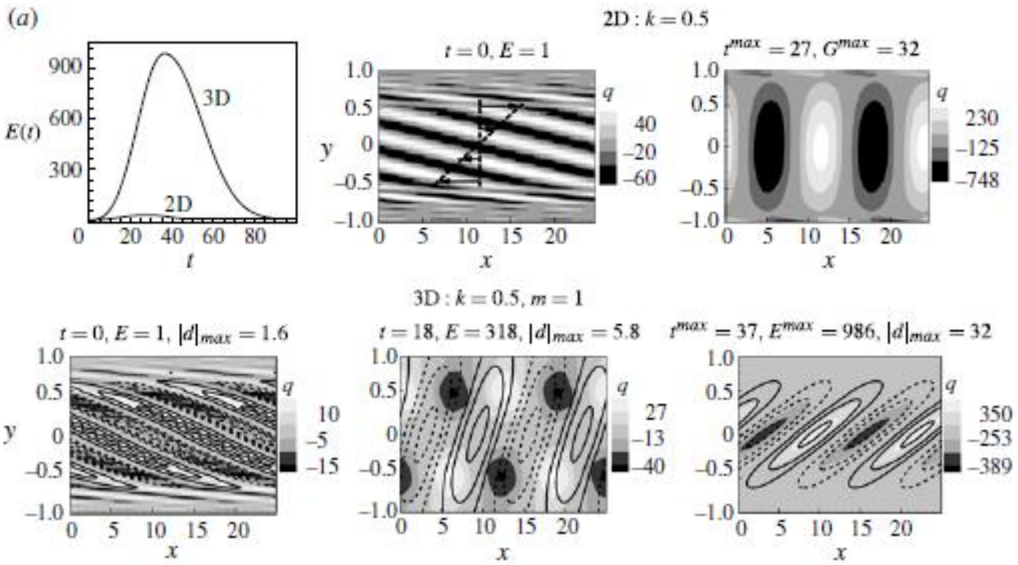

Figure 1. Optimal energy growth for 2D and 3D perturbations on Couette plane parallel shear flows for Re = 5000. The different streamwise and spanwise wavenumbers (k,m) are selected to generate maximal non-modal growth. Solid curves indicate the energy growth evolution, E(t), from the initial optimal perturbations. Note that E_{3Dmax} _ E_{2Dmax} and $t_{3Dmax} > t_{2Dmax}$, where t_{max} is the time of maximal amplification over all times. The structure of the optimal perturbations at selected times is indicated by the contours of the spanwise vorticity q. For the 3D perturbations the planar divergent field d is superimposed and indicated by the solid (positive) and dashed (negative) contours. Note that in 2D, E_{max} is obtained when the eddies are aligned perpendicular to the shear, whereas in 3D it occurs when the eddies are tilted with the shear, and d and q are in (anti) phase when the mean shear is positive (negative). Furthermore, the structures resemble localized plane waves that are tilted with the local maximal shear. Similar results are obtained for Poiseuille and mixing layer shear flows.

NON-LINEAR OPTIMAL PERTURBATION IN SINGLE AND DOUBLE VORTEX SYSTEMS

Navrose[1], Holly G Johnson[2], Vincent Brion[1] & Laurent Jacquin[1]
[1]*Département Aérodynamique Aéroélasticité Acoustique (DAAA), ONERA, Meudon, France*
[2]*Department of Mechanical Engineering, Imperial College London, London, UK*

Optimal perturbation in fluid systems has received significant attention owing to its application in the study of flow transition, mixing and heat transfer. In general, it corresponds to an initial disturbance, with respect to a base state, that optimizes certain flow attributes for a given horizon time (T). The investigation of optimal perturbation in fluid systems has been carried out almost exclusively within the linear framework. In the present work, we demonstrate that for vortex flows the inclusion of non-linear terms in the governing equations can result in higher gain than that predicted by linear analysis. This behaviour is expected to be significant in understanding the route to turbulence in such flows.

We consider the case of an isolated vortex first. The base flow consists of a Lamb-Oseen vortex. The Reynolds number based on the circulation (Γ) of the vortex is $Re = 5000$. Time is non-dimensionalized using the rotation time of the vortex ($4\pi^2a^2/\Gamma$), where a is the dispersion radius of the vortex. The objective is to find the initial perturbation that maximizes the gain of kinetic energy (E) of the perturbation over T. To this end, the method of Lagrange Multipliers is employed. The Langrangian consists of the objective function ($E(T)/E(0)$) constrained by the incompressible Navier-Stokes equations and the corresponding boundary conditions. The direct and adjoint equations are solved iteratively to converge to the optimal solution. The computations are carried out using the spectral element solver NEK5000. Figure 1 shows the variation of gain with $E(0)$ for $T = 4.8$. In general, the value of gain obtained via non-linear analysis is lower than the linear optimal gain. However, there exists a range of $E(0)$ for which the non-linear gain is higher than the linear gain. In this regime, the vorticity field corresponding to the non-linear optimal perturbation is less diffused than that of the linear optimal perturbation. With increase in horizon time, the difference between non-linear and linear optimal gain is found to increase. To compare the effect of the linear and non-linear optimal perturbation on vortex dynamics, direct time integration (DTI) of the governing equations is carried out utilizing each as the initial perturbation. The results show that if DTI is initiated with linear optimal perturbation, the vortex oscillates for short time. If, on the other hand, computations are initiated with the non-linear optimal, the oscillations in the vortex persist for a long time and exhibit a quasi-periodic behaviour.

Next, we investigate non-linear optimal perturbation in a two-vortex system consisting of counter-rotating vortices of equal strength. The Reynolds number based on the circulation (Γ) is $Re = 1000$. The aspect ratio of the vortex pair is $a/b = 0.18$; a is the dispersion radius of a vortex in the pair and b is the distance between the vortex centres. Figure 2 shows the variation of gain with initial energy of the perturbation for $T = 0.5$. Time is non-dimensionalized by $(2\pi b^2)/\Gamma$. Similar to the single vortex system, there exists a range of $E(0)$ for which the non-linear optimal perturbation results in higher gain than the linear optimal perturbation. The structure of the non-linear optimal perturbation exhibits asymmetry about the mid-plane; the perturbations are dominant in one vortex of the pair. DTI of the governing equations initiated with the non-linear optimal perturbation shows significant differences in the evolution of the two vortices in the pair; the one with dominant perturbation exhibits oscillation of the vortex centre similar to that observed in the case of an isolated vortex.

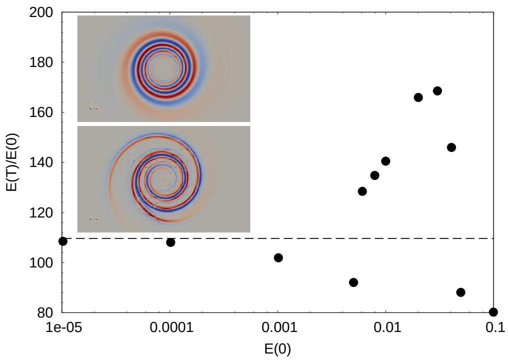

Figure 1. Optimal perturbation in single vortex system for $Re = 5000$: variation of gain with initial energy of the perturbation. The gain obtained by linear analysis is shown via a broken line. The top and bottom insets show the vorticity field associated with the linear and $E(0) = 0.02$ non-linear optimal perturbation respectively, for $T = 4.8$.

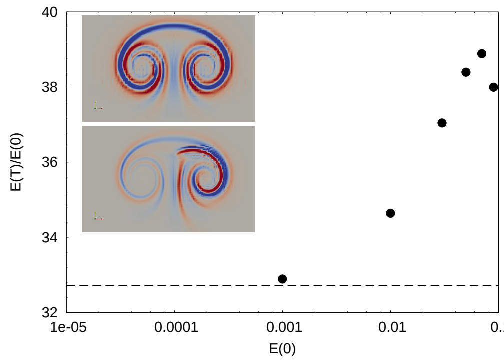

Figure 2. Optimal perturbation in double vortex system for $Re = 1000$: variation of gain with initial energy of the perturbation. The gain obtained by linear analysis is shown via a broken line. The top and bottom insets show the vorticity field associated with the linear and $E(0) = 0.07$ non-linear optimal perturbation respectively, for $T = 0.5$.

ONE-WAY NAVIER-STOKES EQUATIONS: OPTIMAL DISTURBANCES

Georgios Rigas[1], Oliver Schmidt[1], Tim Colonius[1] & Michael Beyar[2]
[1]*California Institute of Technology, Pasadena, CA, USA*
[2]*Boeing Research & Technology, Huntington Beach, CA, USA*

Optimal modes describing the fluctuating hydrodynamic and acoustic fields of slowly-varying flows are obtained in a computationally efficient way by spatially marching the linearized One-Way Navier-Stokes (OWNS) equations [3, 2]. An adjoint-based optimization framework is proposed and demonstrated for calculating optimal boundary conditions and optimal volumetric forcing that maximize the energy of the fluctuating field by iteratively space-marching the direct and adjoint OWNS equations. The resulting optimal OWNS response modes are validated against modes obtained in terms of global resolvent analysis by performing a singular value decomposition of the discretized global resolvent operator.

The above framework is demonstrated by performing a linear analysis of the mean flow of a turbulent Mach 1.5 high Reynolds number jet in order to predict large-scale wavepacket structures and their acoustic radiation. Two scenarios are considered in the present analysis. In the first case, no restriction is applied to the spatial forcing distribution. In the second scenario, the forcing is restricted to the nozzle exit plane. The resulting optimal and suboptimal modes are compared to spectral proper orthogonal modes obtained from a high-fidelity large eddy simulation[1]. For the supersonic jet examined here, we show that volumetric and inlet-restricted forcing produce the same optimal modal shape for the perturbation field in the frequency range dominated by the spatially unstable Kelvin-Helmholtz (K-H) mechanism. For this regime, the optimal forcing is localized in a region close to the nozzle exit and the local K-H mode approximates to a reasonable extent the optimal boundary condition. The optimal response modes are in good agreement with the frequency POD modes extracted from the LES data for both the hydrodynamic and acoustic fields. Good agreement is obtained also for suboptimal modes when compared against the second most energetic POD modes. Although the suboptimal modes at the K-H frequency range have a less pronounced role in terms of amplification, for very low frequencies they dominate the flow response. This explains the failure of Parabolized Stability Equations to capture the flow patterns at low frequencies, since they are typically initialized with the K-H eigenmode. Our findings suggest that, instead of a single spatially unstable mode, a family of spatially stable modes with distributed spatial forcing are responsible for the flow pattern at these frequencies. These modes can be efficiently modeled using optimal OWNS equations, which provide an an efficient framework for capturing modal and non-modal instabilities.

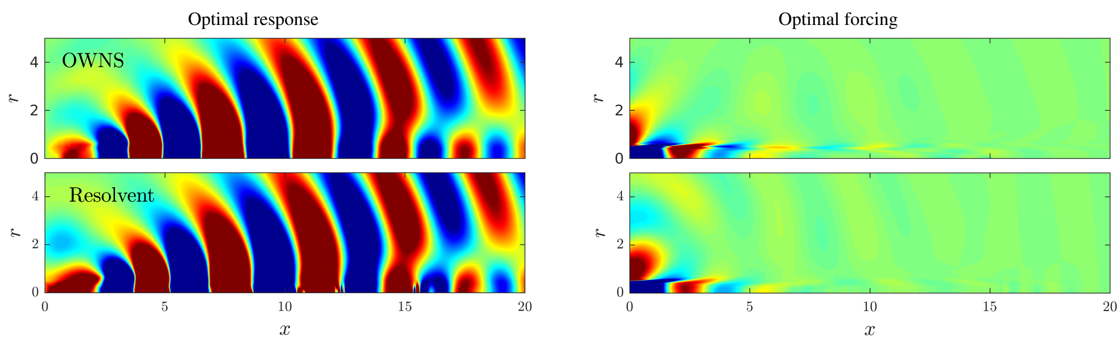

Figure 1. Optimal response modes (left) and volumetric forcing (right) obtained from optimal OWNS equations (top) and global resolvent analysis (bottom). OWNS modes are obtained in a computationally efficient way by iteratively space-marching the OWNS equations. Pressure perturbation field (real part) for frequency $St = 0.2$ with azimuthal wavenumber $m = 0$ for a turbulent Mach 1.5 jet.

We acknowledge the support of the Boeing Company through a Strategic Research and Development Relationship Agreement CT-BA-GTA-1. This research was also supported in part by a grant from the Office of Naval Research (grant No. N00014-16-1-2445) with Dr. Knox Millsaps as program manager.

References

[1] G. .A Brès, V. Jaunet, M. Le Rallic, P. Jordan, T. Colonius, and S. K. Lele. Large eddy simulation for jet noise: the importance of getting the boundary layer right. In *21st AIAA/CEAS Aeroacoustics Conference*, **AIAA 2015-2535**, Dallas, TX, 2015.
[2] G. Rigas, T. Colonius, and M. Beyar. Stability of wall-bounded flows using one-way spatial integration of Navier-Stokes equations. In *55th AIAA Aerospace Sciences Meeting*, **AIAA 2017-1881**, Grapevine, TX, 2017.
[3] A. Towne and T. Colonius. One-way spatial integration of hyperbolic equations. *Journal of Computational Physics*, **300**:844–861, 2015.

EXPERIMENTS WITH DISTURBANCES ON THE FLOW THROUGH A SUDDEN EXPANSION IN A CIRCULAR PIPE

B. Lebon [1,*], M. Q. Nguyen[2], S. Ishizaka[3], Y. Tasaka[3], M. Safdari Shadloo[2], A. Hadjadj[2] & J Peixinho[1]

[1] *Laboratoire Ondes et Milieux Complexes, CNRS and Université Le Havre Normandie, France*

[2] *CORIA, Normandie University, CNRS-University and INSA of Rouen, 76000 Rouen, France*

[3] *Laboratory for Flow Control, Hokkaido University, Sapporo, Hokkaido, Japan*

The study of transition to turbulence in pipe flow with a sudden expansion has been less studied than the uniform pipe case. Recently, Selvam *et al.* [1] have shown that the circular pipe flow with an expansion is sensitive to the disturbance at the inlet and can initiate localised turbulence. Specifically the most energetic modes are located in the center of the pipe, instead of near the wall. This imply that the mechanism leading to the transition to turbulence differs from the one in uniform pipe flow. To experimentally characterise the transition to turbulence, an experimental set-up was design (see figure 1(a)). The flow rate is controlled by valves, allowing an accurate selection of the Reynolds number. The novelty here is the possibility of injecting controlled perturbation five diameters before the expansion in the inlet pipe. Two types of perturbations are investigated: (i) a constant flow jet and (ii) a synthetic jet actuator. At low Reynolds number, a recirculation area (see figure 1(b)) develops at the expansion [2] and interacts with the main flow. This kind of interaction has been study in the case of plane expansion [3] or backward-facing step [4], but a complete experimental investigation is still needed in the circular case. The governing parameters of disturbances are:

- $V_r = U_j/U$ the ratio of jet velocity U_j and inlet bulk velocity U
- $S_t = fd/U$ the Strouhal number, based on the pipe inlet diameter d and the actuator frequency f

The present study aims at characterising the effect of disturbances using flow visualization and PIV measurements. An example of a spatio-temporal diagram of flow visualisation is provided in figure 1(b), where the injection of a constant cross-flow jet initiates localised turbulence. Once the injection is stopped, the flow become laminar again. The lifetime and length of the turbulent patch will be compared with numerical simulations in order to have a better understanding of the transition to turbulence in the flow through a sudden expansion in a circular pipe.

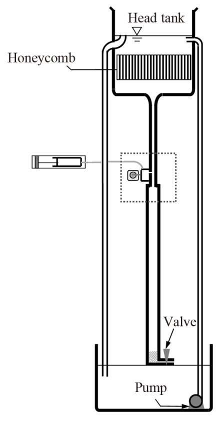

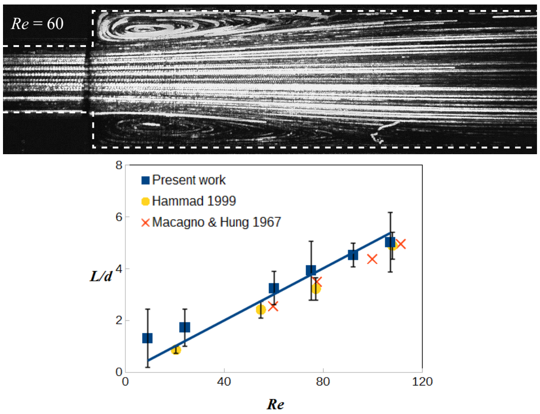

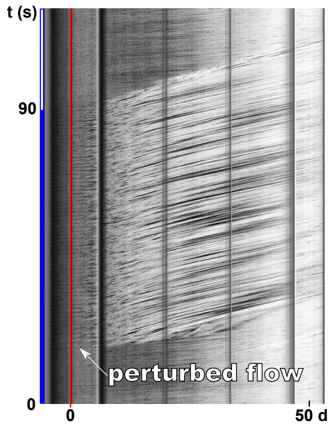

Figure 1. (a) Sketch of the expansion pipe setup. (b) Long-exposure photography of the recirculation region for $Re = 60$ and the axial recirculation length as a function of Re. (c) Spatio-temporal diagram taken at the center of the pipe for a constant flow jet disturbance at $Re = 900$ and $V_r = 0.42$. The disturbance is injected up to $t = 90$ s.

References

[1] K. Selvam, J. Peixinho, and A. P. Willis. Flow in a circular expansion pipe flow: effect of a vortex perturbation on localised turbulence. *Fluid Dyn. Res.*, 48(6):061418, 2016.

[2] H. J. Khaled, M. V. Ötügen, and E. B. Arik. A PIV study of the laminar axisymmetric sudden expansion flow. *Exp. Fluids*, 26(3):266–272, 1999.

[3] R. M. Fearn, T. Mullin, and K. A. Cliffe. Nonlinear flow phenomena in a symmetric sudden expansion. *J. Fluid Mech.*, 211:595–608, 1990.

[4] T. Berk, T. Medjnoun, and B. Ganapathisubramani. Entrainment effects in periodic forcing of the flow over a backward-facing step. *arXiv preprint arXiv:1702.06895*, 2017.

*Corresponding author: benoit.lebon@etu.univ-lehavre.fr

PASSIVE TRANSITION CONTROL IN SUPERHYDROPHOBIC CHANNEL FLOW

F. Picella[1], J.-C. Robinet [1] & S.Cherubini [2]
[2]*DMMM, Politecnico di Bari, Bari, Italia*
[1] *DynFluid, Arts et Métiers Paristech, Paris, France*

SUPERHYDROPHOBIC SURFACES (SHS) are known to relief friction-drag due to the no-slip wall boundary condition. Under certain conditions gas bubbles can be trapped within SHS's micro-sculpture, resulting in a lubricating gas matress onto which a flow can be sustained. Our aim is to investigate if such bio-mimetic surfaces can be engineered in order to obtain a form of PASSIVE CONTROL capable of delaying transition and reduce drag in a shear-dominated configuration, namely transitional channel flow.

Being still out of reach discretising both the micro and macroscopic scales at once, we have modeled SHS by using a Robin (mixed Neumann-Dirichlet) boundary condition, therefore introducing a *slip-length*, which is a widespread solution in literature[1]. SHS is therefore flat and inconditionally stable. It is known that both in laminar [2] and turbulent [3] regimes SHS are capable of increasing critical Reynolds number and decreasing Re_τ respectively by throttling the slip length. On the other hand macroscopically homogeneous SHS have proven to be slightly affected by such *gas lubricated surface* for slip length sitting in a experimentally observable range. Transition is generally characterised by the appearance of spatially localized COHERENT STRUCTURES. Our gist is to *warp* these latter in order to control transition, by the use of spatially inhomogeneous SuperHydrophobic Patches (SHP). We have chosen to focus on the K-type transition scenario for Plane Poiseuille Flow (PPF) [4], since it is amongst the others the most influenced by near-wall structures (Tollmien-Schlischting waves), hence more probably by our wall-confined passive control technique. It has been found that, depending on the initial perturbation (IP)–SHP alignment, λ vortices can be stretched, shrinked nor annihiliate for a given IP amplitude.

Despite the fact that both laminar and turbulent regimes are mildly affected, our preliminary results shows how transition can be substantially advanced//retarded depending on the spatial localization of superhydrophobic patches.

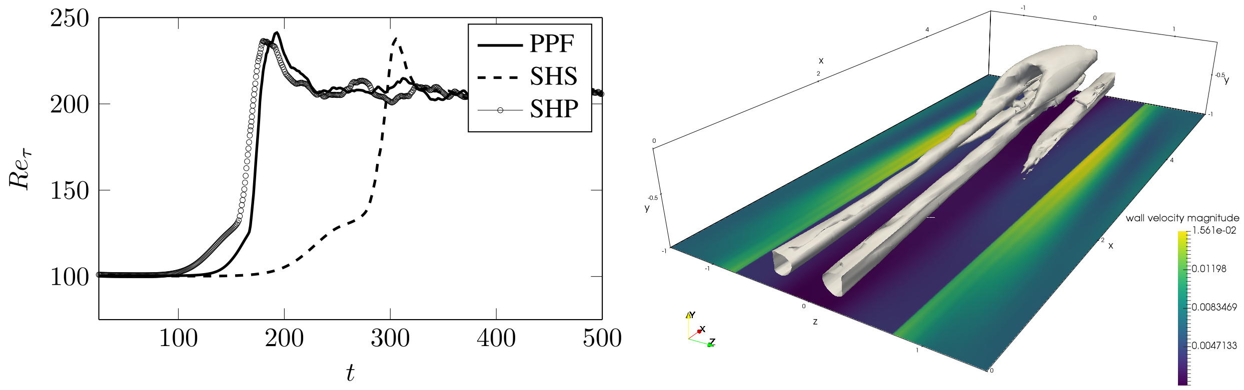

Figure 1. Detecting Transition with Re_τ and visualizing warped hairpin onto SHP, $\lambda_2 = -0.005$

References

[1] Jin Lee, Thomas O. Jelly, and Tamer A. Zaki. Effect of reynolds number on turbulent drag reduction by superhydrophobic surface textures. *Flow, Turbulence and Combustion*, **95**(2):277–300, 2015.

[2] Taegee Min and John Kim. Effects of hydrophobic surface on skin-friction drag. *Physics of Fluids*, **16**(7):L55–L58, 2004.

[3] Hyunwook Park, Hyungmin Park, and John Kim. A numerical study of the effects of superhydrophobic surface on skin-friction drag in turbulent channel flow. *Physics of Fluids*, **25**(11):110815, 2013.

[4] Philipp Schlatter, Steffen Stolz, and Leonhard Kleiser. LES of transitional flows using the approximate deconvolution model. *The international journal of heat and fluid flow*, **25**(3):549–558, June 2004.

[5] K. H. Yu, C. J. Teo, and B. C. Khoo. Linear stability of pressure-driven flow over longitudinal superhydrophobic grooves. *Physics of Fluids*, **28**(2):022001, 2016.

TRANSITION TO TURBULENCE IN A SUDDEN EXPANSION PIPE FLOW

Minh-Quan Nguyen[1], Benoit Lebon [2], Mostafa Safdari-Shadloo [1,*], Jorge Peixinho[2], Abdellah Hadjadj[1]
[1] *CORIA-UMR 6614, Normandie University, CNRS-University and INSA of Rouen, 76000 Rouen, France*
[2]*Laboratoire Ondes et Milieux Complexes, CNRS and Université Le Havre Normandie, France*

Flow in a sudden expansion pipe is a basic fluid mechanics problem that has both fundamental and practical interests. One of the crucial issue in studying flow bifurcation and transition to turbulence in pipes is a gap of critical Reynolds number predicted by simulations and the one found in experiments. This gap is believed to be caused by the imperfections that are always present in the experiments. Beside the natural transition, which is difficult to predict, the simulations very often use finite-amplitude forced perturbations to trigger the transition. Better understanding of this "forced" turbulence state could help to understand the difference between experimental and numerical predictions. The recent numerical investigation of Sanmiguel-Rojas & Mullin [2] shows the existence of a hysteresis cycle when varying the Reynolds number ($Re = Ud/\nu$, with d the inlet diameter, U the mean inlet velocity and ν the kinematic viscosity) around its critical value. The extent of this hysteresis loop is surprisingly large (varying from $Re = 1450$ to 1850). The underlying mechanisms that govern the transition are far from being completely understood, and the transition mechanism is extremely sensitive to the shape and energy of the initial perturbation. Hence, one need to know how the transition occurs precisely and how long the system stands before laminar or turbulent states occur. Also, the question of the existence or not of a hysteresis phenomenon must be clearly answered. In this study, we further investigated this problem using a spectral element code (based on Nek5000 [1] solver) along with a vortex perturbation method with a given amplitude $\mathcal{A}$. The simulation set-up is described in [3]. We found that the turbulence state seems to be different while varying the two main parameters: Re and $\mathcal{A}$. The space-time diagrams, plotted below, show the signature of the different instabilities, that can be summarized as follow:

- Periodical burst that appear around $25\,d$ after the expansion for $Re = 1300$ and $\mathcal{A} = 0.5$.
- Steady production of turbulence around $15\,d$ after the expansion for $Re = 2000$ and $\mathcal{A} = 0.2$.
- Any change of physical parameters (Re or $\mathcal{A}$) or numerical (order of time interpolation) will generate turbulence (around 10 to $15\,d$ after the expansion) that get carried downstream and decays: see figure 1(b) and 1(c).
- Under certain conditions, turbulence can be re-generated far downstream (around 50 d after the expansion) and at later times: see space-time diagram in figure 1(c) at $t = 1000$ and the 3D flow structure in figure 1(a).

Full details, including the development of 3D instability structures along with the pattern of unstable modes, will be presented during the colloquium.

(a) $Re = 1400$, $\mathcal{A} = 0.2$ (b) $Re = 1300$, $\mathcal{A} = 0.2$ (c) $Re = 1400$, $\mathcal{A} = 0.2$

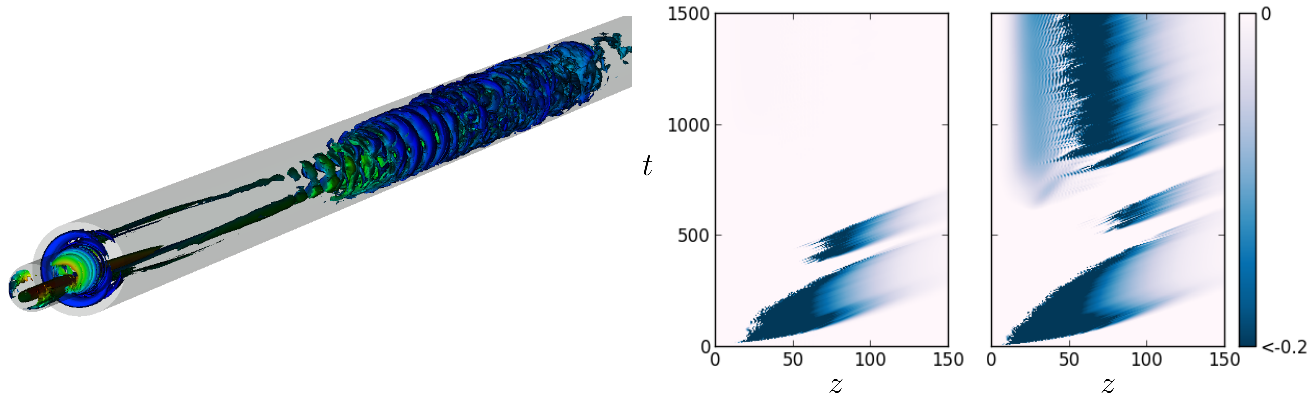

Figure 1. (a)- Iso-contour of λ_2 coloured by velocity magnitude. (b,c)- Spatio temporal diagram of the perturbed axial velocity: $v_z(t) - v_z(t = 0)$ for different Re and $\mathcal{A}$. Here, t is the simulation time expressed in d/U and z the distance from the expansion section expressed in d.

References

[1] P. Fisher, J. Kruse, J. Mullen, H. Tufo, J. Lottes, and S. Kerkemeier. nek5000: Open source spectral element CFD solver.

[2] E. Sanmiguel-Rojas and T. Mullin. Finite-amplitude solutions in the flow through a sudden expansion in a circular pipe. *J. Fluid Mech.*, **691**:201–213, 2012.

[3] K. Selvam, J. Peixinho, and A. P. Willis. Flow in a circular expansion pipe flow: effect of a vortex perturbation on localised turbulence. *Fluid Dyn. Res.*, **48**(6):061418, 2016.

*Corresponding author: msshadloo@coria.fr

ROUTES TO CHAOS FROM AXISYMMETRIC THERMAL VERTICAL VORTICES IN A ROTATING CYLINDER

Damián Castaño[1], María Cruz Navarro [1] & Henar Herrero [1]
[1]*Dpto. Matemáticas, Universidad de Castilla-La Mancha, 13071 Ciudad Real, Spain*

In this work we study several routes of the transition from a steady axisymmetric vertical vortex to a chaotic flow in a rotating cylinder depending on thermal gradients and rotation rates. The analysis is done using nonlinear simulations. For a fixed rotation rate, the chaotic regime appears, as thermal gradients increase, after a sequence of supercritical Hopf bifurcations to periodic, quasiperiodic and chaotic flows in a scenario similar to the Ruelle-Takens-Newhouse route to chaos. For moderate values of the rotation rate we find vortices that tilt and displace from the center of the cylinder in a periodic, quasiperiodic and finally chaotic movement around the central axis. For larger rotation rates the axisymmetric vortex splits into two symmetric vortices that move periodically around the central axis, and lose the symmetry merging again in one non-axisymmetric vortex that moves around the central axis quasiperiodically and later chaotically. The transitions to chaos when the rotation rate is varied at fixed thermal gradients reveal also the appearance of periodic, quasiperiodic and chaotic states in different routes. Tilted single vortices, double vortices and more complex structures with multiple vortices are reported in this case. The transitions are studied through a force balance analysis. Results are of interest as they connect to the behavior of some atmospheric vertical vortices. These results are a continuation of those in Ref. [1], and have been published in Ref. [2].

References

[1] D. Castaño, M.C. Navarro and H. Herrero. Double vortices and single-eyed vortices in a rotating cylinder under thermal gradients. *Computers and Mathematics with Applications* **73**: 2238-2257, 2017.
[2] D. Castaño, M.C. Navarro and H. Herrero. Routes to chaos from axisymmetric vertical vortices in a rotating cylinder. Submitted, 2017.

EXPERIMENTAL STUDY OF A ROTATING SPLIT-CYLIDNER FLOW. FIRST RESULTS

Jesús O. Rodríguez-García[1] & Javier Burguete [1]
[1]*Dpto. de Física y Matemática Aplicada, Universidad de Navarra, C/ Irunlarrea 1, 31008 Pamplona, Spain*

There exist lots of natural and industrial processes where rotating and turbulent flows are present like tornadoes or industrial mixers. This fact has provoked much research to better understand this kind of flows. On one hand, geophysical flows have a complex behavior which is mainly turbulent, appearing different instabilities, and it isn't fully understood. On the other hand, this kind of behavior also appears in many enclosed flows which rules the dynamic of the system, like liquid mixing processes or liquid transport through pipes. These different situations can be considered as confined systems in which lots of questions remain unanswered yet.
In order to better study these flows, different experiments using a von Kármán flow driven by propellers have been performed in our group (see [1], [6], [4]) finding very rich phenomena. Now, we have developed a new experimental device motivated by different numerical simulations (see [2], [5], [3]).
The new experimental setup consists in a split-cylinder in which each half of the cylinder moves jointly with each end cap (see Fig. 1). Both halves can move in co-rotation or in counter-rotation. Moreover, we can set the rotating velocity of both halves independently. In this configuration the internal radius of the cylinder R is fixed, but we can change the length L of both halves using wider end caps, so we can change the aspect ratio defined as $\Gamma = 2L/R$.

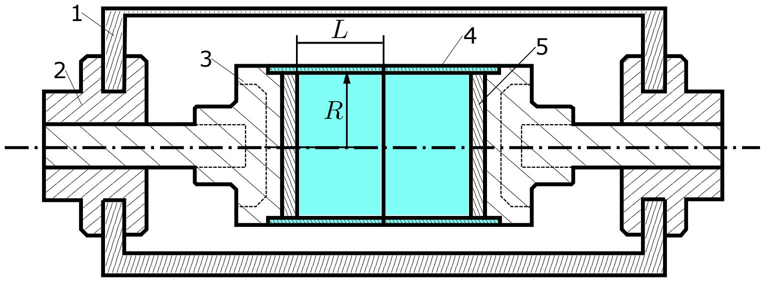

Figure 1. Cross section of the experimental device: (1) aluminum cell; (2) shaft backing; (3) shaft set; (4) methacrylate split-cylinder; (5) end cap. All the cell is filled with the working fluid.

With the new setup we can study the laminar flow produced at low Reynolds numbers (Re) and the transition to turbulence or the different symmetry-breaking that should appear when the Re increases according to [2], [5] and [3]. In order to sweep a large Re range we can use silicone-oil ($140cSt$ at $40°C$) or water as working fluid. The velocity field developed inside the split-cylinder is measured using both experimental techniques: LDV and PIV. More concretely, we measure the velocity of silver coated hollow glass spheres ($D = 14\mu m$, $\rho = 1.65g/cm^3$) seeded inside the split-cylinder.
The first results have been obtained in co-rotation applying an asymmetric rotation velocity. We have set a main rotating velocity Ω and a differential rotating velocity ω so the right-half rotation velocity is $\Omega + \omega$ and the left-half rotation velocity is $\Omega - \omega$. Assuming that ν is the kinematic viscosity of the working fluid, we can characterize the flow inside the split-cylinder in function of the Re and the Rossby number Ro defined as follows

$$Re = \frac{\Omega R^2}{\nu}, \quad Ro = \frac{\omega}{\Omega}. \tag{1}$$

Here, we will present the 2D spatial average flow and the time series of the behavior of the flow for the experimental parameters.

References

[1] A. de la Torre and J. Burguete. Slow Dynamics in a Turbulent Von Kármán Swirling Flow. *PRL*, **99**:054101, 2007.
[2] P. Gutierrez-Castillo and J. M. Lopez. Instabilities of the sidewall boundary layer in a rapidly rotating split cylinder. *J. Mechanics B: Fluids*, **52**:76–84, 2015.
[3] P. Gutierrez-Castillo and J. M. Lopez. Nonlinear mode interactions in a counter-rotating split-cylinder flow. *J. Fluid Mech.*, **816**:719–745, 2017.
[4] O. Liot and J. Burguete. Bifurcation induced by the aspect ratio in a turbulent von Kármán swirling flow. *Phys. Rev. E*, **95**:013101, 2017.
[5] J. M. Lopez and P. Gutierrez-Castillo. Three-dimensional instabilities and inertial waves in a rapidly rotating split-cylinder flow. *J. Fluid Mech.*, **800**:666–687, 2016.
[6] M. López-Caballero and J. Burguete. Inverse Cascades Sustained by the Transfer Rate of Angular Momentum in a 3D Turbulent Flow. *PRL*, **110**:124501, 2013.

LINEAR EVOLUTION OF COMPRESSIBLE GÖRTLER INSTABILITY TRIGGERED BY FREE-STREAM VORTICAL DISTURBANCES

Samuele Viaro[1] & Pierre Ricco [1]
[1]*The University of Sheffield, Sheffield, UK*

A rigorous theory for boundary-layer receptivity to free-stream perturbations must include the interaction of outer on-coming free-stream disturbances (region FS, Fig.1a) with boundary-layer perturbations (region III, Fig.1a) and the correct initial perturbation field in the proximity of the leading edge, uniquely determined by the free-stream flow. We adopt this theoretical framework by combining the work of [1] and [2] to study the receptivity of Görtler unstable compressible vortices generated by free-stream vortical disturbances (FSVD). The equations describing the boundary-layer dynamics are the unsteady compressible boundary-region equations, i.e. the full Navier-Stokes equations with the streamwise pressure gradient and the streamwise viscous diffusion terms neglected. Asymptotic matching allows initial and boundary conditions to be directly connected to the FSVD imposed on the mean oncoming flow (Fig.1a). Neglecting the interaction with free-stream disturbances, an eigenvalue (EV) framework was derived from the previous initial boundary value (IBV) framework. Numerically, the system of equations for both frameworks are solved with in-house finite difference codes of the second order accuracy. The influence of frequency F, curvature and compressibility along the scaled streamwise coordinate $\hat{x}$ is investigated using flow parameters from wind tunnel studies on subsonic and supersonic boundary-layers. The main findings are summarized as follows:

- curvature effects exponentially amplify the instabilities triggered by FSVD;
- compressibility, high-frequency disturbances and small curvature have a stabilizing effect on the flow;
- perturbations with increased stability are shifted away from the wall, inducing regions of unperturbed flow;
- the streamwise wavelength of the perturbations approaches the free-stream value as the flow stabilizes;
- only the IBV framework can fully capture the growth rate of the perturbations σ_{Re} =fn$(\hat{x}, \eta)$;
- sufficiently downstream from the leading edge, the EV solution could be justifiable (Figure 1b).

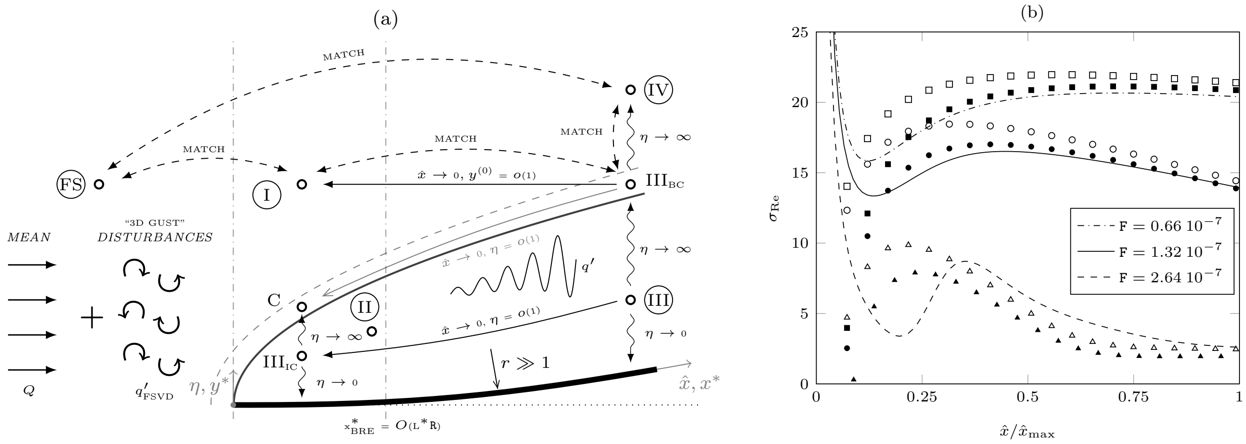

Figure 1: Sketch of the asymptotic matching between regions of the domain (a). Streamwise evolution of the growth rate σ_{Re} from the IBV solution at $\eta = 2.0$ (lines), parallel EV solution (empty symbols) and non-parallel EV solution (full symbols) for $r^* = 10$m, M $= 0.5$ (b).

References

[1] P. Ricco and X. Wu. Response of a compressible laminar boundary layer to free-stream vortical disturbances. *J. Fluid Mech.*, **587**:97–138, 2007.
[2] X. Wu, D. Zhao, and J. Luo. Excitation of steady and unsteady Görtler vortices by free-stream vortical disturbances. *J. Fluid Mech.*, **682**:66–100, 2011.

Boundary-layer transition over concave surfaces caused by centrifugal forces

Margio Méndez-González[1], Mostafa Safdari-Shadloo[1,*], Abdellah Hadjadj[1], Antoine Ducoin[2]
[1]CORIA Laboratory-UMR 6614, Normandie University, CNRS-University & INSA de Rouen, 76000 Rouen, France
[2]LHEEA Laboratory, Ecole Centrale de Nantes (CNRS UMR 6598), 44300 Nantes, France

Boundary-layer instabilities cannot develop similarly over concave and flat plates. The boundary layer forming on concave surfaces is known as the Görtler boundary layer [1] and is different from that of a flat plate. The prominent characteristic of Görtler flows is the presence of a centrifugal force acting on the fluid in the wall-normal direction. This resulting force makes the flow prone to centrifugal instabilities that may be triggered by radial displacements of the fluid caused by different type of perturbations. These centrifugal instabilities, that start the transition process, are characterized by being streamwise-oriented and having a counter-rotating motion; and are known as Görtler vortices [2].

As the flow develops in the streamwise direction, three different regions can be distinguished, namely linear, nonlinear and transitional regions [3]. The beginning of the nonlinear region is identified with the departure from the Blasius solution due to the inception of the Görtler vortices. These vortices generate a spanwise variation of the streamwise velocity resulting in a wavy velocity profile that can be divided into two regions, an upwash and a downwash region. Downstream, the Görtler vortices develop into secondary instabilities that are identified with a meandering motion (sinuous mode) and the generation of horseshoe vortices (varicose mode). Finally, in the transition region, the secondary instabilities breakdown into turbulence and a homogenous turbulent flow in the spanwise direction is observed where the upwash and downwash regions are no longer discriminated.

Although some efforts have been made to characterize flows over concave surfaces, different transition scenarios caused by such instabilities are not yet well understood. Highlighting the most recent studies, Tandiono et al. [3] experimentally analyzed a domain in which the streamwise length was not large enough to obtain a turbulent homogeneous flow in the spanwise direction; and, the upwash and downwash regions could still be observed. Numerically, Schrader et al. [4] performed a spatial direct numerical simulation (DNS) but only spanwise average values were reported and, thus, there was no spanwise local information that could allow to determine the length of this region. Hence, the present work includes spanwise local characterization of the transition region that can allow to determine its length and the start of a complete spanwise homogenous turbulent flow.

Additionally, most DNS studies of Görtler vortices have considered a temporal framework and there are only few DNS studies reporting the spatio-temporal development of the Görtler instabilities [4,5]. Furthermore, the breakdown to turbulence is not well documented and to the best of the author's knowledge the details of turbulent flow caused by Görtler breakdown has not been reported in the literature so far. Therefore, in order to enrich the available literature and to better highlight the transition mechanism, the present study aims at characterizing the transition scenarios in spatially-evolving flows over concave walls through fully resolved DNS. The study includes a parametric analysis in which concave plates with different radii (R) are tested with a series of wall roughness elements utilized as source of excitation. It is found that the inception of transition is postponed for smaller wall curvatures; however, the transition Görtler number is identical, for all cases, when the streamwise coordinate is non-dimensionalized. Moreover, only with high-resolution simulations, the transition region, characterized by the breakdown of the typical mushroom structure created in the upwash region [2], can be captured. Due the wall roughness elements imposed at the inlet, a clean transition is observed for the very first time where symmetric mushroom structures are elongated and transformed into a filament structure prior to their breakdown. Three-dimensional coherent structures in the transition region are then utilized to explain some of the observed phenomena.

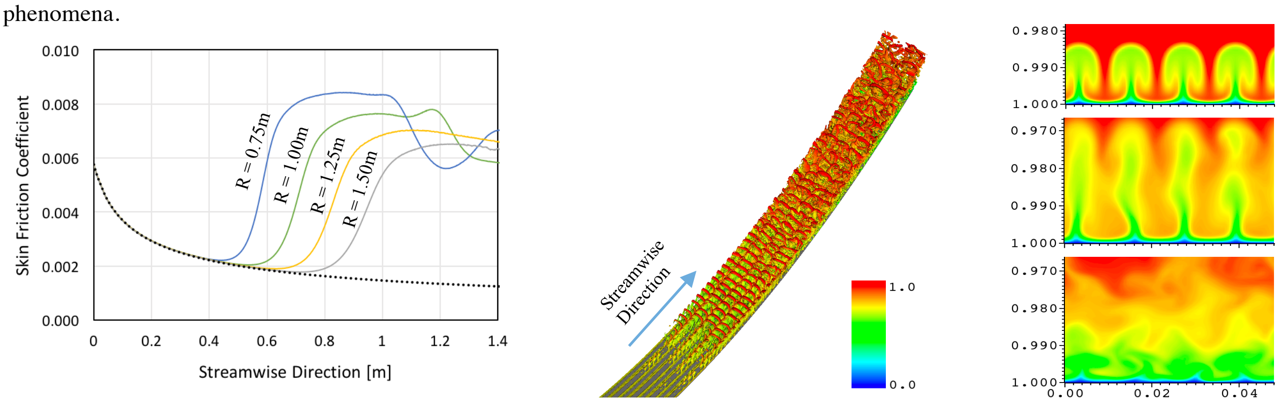

Figure 1. At left, streamwise wall shear stresses development which depart from the Blasius solution (dotted line) showing a delay in the start of the transition process due to a decrease in the curvature. At center, iso-surfaces of λ_2 colored with U/U_∞ showing the breakdown into turbulence of the horseshoe vortices for the case with concave plate with R = 1m. At right, U/U_∞ at different streamwise positions (x = 1.1m, 1.9m, 2.4m) showing the development and breakdown of mushroom structures (vertical axis: radial coordinate, horizontal axis: spanwise coordinate, in meters) also for the case R = 1m. Incompressible flow. $Re_x = 1.3x10^4$ at entrance.

References

[1] Görtler, H. On the three-dimensional instability of laminar boundary layers on concave walls. NACA-TM-1375. 1954
[2] Floryan, J. M. On the Görtler instability of boundary layers. Prog. Aerosp. Sci. **28** (3), 235-271. 1991
[3] Tandiono, S., Winoto, H. & Shah, D. A. Wall shear stresses in Görtler vortex boundary layer flow. Phys. Fluids. **21**, 084106. 2009
[4] Schrader, L.-U., Brandt, L., Zaki, T. A. Receptivity, instability and breakdown of Görtler flow. J. Fluid Mech. **628**, 362-396. 2011
[5] Ducoin, A., Shadloo, M. S., Roy, S. Direct Numerical Simulation of flow instabilities over Savonius style wind turbine blades. Renewable Energy.**105**, 374-385. 2017

*Corresponding Author: msshadloo@coria.fr

NONLINEAR THERMOACOUSTICS: FLAMES ON THE EDGE OF CHAOS

Matthew Juniper[1]
[1] *Engineering Department, University of Cambridge, Trumpington Street, Cambridge, UK*

Thermoacoustic oscillations occur when a flame is confined within an acoustic cavity, such as a combustion chamber. Their amplitude grows if the oscillating flame releases more heat at times of higher pressure and less heat at times of lower pressure. The phase between the pressure and the additional heat release is critical. It can vary from cycle to cycle, resulting in quasiperiodic, multi-periodic, or chaotic oscillations, as observed in experiments and numerical simulations.

Simulations also reveal a multitude of periodic and quasiperiodic unstable attractors, which attract the system in many directions in phase space and repel in one direction. The system's state can pass within the vicinity of several unstable attractors before arriving at a stable attractor, which has similar features to bypass transition to turbulence in hydrodynamics. Sometimes small differences in initial states lead to diverging paths in phase space and different final states.

In some linearly stable thermoacoustic systems, thermoacoustic oscillations can be triggered by a small pulse. A simple thermoacoustic system containing a stable fixed point, an unstable periodic solution and a stable periodic solution is examined. The 'minimal seed' is found with nonlinear adjoint looping. Growth to the stable periodic solution is shown to exploit non-normal transient growth around the unstable periodic solution, rather than non-normal transient growth away from the fixed point.

CLOSED-LOOP FLOW CONTROL USING A LINEARIZED APPROACH AROUND THE MEAN FLOW

Colin Leclercq[1], Charles Poussot-Vassal [2], Denis Sipp [1] & Éric Garnier [1]
[1] *ONERA, DAAA, Meudon, France*
[2] *ONERA, DCSD, France*

Closed-loop flow control requires the synthesis of a model capturing the input-output behaviour between actuators and sensors. System identification techniques can be used to obtain the relationship between inputs and outputs directly from data [3, 4], but lack physical insight. Alternatively, physics-based models can be derived by projecting the governing equations onto an appropriate basis of modes (POD modes, global modes, BPOD modes, etc.) [6, 1]. In the case of linear models, the Navier–Stokes equations are linearized about their fixed point: the base flow. For strongly nonlinear flows, this approach may be ineffective as the system evolves far from the fixed point. However, *dynamic linearity* may still occur, where the response to a small-amplitude momentum forcing $a(t)\mathbf{f}_c$ is a small perturbation $\mathbf{u}_c(t)$ of the natural dynamics [3, 4]. We therefore seek to obtain a linear model by considering small perturbations of the *mean flow* $\overline{\mathbf{u}}$ rather than the base flow $\mathbf{u}_b$. This approach involves the *resolvent* operator $\mathcal{R}(\omega, \mathcal{L}_{\overline{\mathbf{u}}})$, which depends on the angular frequency ω and the Jacobian $\mathcal{L}_{\overline{\mathbf{u}}}$ about the mean flow [5, 2]. The open-loop transfer function between the Fourier transforms of the forcing amplitude a and of a measurement $m = \langle \mathbf{m}, \mathbf{u}_c \rangle$ is simply given by

$$G(\omega) = \langle \mathbf{m}, \mathcal{R}(\omega, \mathcal{L}_{\overline{\mathbf{u}}})\mathbf{f}_c \rangle, \tag{1}$$

where $\langle \cdot, \cdot \rangle$ is the canonical inner product between two complex fields, $\mathbf{f}_c$ and $\mathbf{m}$ are two fields characterising the actuator and the sensor, and $\|\mathbf{f}_c\| = 1$. This expression can then be used to design a linear controller, which is valid in the vicinity of the unperturbed mean flow. As control is applied, the flow drifts towards a new mean state, and the control law may then be adapted to follow these changes. Since the mean flow incorporates information about nonlinearities, we hope to demonstrate that the method efficiently captures the input-output behaviour in flows at large Reynolds numbers, while being much simpler to implement than more traditional POD-based models [6].

As a first step, the method is validated on the incompressible two-dimensional cavity flow described in Barbagallo *et al.* [1] (see figure 1). We will then assess the efficiency of the approach on a noise-amplifier flow (backward facing step) and at higher Reynolds number $Re = O(10^{4-5})$, using ZDES models of these flows.

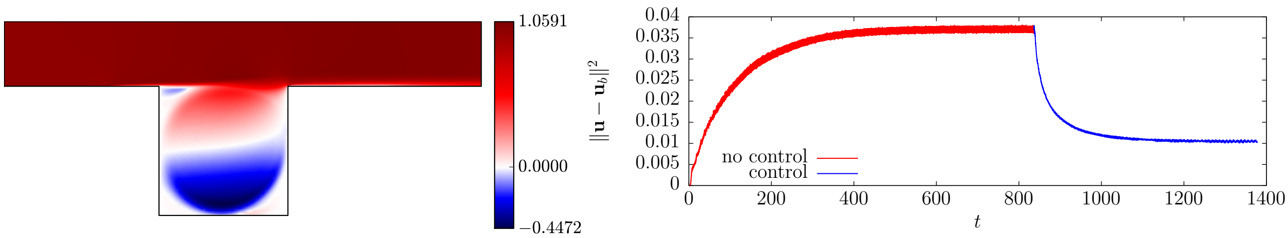

(a) (b)

Figure 1: (a) Streamwise velocity component of the mean flow $\overline{\mathbf{u}}$ over an open cavity at $Re = 7500$ (same model as [1], using FreeFem++). (b) Timeseries of the perturbation kinetic energy with respect to the base flow; the flow is initalized with the base flow and a small perturbation parallel to the most unstable eigenmode. The controller, designed from within the limit cycle, leads to a large decrease ($> 70\%$) of the perturbation kinetic energy before saturation to a new mean state. The actuator is located at the upstream edge while the shear stress sensor is near the downstream edge [1].

References

[1] A. Barbagallo, D. Sipp, and P. J. Schmid. Closed-loop control of an open cavity flow using reduced-order models. *J. Fluid Mech.*, **641**:1–50, 2009.
[2] S. Beneddine, D. Sipp, A. Arnault, J. Dandois, and L. Lesshafft. Conditions for validity of mean flow stability analysis. *J. Fluid Mech.*, **798**:485–504, 2016.
[3] A. S. Dahan, J. A .and Morgans and S. Lardeau. Feedback control for form-drag reduction on a bluff body with a blunt trailing edge. *J. Fluid Mech.*, **704**:360–387, 2012.
[4] L. Dalla Longa, A. S. Morgans, and J. A. Dahan. Reducing the pressure drag of a d-shaped bluff body using linear feedback control. *Theo. Comput. Fluid Dyn.*, pages 1–11, 2017.
[5] B. J. McKeon and A. S. Sharma. A critical-layer framework for turbulent pipe flow. *J. Fluid Mech.*, **658**:336–382, 2010.
[6] M. Samimy, M. Debiasi, E. Caraballo, A. Serrani, X. Yuan, J. Little, and J. H. Myatt. Feedback control of subsonic cavity flows using reduced-order models. *J. Fluid Mech.*, **579**:315–346, 2007.

EFFECTS OF POROUS COATINGS ON FLOWS AROUND A 3D HEMISPHERE : APPLICATION TO FLOW CONTROL

Chloé Mimeau[1], Iraj Mortazavi [1] & Georges-Henri Cottet [2]
[1] *Laboratory M2N, CNAM, Paris, France*
[2]*Laboratory Jean Kuntzmann, Université Grenoble-Alpes, Grenoble, France*

Flows throughout porous media may be observed in multiple natural structures like vegetation canopies, birds' covert feathers or endothelial glycocalyx (also called "sweet shield") of blood vessels. The presence of such porous layers actually enables a damping of the flow-induced surface instabilities, therefore smoothing the flow dynamics in the vicinity of the solid-porous-fluid interface. Based on these observations, we perform in this work direct numerical simulations (DNS) of flow past a 3D hemisphere totally or partially covered with a porous layer. The main reason for choosing the hemisphere geometry is its similarity to the side view mirrors of a ground vehicle and the possible extension of this study to passive flow control and drag reduction.

In this study the hemisphere is covered with a permeable coating of thickness $\tau = 10\%$ of the hemisphere diameter and four different geometrical configurations are considered. The configuration 1 corresponds to a porous layer applied on the whole hemisphere surface, configuration 2 involves two porous poles on top and bottom of the body, configuration 3 contains a porous zone corresponding to the rotation of the previous poles around the z-axis (this case is denoted as "ring inlay") and configuration 4 implements an "annular coating", consisting in a thin porous ring. The simulations are performed at a low and a moderate Reynolds number, namely $Re = 300$ and $Re = 1000$. The results are compared to the one obtained with a fully solid sphere in terms of aerodynamic forces, phase diagrams and time averaged/instantaneous vorticity fields. It turns out that, for both Reynolds numbers, configuration 1 (porous layer) allows to recover a planar symmetric wake (which was not the case with the solid hemisphere) and configuration 3 (ring inlay) provides the best results in terms of drag reduction with -21% at $Re = 300$ and -16% at $Re = 1000$ compared to the solid body (cf Fig. 1).

The numerical method used in this study is an hybrid vortex-penalization method. The resolution of the fluid flow is performed with a semi-Lagrangian method called the remeshed vortex method [2] and the modeling of flow in solid-fluid-porous media is realized through an immersed boundary approach called the Brinkman penalization method consisting in adding a forcing term, derived from the Darcy equation, in the Navier-Stokes equations [1].

A 3D linear global stability analysis [3] is being developped at $Re = 300$ in the context of the present hybrid vortex penalization method. It will allow to study the effects of porous coatings on the unstable global mode in flow past a hemisphere and to explain the delay in transition achieved with configurations 1 and 3.

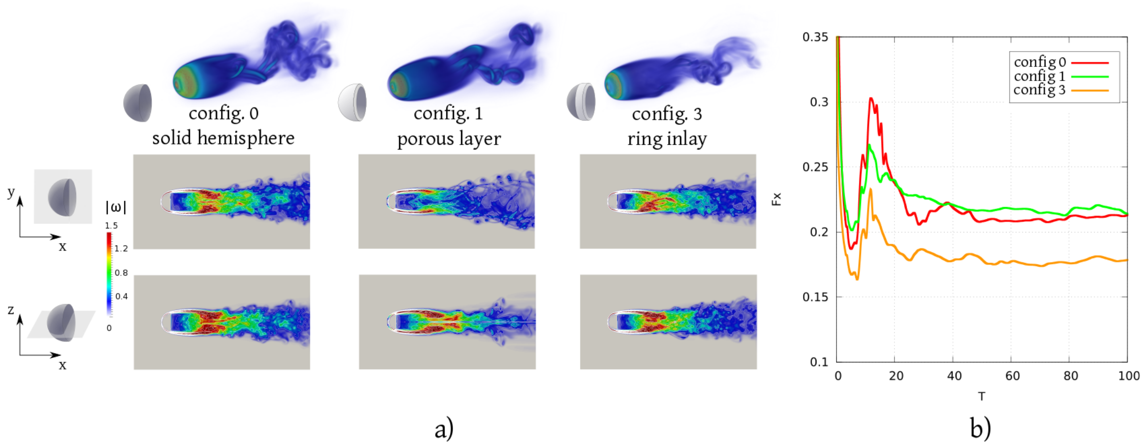

Figure 1. Effects of porosity around a 3D hemisphere at Re = 1000. a) Comparison of the vorticity (a) and the drag force Fx (b).

References

[1] P. Angot, C.-H. Bruneau, and P. Fabrie. A penalization method to take into account obstacles in incompressible viscous flows. *Numer. Math.*, **81**:497–520, 1999.

[2] G.-H. Cottet and P. Koumoutsakos. *Vortex Methods - Theory and Practice*. Cambridge University Press, 2000.

[3] J.-C. Loiseau, J.-C. Robinet, S. Cherubini, and E. Leriche. Investigation of the roughness-induced transition: global stability analyses and direct numerical simulations. **760**:175–211, 2014.

A method to study flow structures

Soledad Le Clainche[1] & José M. Vega[1]
[1]*School of Aerospace Engineering, Universidad Politécnica de Madrid, Madrid, Spain*

The main goal of this work is based on studying complex flows. These types of flows are found in nature or in several industrial applications, such as aerospace engineering, food processing or even physiological fluids. For this reason, studying and understanding complex flow behavior is a research topic of high interest. We present a method, higher order dynamic mode decomposition (HODMD)[1] that is suitable to analyze flow structures. This method combines singular value decomposition (SVD) with DMD [2] and Takens' delay embedding theorem [3] to approximate flow dynamics. HODMD has been successfully applied to study several types of cases that cover from non-linear dynamical systems, to complex fluid dynamic problems [4]. We will present the good performance of HODMD applied to study noisy experimental data (transitional or thermal flow), and its extrapolation properties, which make this method a suitable tool that can be used to reduce the computational cost in numerical simulations. Finally, we will briefly introduce the spatio-temporal HODMD analysis [5], to calculate flow structures, defined as traveling waves. Some examples of the wake of a wind turbine or the thermal convection in a rotating spherical shell will be presented at the time of the conference.

References

[1] S. Le Clainche, J.M. Vega, Higher order dynamic mode decomposition, SIAM J. of Appl. Dyn. Sys., 16(2), 882-925, 2017.
[2] P. J. Schmid, Dynamic mode decomposition of numerical and experimental data, J. of Fluid Mech. 656, 5–28, 2010.
[3] F. Takens, Detecting strange attractors in turbulence, Lecture Notes in Math., D.A. Rand and L.-S. Young, eds., Springer, Berlin, New York, 898, 366–381, 1981.
[4] S. Le Clainche, J.M. Vega, J. Soria, Higher order dynamic mode decomposition of noisy experimental data: the flow structure of a zero-net-mass-flux jet (submitted to Exp. Therm. and Fluid Sci.)
[5] S. Le Clainche, J.M. Vega, Spatio-Temporal Koopman Decomposition (submitted to J. of Nonlin. Sci.)

SPECTRAL PROPER ORTHOGONAL DECOMPOSITION AND ITS CONNECTION WITH DYNAMIC MODE DECOMPOSITION AND RESOLVENT ANALYSIS

Aaron Towne[1], Oliver T. Schmidt [2] & Tim Colonius [2]
[1] *Center for Turbulence Research, Stanford University, Stanford, CA, USA*
[2] *Department of Mechanical and Civil Engineering, California Institute of Technology, Pasadena, CA, USA*

Modern numerical and experimental investigations of turbulent flows lead to enormous data sets that are often interrogated using modal decomposition techniques such as proper orthogonal decomposition (POD) [2] and dynamic mode decomposition (DMD) [5]. The majority of applications of POD have used a version of the method that generates modes that depend only on spatial coordinates. This talk will focus on a lesser-used form of POD called spectral proper orthogonal decomposition. To be clear, we are *not* referring to the recent method of Sieber et al. [6] that was given the same name; instead, we are using the terminology of Picard & Delville [4] to describe a space-time formulation of POD for stationary flows that goes back to the original work of Lumley [2]. The first part of the talk will compare spectral POD with the more familiar "space-only" form of POD as well as dynamic mode decomposition. We will show that spectral POD is better suited than space-only POD for identifying physically meaningful coherent structures and that spectral POD modes can be viewed as optimal averages of DMD modes computed for an ensemble of realizations of a stationary flow. In the second part of the talk, a connection will be made between spectral POD and resolvent analysis, which is often used to model linear non-modal growth mechanisms in turbulent flows [3]. We will show that spectral POD and resolvent modes are identical when the resolvent-mode expansion coefficients are uncorrelated. More generally, we will show that the expansion coefficients must be regarded as statistical quantities in order for the resolvent-mode expansion to properly capture the flow statistics and that treating them as deterministic quantities, as is done in most existing models, imposes a fundamental limitation on the quality of the flow approximation that depends on the low-rank nature of spectral POD modes rather than the resolvent modes. These results will be demonstrated using two example problems: the linearized Ginzburg-Landau equation and a turbulent jet. The Ginzburg-Landau problem provides a simple model that can be used to highlight our theoretical results. For example, Figure 1 shows the equivalence of spectral POD and resolvent modes under white-noise forcing. The second problem relies on an extensive LES database [1] and enables comparisons between the different methods for a realistic application.

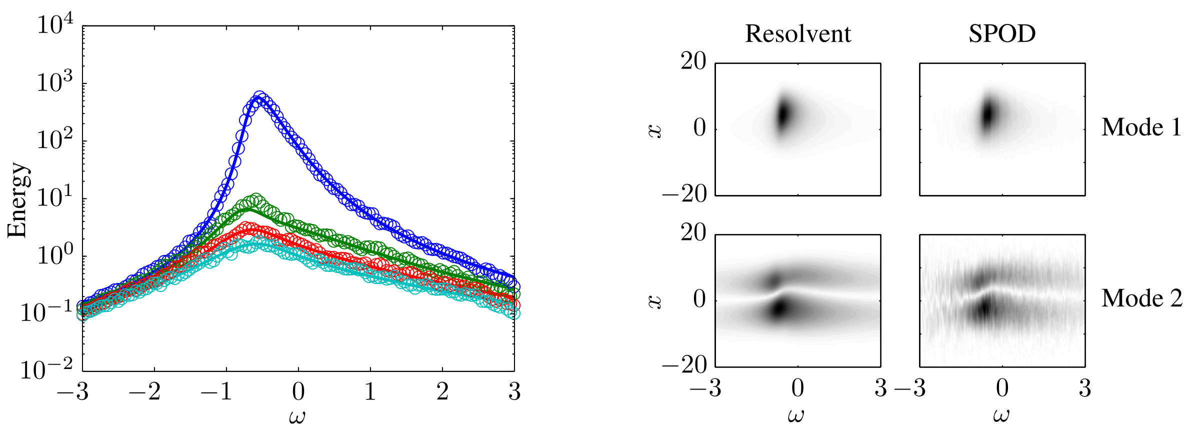

Figure 1. Equivalence of spectral POD and resolvent modes for white-noise forcing of the linearized Ginzburg-Landau equation. Left: SPOD eigenvalues (circles) and resolvent gain (lines). Right: energy-weighted mode-shapes.

References

[1] G. A. Brès, V. Jaunet, M. Le Rallic, P. Jordan, A. Towne, O. Schmidt, T. Colonius, A. V. G. Cavalieri, and S. K. Lele. Large eddy simulation for jet noise: azimuthal decomposition and intermittency of the radiated sound. *AIAA Paper #2016-3050*, 2016.

[2] J. L. Lumley. *Stochastic tools in turbulence*. Academic Press, New York, 1970.

[3] B. J. McKeon and A. S. Sharma. A critical-layer framework for turbulent pipe flow. *J. Fluid Mech.*, **658**:336–382, 2010.

[4] C. Picard and J. Delville. Pressure velocity coupling in a subsonic round jet. *Int. J. Heat Fluid Fl.*, **21**(3):359–364, 2000.

[5] P. J. Schmid. Dynamic mode decomposition of numerical and experimental data. *J.Fluid Mech.*, **656**:5–28, 2010.

[6] M. Sieber, C. O. Paschereit, and K. Oberleithner. Spectral proper orthogonal decomposition. *J. Fluid Mech.*, **792**:798–828, 2016.

LOW-RANK BEHAVIOR OF TURBULENT JETS

Oliver T. Schmidt[1], Georgios Rigas [1] & Tim Colonius [1]
[1]*California Institute of Technology, Pasadena, CA 91125, USA*

Large-scale coherent structures are educed from three large-eddy simulations of turbulent isothermal jets at different Mach numbers by means of spectral proper orthogonal decomposition. The modal energy spectra reveal a low-rank behavior that leads to a preferred amplification of Kelvin-Helmholtz-type wavepackets within certain frequency bands. We investigate the linear frequency response of the turbulent mean flow using the same numerical framework as in [2], and demonstrate that a resolvent analysis is capable of predicting the jet's statistical low-rank behavior and the associated modal structures accurately. The results also explain why previous wavepacket models based on the parabolized stability equations were largely successful in predicting modal shapes for certain frequencies, but not at others, particularly for the axisymmetric mode. A good qualitative agreement is found between the optimal resolvent gains and empirical modal energies in terms of their relative order and frequency dependance in figure 1(a-b). The leading $m = 1$ mode is dominant up to St ≈ 1. The predicted abrupt change to low-rank behavior is clearly observed for $m = 0$. The five leading SPOD and optimal resolvent response modes are compared in figure 1(c-l) for St $= 0.6$. Both analyses identify a Kelvin-Helmholtz (K-H) type instability as the dominant coherent structure. We show in detail that two different mechanisms are at work in the turbulent jet: the modal spatial instability of the initial shear layer, and non-modal spatial growth downstream of the potential core. The latter is optimally triggered through the Orr-mechanism[3], but is likewise observed in the empirical modes. According to [1], low-rank behavior in weakly non-parallel open flows such as jets is expected if the mean flow is convectively unstable. We note that this classification into modal and non-modal refers to the classical spatial, quasi-parallel stability analysis. In our resolvent analysis, the response is always non-modal in the sense that it is a superposition of a stable spectrum of modes. The better distinction is between low rank behavior associated with the dominant K-H mode and non-low-rank behavior at low frequencies. According to [1], low-rank behavior is expected for this open, convectively unstable flow, but these results show a different behavior at low frequencies.

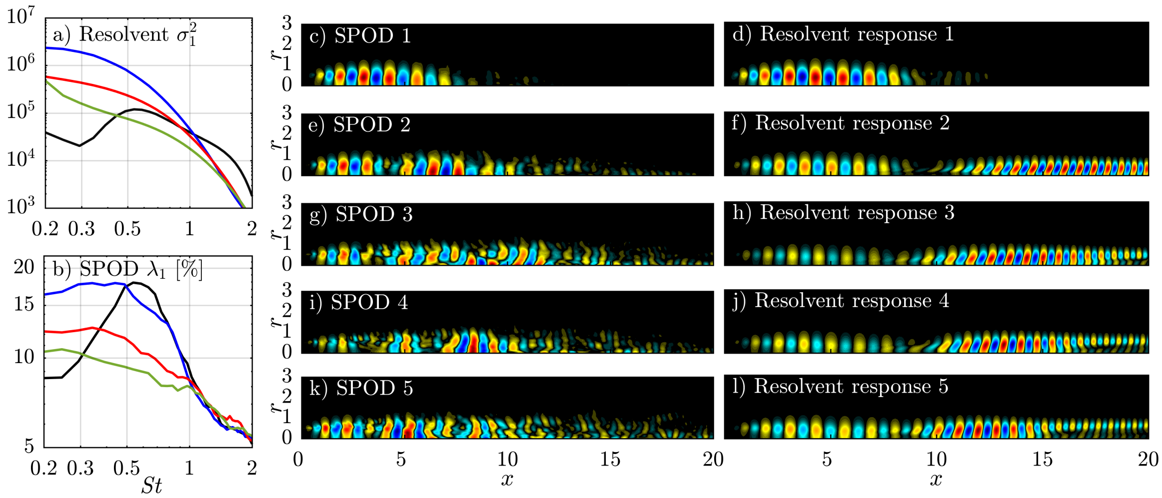

Figure 1. Empirical SPOD modes (left) and optimal resolvent response modes (right) for St $= 0.6$ and $m = 0$. The normalized pressure is shown. The leading resolvent response in (b) accurately models leading SPOD mode in (a). Suboptimal resolvent and higher SPOD modes exhibit similar structures, but should not be compared one by one because of their similar gains.

We acknowledge the support of the Office of Naval Research (grant No. N00014-16-1-2445) with Dr. Knox Millsaps as program manager. This research was also supported in part by the Boeing Company through a Strategic Research and Development Relationship Agreement (CT-BA-GTA-1).

References

[1] S. Beneddine, D. Sipp, A. Arnault, J. Dandois, and L. Lesshafft. Conditions for validity of mean flow stability analysis. *Journal of Fluid Mechanics*, **798**:485–504, 2016.

[2] O. T. Schmidt, A. Towne, and T. Colonius. Intrinsic and extrinsic linear dynamics of a high-reynolds number turbulent jet. In *Euromech Colloquium 571 / IUTAM Symposium*. American Institute of Aeronautics and Astronautics (AIAA), 2016.

[3] G. Tissot, M. Zhang, F. C. Lajús, A. V. G. Cavalieri, and P. Jordan. Sensitivity of wavepackets in jets to nonlinear effects: the role of the critical layer. *Journal of Fluid Mechanics*, **811**:95–137, 001 2017.

DELAY OF THE PIPE FLOW INSTABILITY VIA POLYMER SOLUTE

K.Y. Volokh[1]*
[1] *Faculty of Civil and Environmental Engineering, Technion - I.I.T., Israel*

The remarkable phenomenon of the drag reduction via addition of small amounts of polymer molecules to a Newtonian solvent was observed experimentally long ago. However, the theoretical explanations of this observation are not overwhelming yet. In this talk, we present a possible theoretical account of the phenomenon. It is based on the use of the Navier-Stokes model with viscous strength for the solvent and the upper-convected Maxwell model for the polymer solute. Simple analytical calculation shows that the laminar flow of the solvent is stabilized by an addition of the polymer solute and, thus, the transition to the chaotic and slower on average turbulent motion is suppressed.

E-mail: cvolokh@technion.ac.il

*E-mail: cvolokh@technion.ac.il

NUMERICAL BIFURCATION ANALYSIS OF THREE-DIMENSIONAL STEADY FLOWS IN A SUDDEN EXPANSION

Y. Guevel[1], G. Girault[1,2], and J.M. Cadou[1]
[1] *Univ. Bretagne Sud, FRE CNRS 3744, Institut de Recherche Dupuy de Lome, Lorient, France,*
[2] *Centre de recherche des Ecoles de Saint-Cyr Coëtquidan, Ecoles Militaires de Coëtquidan, Guer, France*

This study is focused on the parametric analysis of the three-dimensional flow in a sudden expansion. Bifurcation analysis methods based on the Asymptotic Numerical Method [4, 5, 6] are used. Those specific methods allow us to follow regular solution paths, to detect critical solutions and to automatically switch branches. High performance computing is implemented in an open-source multi-physical software ELMER [3], coupled with the direct Solver MUMPS [1] and the multi-threading library OpenBlas [7]. It makes it possible to perform bifurcation analysis for models with high number of degrees of freedom (10^7 d.o.f.), in affordable computing times.
Remarks are made for the branch-switching method in the case of symmetry breaking bifurcations. New results of primary and higher rank bifurcations are presented.
It is proposed to investigate, for one expansion ratio, fundamental and bifurcated branches in order to reveal primary and secondary bifurcation. Additionally, branch switching method based on power series analysis is successfully tested. Thus, it is established the corresponding bifurcation diagram (see Fig.1). Evolution of the critical Reynolds number for the primary bifurcation according to the span-wise aspect ratio is obtained. Finally, in-depth analysis permit to obtain several kinds of bifurcation. Velocity and pressure for flows and branch switching specific vectors (see Fig.1) are depicted. It is also confirmed the existence of a span-wise symmetry breaking bifurcation for smaller aspect ratio than expected [2, 6].

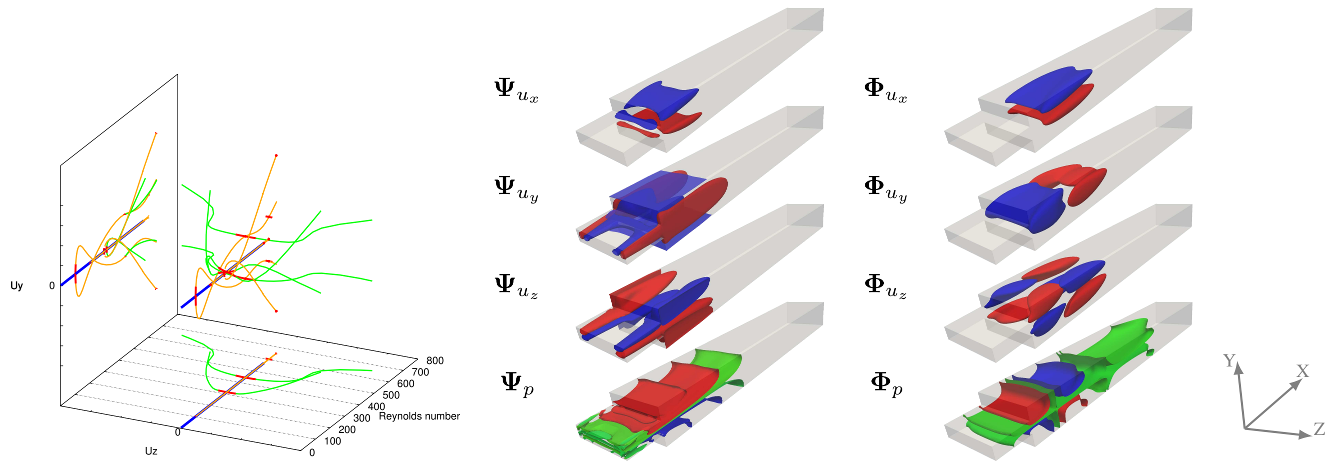

Figure 1. (Left) Bifurcation diagram for the case $E = 3$, $A_i = 8$, $L = 55h$. (Middle) Left bifurcation mode $\mathbf{\Psi}_{PB1}$ and (Right) bifurcation mode $\mathbf{\Phi}_{PB1}$ for the first primary bifurcation "PB1". Velocity components and pressure for $E = 3$, $A_i = 5$, $L = 30h$.

References

[1] Patrick R. Amestoy, Iain S. Duff, Jean-Yves L'Excellent, and Jacko Koster. A fully asynchronous multifrontal solver using distributed dynamic scheduling. *SIAM Journal on Matrix Analysis and Applications*, **23**(1):15–41, 2001.

[2] T. P. Chiang, T. W. Sheu, R. R. Hwang, and A. Sau. Spanwise bifurcation in plane-symmetric sudden-expansion flows. *Phys. Rev. E*, **65**(1):016306, January 2002.

[3] CSC - IT Center for Science. ELMER - Finite Element Solver for Multiphysical Problems. *www.csc.fi/elmer*, 1995.

[4] Y. Guevel, H. Boutyour, and J. M. Cadou. Automatic detection and branch switching methods for steady bifurcation in fluid mechanics. *Journal of Computational Physics*, **230**(9):3614 – 3629, 2011.

[5] Yann Guevel. *Numerical methods suitable for solving the Navier-Stokes equations*. Theses, IRDL FRE CNRS 3744,Université Bretagne Sud, January 2016.

[6] Marc Medale and Bruno Cochelin. High performance computations of steady-state bifurcations in 3D incompressible fluid flows by Asymptotic Numerical Method. *Journal of Computational Physics*, **299**:581 – 596, 2015.

[7] Zhang Yunquan Zhang Xianyi, Wang Qian. Model-driven level 3 blas performance optimization on loongson 3a processor. In *2012 IEEE 18th International Conference on Parallel and Distributed Systems (ICPADS),*, 2012.

THREE-DIMENSIONAL INSTABILITY OF THE FLOW AROUND A SPHERE

Andrea Sansica[1,2], Jean-Christophe Robinet [2], Frédéric Alizard[2] & Eric Goncalves[3]
[1] *Centre National d'Études Spatiales, Direction des Lanceurs, Paris, France*
[2] *Laboratory of Fluid Dynamics, ENSAM, Paris, France*
[3] *Pprime Institute, ISAE-ENSMA, Poitiers, France*

The onset of large scale unsteadiness for viscous fluids past axisymmetric bodies represents one of the major subject of study for several modern engineering applications, especially in the field of launcher after-bodies. In this respect, the wake behind a sphere may be considered as a representative simplified case for axisymmetric bodies. Both numerical simulations and experiments [1, 2, 4, 5, 6] carried out at low Reynolds numbers reveal that a first bifurcation occurs when a critical Reynolds number is reached ($Re_{c,1} \approx 210$), yielding to the loss of axial symmetry of the steady base flow. The wake is consequently shifted along the normal direction and exhibits a pair of steady streamwise vortices that extend on a very long distance downstream of the body. Although the flow is no longer axisymmetric, a reflectional symmetry of a plane in the streamwise direction still exists. When the Reynolds number is further increased beyond a second critical value ($Re_{c,2} \approx 270$) the flow undergoes a supercritical Hopf bifurcation and is dominated by a low-frequency shedding of hairpin-like vortices in a Strouhal number range between $St \approx 0.1 - 0.2$. The objective of this study is to carry out a fully three-dimensional linear stability analysis without any assumption on the base flow and follow the evolution of the two bifurcations with the Mach number, as a follow up of the study by [3]. The analysis is performed for a Reynolds number range between $200 - 320$ and up to supersonic velocities. The density gradient contours in a Schlieren-like flow visualization for the baseflow at $Re = 280$ and $M = 1.2$ in Fig. 1-left shows that a bow shock is created. The iso-surface of the zero-streamwise velocity is also reported and shows the axisymmetric configuration of the separation behind the sphere. The dominant eigenmodes of are extracted by means of an Arnoldi algorithm coupled to the the linearized full Navier-Stokes equations. In this way, it is possible to draw a stability map (Fig. 1-right) that shows for each Reynolds-Mach number combination whether the leading eigenmode is a steady axisymmetric (full circle), steady planar-symmetric (full triangle) or unsteady planar-symmetric (empty triangle) mode. The effect of the increasing Mach number is to stabilize the flow and to move the two bifurcations towards higher Reynolds numbers and close to each other. The evolution of the eigenfunctions with the Mach number will also be shown.

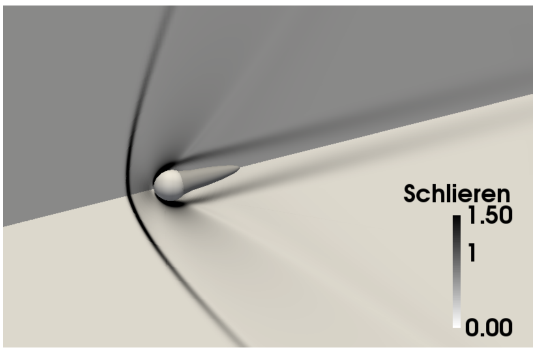

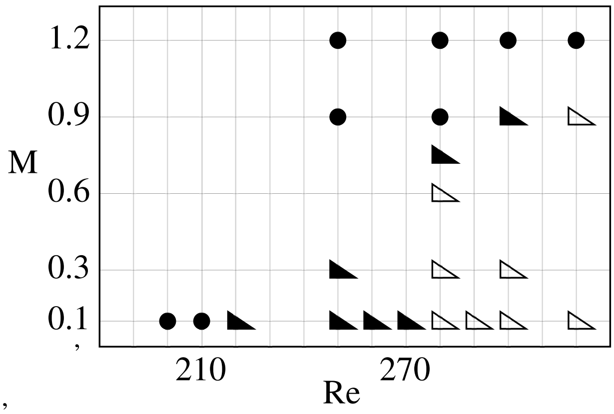

Figure 1. Left: Baseflow at $Re = 280$ and $M = 1.2$; Contours of the gradient of density and zero-streamwise velocity iso-surface. Right: Stability map; Symbols are: full circle=steady axysimmetric, full triangle=planar-symmetric and empty triangle=unsteady planar-symmetric.

References

[1] K. Gumowski, J. Miedzik, S. Goujon-Durand, P. Jenffer, and J. E. Wesfreid. Transition to a time-dependent state of fluid flow in the wake of a sphere. *Phys. Rev. Lett.*, **77**:055308(R), 2008.

[2] T.A. Johnson and V.C. Patel. Flow past a sphere up to a reynolds number of 300. *J. Fluid Mech.*, **378**:19–70, 1999.

[3] T. Nagata, T. Nonomura, S. Takahashi, Y. Mizuno, and K. Fukuda. Investigation on subsonic to supersonic flow around a sphere at low reynolds number of between 50 and 300 by direct numerical simulation. *Physics of Fluids*, **58**:056101, 2016.

[4] D. Ormières and M. Provansal. Transition to turbulence in the wake of a sphere. *Phys. Rev. Lett.*, **81**(1):80–83, 1999.

[5] L. Schouveiler and M. Provansal. Self-sustained oscillations in the wake of a sphere. *Phys. Fluids*, **14**:3846 – 3854, 2002.

[6] A.G. Tomboulides, S.A. Orszag, and Karniadakis G.E. Direct and large-eddy simulation of axisymmetric wakes. AIAA âĂŞ 31st Aerospace Sciences Meeting & Exhibit, 1993.

SUBCRITICAL AND SUPERCRITICAL TRANSITION IN CURVED PIPES

Jacopo Canton, Ramis Örlü & Philipp Schlatter
Linné FLOW Centre, KTH Mechanics, Stockholm, Sweden

The flow through curved pipes has received increasing attention in the past decades, but several phenomena still miss an exhaustive explanation. Bent pipes are fundamental components in various industrial devices (for a review see Ref. [8]), and are also studied in the medical field, being an integral part of vascular and respiratory systems [2, 3]. The present work focuses on the flow inside a toroidal pipe, which constitutes the common asymptotic limit between two 'real' flow cases: the spatially developing and the helical pipes. The flow is determined by the Reynolds number Re and a single geometrical parameter: the curvature δ (the ratio between pipe and torus radii).
The transition to turbulence of this flow has received a considerable amount of interest in the past decades. The recent works by Canton *et al.* [4] and Kühnen *et al.* [6] determined that the flow is linearly unstable, and undergoes a Hopf bifurcation, for any curvature greater than zero and for $Re \approx 4000$. Different eigenmodes, in the shape of travelling waves, contribute to the neutral curve for the flow (see figure 5 in Ref. [4]). This behaviour is in contrast to the flow in a straight pipe which undergoes subcritical transition for $Re \gtrsim 2000$ [1].
The transition scenario is different for low curvatures: while for $\delta \geq 0.028$ direct numerical simulations (DNS) confirm the presence of a Hopf bifurcation [4], for $\delta < 0.028$ no clear boundary has been observed. For low curvatures a bent pipe appears to behave similarly to a straight pipe: the flow undergoes transition to turbulence despite being linearly stable to infinitesimal perturbations [6, 7]. We investigate this complex behaviour by means of nonlinear DNS performed with the spectral element code Nek5000 [5] and, in order to isolate the dominant structures in the flow, we analyse the flow by three-dimensional proper orthogonal decomposition (POD). We also analyse the transition process by quantifying the intermittency level and measuring the lifespan of turbulent events. Preliminary results indicate that, indeed, the flow does not abruptly transition from the steady to the unsteady regime. Instead, transition occurs over a range of curvatures and Reynolds numbers indicating a subcritical behaviour.

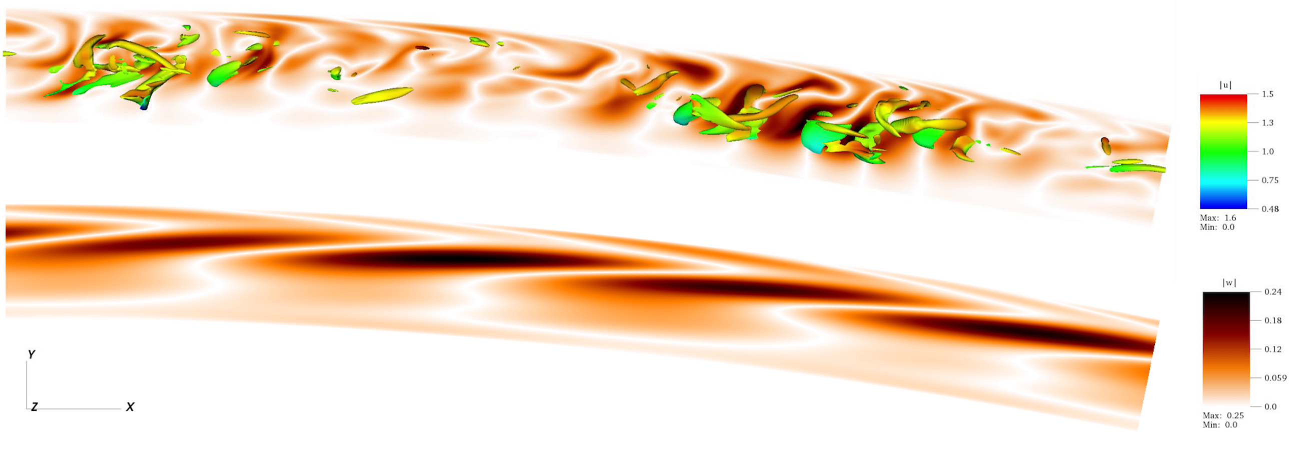

Figure 1. *(Top):* Instantaneous flow field for $\delta = 0.01$ and $Re = 3000$ represented by isocontours of negative λ_2 coloured by streamwise velocity magnitude (u) and azimuthal velocity magnitude (w) on a longitudinal section. *(Bottom):* Corresponding most energetic POD mode showing a travelling wave with a wavelength of about 5 pipe diameters.

References

[1] D. Barkley. Theoretical perspective on the route to turbulence in a pipe. *J. Fluid Mech.*, **803**:P1, 2016.
[2] S. A. Berger, L. Talbot, and L.-S. Yao. Flow in curved pipes. *Annu. Rev. Fluid Mech.*, **15**:461–512, 1983.
[3] K. V. Bulusu, S. Hussain, and M. W. Plesniak. Determination of secondary flow morphologies by wavelet analysis in a curved artery model with physiological inflow. *Exp. Fluids*, **55**:1832, 2014.
[4] J. Canton, P. Schlatter, and R. Örlü. Modal instability of the flow in a toroidal pipe. *J. Fluid Mech.*, **792**:894–909, 2016.
[5] P. F. Fischer, J. W. Lottes, and S. G. Kerkemeier. Nek5000 Web page, 2008. http://nek5000.mcs.anl.gov.
[6] J. Kühnen, P. Braunshier, M. Schwegel, H. C. Kuhlmann, and B. Hof. Subcritical versus supercritical transition to turbulence in curved pipes. *J. Fluid Mech.*, **770**:R3, 2015.
[7] K. R. Sreenivasan and P. J. Strykowski. Stabilization effects in flow through helically coiled pipes. *Exp. Fluids*, **1**:31–36, 1983.
[8] S. Vashisth, V. Kumar, and K. D. P. Nigam. A review on the potential applications of curved geometries in process industry. *Ind. Eng. Chem. Res.*, **47**:3291–3337, 2008.

ONE-WAY NAVIER-STOKES EQUATIONS: GLOBAL STABILITY ANALYSIS VIA EFFICIENT SPATIAL MARCHING.

Tim Colonius[1], Georgios Rigas[1], Aaron Towne[2] & Michael Beyar[3]
[1]*California Institute of Technology, Pasadena, CA, USA*
[2]*Stanford University, Palo Alto, CA, USA*
[3]*Boeing Research & Technology, Huntington Beach, CA, USA*

Hydrodynamic stability analysis is a critical tool for transition prediction in the laminar regimes, and, when applied to the mean of a turbulent mean flow has been used to predict coherent structures in some flows. Stability tools have been successfully applied to canonical two-dimensional flows over the last years. However, practical flows of relevance to the aviation industry are often three-dimensional (3D). For 3D flows questions of stability, receptivity, secondary flows, and coherent structures, require the solution of large 3D, partial-derivative eigenvalue problems.

A method for constructing well-posed one-way equations for calculating disturbances of slowly-varying flows was recently introduced[2]. The linearized Navier-Stokes equations are modified such that upstream propagating modes are removed from the operator. The resulting equations, termed one-way Navier-Stokes (OWNS) equations, are stable and can be solved efficiently in the frequency domain as a spatial initial value problem in which initial perturbations are specified at the domain inlet and propagated downstream by spatial integration. Since the method accurately tracks the full spectrum of downstream propagating modes, it is well suited for studying multi-modal interactions and non-modal instabilities, situations for which the traditional parabolized stability equations (PSE) are not well suited. The regularization of the governing equations permits a very fast spatial marching procedure that results in a huge reduction in computational expense.

The OWNS equations have been applied in a variety of slowly-varying flows, including wall-bounded flows and jet flows in subsonic and supersonic regimes [2, 1]. Specifically, we have examined the spatial stability of canonical two- and three-dimensional boundary layers, corresponding to the Blasius and the Falkner-Skan-Cooke flows for predicting the evolution of unstable Tollmien-Schlichting waves and crossflow vortices, respectively. Also, turbulent circular and non-circular jets, with two and three inhomogeneous directions, have been examined in order to predict large-scale wavepacket structures and their acoustic radiation. Finally, the OWNS framework has been also adapted to perform resolvent analysis, which is the topic of a companion contribution in this volume.

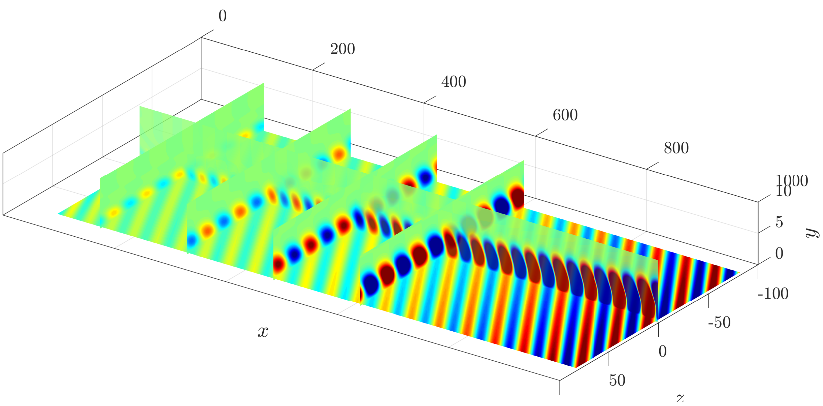

Figure 1. Three-dimensional stationary crossflow disturbance in physical space obtained from OWNS. Falkner-Skan-Cooke boundary layer with spanwise wavenumber $\beta = 0.19$ and frequency $\omega = 0$. Contours of the real part of streamwise velocity perturbation are shown.

We acknowledge the support of the Boeing Company through a Strategic Research and Development Relationship Agreement CT-BA-GTA-1. This research was also supported in part by a grant from the Office of Naval Research (grant No. N00014-16-1-2445) with Dr. Knox Millsaps as program manager.

References

[1] G. Rigas, T. Colonius, and M. Beyar. Stability of wall-bounded flows using one-way spatial integration of Navier-Stokes equations. In *55th AIAA Aerospace Sciences Meeting*, **AIAA 2017-1881**, Grapevine, TX, 2017.

[2] A. Towne and T. Colonius. One-way spatial integration of hyperbolic equations. *Journal of Computational Physics*, **300**:844–861, 2015.

INSTABILITY OF THE FLOW ACROSS A CIRCULAR APERTURE IN A THICK PLATE

Raffaele Longobardi[1,2], David Fabre [1] & Paolo Luchini [2]
[1]*Institut de Mécanique des Fluides de Toulouse (IMFT), Toulouse, France*
[2]*DIIN, Universitá degli studi di Salerno, Fisciano, Italy*

Jet flows are well known to be strongly convectively unstable, i.e. they strongly amplify hydrodynamic perturbations in the downstream direction. In the case the jet is formed by the flow through a circular aperture, experiments and simulations [3, 4] show that if the plate is thick enough, strong periodic oscillations can occur and lead to characteristic whistling tones, suggesting the existence of a feedback mechanism leading to self−sustained oscillations. The objective of this work is to clarify this mechanism using linearized Navier-Stokes equations. We show that, contrary to previous expectations, the feedback mechanism is not related to acoustics but that an instability can exist in a purely incompressible framework [2].
Under the hypothesis of small-amplitude perturbations, we first solve a non−homogenous linear forced problem with an imposed oscillating flow rate through the aperture. The solution allows to compute the *impedance* of the hole, defined as the pressure jump divided by the flow rate. We compute the impedance as function of the frequency ω, the Reynolds number and the ratio between the length of the hole and its diameter β. For thin holes, we compare our viscous results with existing models derived in the inviscid case [1]. Moreover, we show that for thick holes the impedance can have a negative real part, indicating that the flow can act as an energy source when coupled to an outer system, for instance an acoustic resonator.
In a second step, we conduct a global stability analysis, which consists of solving a homogeneous linear eigenvalue problem. We confirm the existence of globally unstable mode in the range of parameters predicted by the impedance criteria. Analyzing the structure of the global modes, we show that the instability is associated to the existence of a recirculation region in the thickness of the hole.
Note that to solve both the homogenous and nonhomogenous linear problems we had to design a specific method in order to overcome the problems associated to the boundary condition in the farfield of the jet because of the very strong spatial amplification. An original method using a complex mapping of the axial coordinate is introduced. It is shown that this method greatly increases the range or Reynolds numbers investigated.

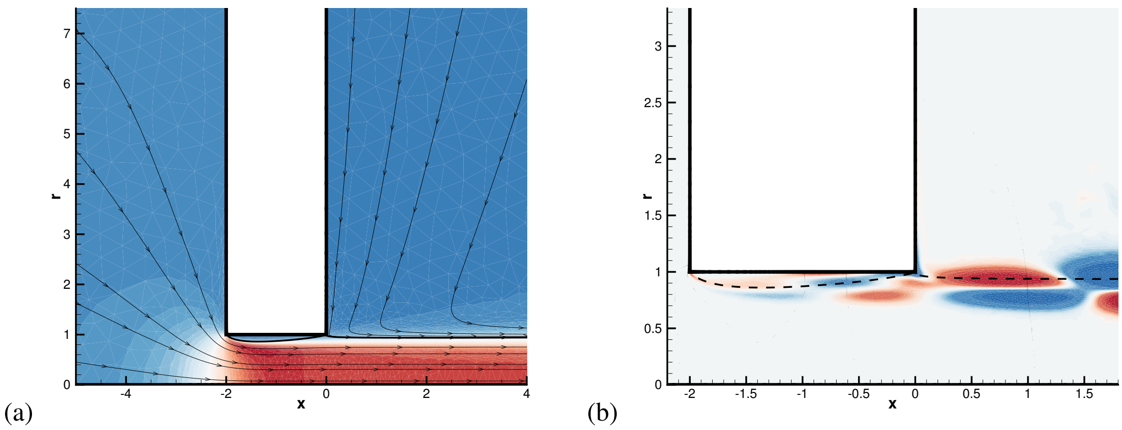

Figure 1. (a) Axial component of the baseflow at Re=1500 and $\beta = 1$. (b) Vorticity of the perturbation of the forced problem at Re=1600, $\beta = 1$ and $\omega = 2.07$; the dashed line shows the boundary of the recirculation region.

References

[1] MS Howe. On the theory of unsteady high reynolds number flow through a circular aperture. In *Proceedings of the Royal Society of London A: Mathematical, Physical and Engineering Sciences*, **366**, pages 205–223. The Royal Society, 1979.
[2] MA Langthjem and M Nakano. Numerical study of the hole-tone feedback cycle based on an axisymmetric formulation. *Fluid dynamics research*, **42**(1):015008, 2010.
[3] Jialin Su, Jochen Rupp, Andrew Garmory, and Jon F Carrotte. Measurements and computational fluid dynamics predictions of the acoustic impedance of orifices. *Journal of Sound and Vibration*, **352**:174–191, 2015.
[4] Dong Yang and Aimee S Morgans. The acoustics of short circular holes opening to confined and unconfined spaces. *Journal of Sound and Vibration*, **393**:41–61, 2017.

RECEPTIVITY OF A COMPRESSIBLE BOUNDARY LAYER TO INTERACTIONS BETWEEN IMPINGING ACOUSTIC WAVES

Carlos G. Hernandez[1] & Xuesong Wu [1,2]
[1]*Department of Mathematics, Imperial College London, 180 Queen's Gate, London SW7 2AZ, UK*
[2]*Department of Mechanics, Tianjin University, Tianjin 300072, PR China*

In this talk, we show that two acoustic waves impinging on a compressible boundary layer at certain angles may interact to generate a forcing in resonance with a nearly neutral Tollmien-Schlichting wave. The latter is thus excited near the lower branch of the neutral curve and subsequently undergoes exponential amplification.

The ability of a flow in a boundary layer to convert external perturbations (sound, heat, turbulence, vibrations of a wing surface) into instability modes is termed receptivity of a boundary layer. According to Morkovin [1], the first who coined the term "Receptivity", this represents the first stage of the transition process, which can consist of different steps depending on the type of flow and the strength of the external disturbance. The main goal of receptivity is therefore the determination of the amplitudes of the generated T-S waves and, related to the former, to find out which types of external disturbances can more easily provoke these instability waves.

It was not until 1947 [2] that low-turbulence wind tunnels were available and serious boundary layer receptivity studies were carried out experimentally. On the other hand, the analysis of the receptivity of a boundary layer to acoustic perturbations began with Fedorov [3], who was the first to study the interaction of sound waves with a growing boundary layer, leading to some scattering but not to the excitation of T-S waves; later on, almost at the same time both Ruban [4] and Goldstein [5] described the mechanism by which relatively weak sound waves interact with a small defect along a flat plate's surface to excite T-S waves downstream.

We will begin our analysis with a survey of the different scenarios featuring resonant interactions leading to excitation of T-S waves. Later on, a triple-deck formalism consisting on the upper, main and lower decks is adopted (via asymptotic analysis of the Navier-Stokes equations in the limit $Re \to \infty$). In order to obtain the uniformly valid solution near the neutral point, it is necessary ot include the non-parallel flow effect, which becomes important in an $O(Re^{-3/16})$ neighbourhood [6], [7]. Asymptotic expansions for the fluid variables will be constructed across the decks and suitable matching and boundary conditions will be derived. Finally, expressions for the coupling coefficient and the T-S wave's amplitude will be presented, for a wide range of values of β_{TS}, β_S, ω_S, α_S and Mach number.

The receptivity mechanism is similar to that due to the interaction between acoustic and vortical disturbances [8], but a difference is that both acoustic waves penetrate into the lower deck where they interact to make an extra contribution in addition to that from the interaction in the upper deck, The mechanism operates in both subsonic and supersonic regimes, but it is found to be particularly efficient in the latter regime when the sound waves have low frequencies of the same order of magnitude as the instability mode. The present mechanism is found to be very efficient when compared to the interaction of a sound wave and a convective gust [8].

Unlike the mechanism in the Goldstein-Ruban theory, the scale conversion does not require any wall roughness and therefore operates over smooth surfaces, like a flat plate. This roughness-free interaction is also observed between a sound and a vortical wave, as described in [8].

References

[1] Morkovin M.V.; 1969 Critical evaluation of transition for laminar to turbulent shear layers with emphasis on hypersonically traveling bodies. Air Force Flight Dynamics Laboratory Rep. AFFDL-TR-68-149.
[2] Schubauer G.B. and Skramstad H.K.; 1947 Laminar-boundary-layer oscillations and transition on a flat plate. NACA Report 909, 327-357.
[3] Fedorov A.V.; 1982 Generation of instability waves in a boundary-layer flow of compressible gas exposed to an acoustic field. Numerical Methods in Continuum Mechanics (Novosibirsk). 13, 106.
[4] Ruban A.I.; 1984 On Tollmien-Schlichting wave generation by sound. Izv. Akad. Nauk SSSR Mekh. Zhid. Gaza 5,44. 154-189.
[5] Goldstein M.E.; 1985 Scattering of acoustic waves into Tollmien-Schlichting waves by small streamwise variation in surface geometry. Journal of Fluid Mechanics. 154, 509.
[6] Ruban A.I.; 1983 Nonlinear equation for the amplitude of Tollmien-Schlichting waves in the boundary layer On Tollmien-Schlichting wave generation by sound. Izv. Akad. Nauk SSSR Mekh. Zhid. Gaza 6, 60-67.
[7] Hall P and Smith F.T.; 1984 On the effects of non-paralellism, three-dimensionality and mode interaction in nonlinear boundary-layer stability. Studiesin Applied Mathematics 71, 91-120.
[8] Wu X.; 1999 Generation of Tollmien-Schlichting waves by convective gusts interacting with sound. Journal of Fluid Mechanics. vol. 397, 285-316.

EUROPEAN MECHANICS SOCIETY

EUROMECH COLLOQUIUM 591

Three dimensional instability mechanisms in transitional and turbulent flows

Bari, Italy / 18-20 September 2017